Technical Report: NAVTRADEVCEN 838-2

INVESTIGATION AND EVALUATION OF UDOFTT MATHEMATICAL PROCEDURES

Morris Rubinoff
Harry J. Gray, Jr.
William C. Sleemer
Alvin L. Vivatson

University of Pennsylvania
The Moore School of Electrical Engineering
Philadelphia, Pennsylvania

401748

7 December 1962

Prepared for

U.S. NAVAL TRAINING DEVICE CENTER

Port Washington, New York

Contract No. N61339-838

ABSTRACT

This was an investigation of the mathematical methods used in UDOFTT. The investigation has provided an evaluation, both from a theoretical and an experimental aspect, of the mathematical methods used in UDOFTT. These mathematical methods were the numerical methods that were used to solve the simultaneous system of nonlinear differential equations of flight for the F-100A. The investigation was initiated with a study and summary of the mathematical theory that led to the development of stability charts for numerical quadrature formulas. Next, the theory, which treated a single linear inhomogeneous differential equation, was extended to a simultaneous set of such equations and then to a primitively nonlinear differential equation. This last equation led to the conjecture that stability charts could be applied to nonlinear differential equations in order to establish both stability and accuracy of their solutions. Finally, the last effort experimentally evaluated the accuracy of the numerical methods used by UDOFTT, as applied to the nonlinear differential equations of motion of the F-100A trainer. This was accomplished by first programming certain maneuvers to start from various initial conditions, and then by flying the trainer through the programmed maneuvers using different quadrature intervals. Quadrature intervals over the range of 100 msec. to 10 msec. were used and the resulting flights were compared by means of a set of flight variables that were obtained in digital print-outs.

FOREWORD

The mathematical procedures used in the Universal Digital Operational Flight Trainer Tool (UDOFTT) have been under investigation since the concept of real-time digital flight simulation was first envisioned. The first step was the development of a numerical integration procedure capable of solving, in real time, a system of six simultaneous non-linear differential equations necessary for the activation of a flight trainer. The problem was investigated through the theory of stability charts and their use in the synthesis of numerical quadrature formulae.

Initially the theory was developed to treat one linear inhomogeneous differential equation. The natural frequency of the equation was computed and for this frequency, a quadrature interval was found for which the solution was stable. The theory was then applied to a set of linear inhomogeneous equations with the result that by plotting the frequency curve of the system of equations on the stability chart an immediate choice of quadrature intervals for which the solution will be stable can be made.

The present study was an experimental investigation of the mathematical methods used in UDOFTT and the variation in the accuracy and stability of these methods with a change in interval length and under the stress of different flight maneuvers. A by-product of this investigation was the determination that stability chart theory can be applied to a primitively non-linear differential equation when there is close agreement between the frequencies of the true solution and those in the numerical solution.

The flight maneuvers chosen to test the integration procedures were of both high and low frequency types. The integration interval was varied between 10 and 100 milliseconds using both the O_{33} and O_{30} C_{31} quadrature formulae. The results showed that the accuracy and stability for all intervals chosen using both formulae were as they are predicted by the stability charts, both accurate and stable for the 10 to 70 millisecond intervals.

It can be concluded from this study that the O_{33} Mod Gurk quadrature formula can be utilized for the simulation of most airplanes even though the system of equations describing the planes are not truly linear. The knowledge of the accuracy and stability of the chosen quadrature formula for the given integration interval can be predicted beforehand through the use of the stability charts. Further if an increase or decrease in computation time is needed, for example on a dual or triple cockpit activation system, the interval length can be extended to 70 milliseconds without loss of accuracy or stability.

E. M. Colletti

E. M. COLLETTI
Computer Branch
U. S. Naval Training Device Center

TABLE OF CONTENTS

LIST OF ILLUSTRATIONS

LIST OF TABLES

I. INTRODUCTION

1. Historical Background

Speculation as to the feasibility of real-time simulation of airplane flight using digital computers dates back to the middle 1940's when the U.S. Navy Special Devices Center launched a study to examine the problem. At first glance it appeared that such digital simulation should be feasible, but the primitive status of the digital computer art and the lack of certain mathematical assurances led to early discouragement, at least for the immediate future.

In 1950 the feasibility study was re-instituted at the Moore School where it was at first concluded that feasibility was marginal for as simple an airplane as the F9F but that feasibility might be accomplished through the use of certain special-purpose techniques aimed at increased computational speed. These techniques proved successful and the result was a design for a Universal Digital Operational Flight Trainer (UDOFT) which was eventually constructed as a trainer tool (UDOFTT).

Concurrently, the mathematical problem underlying successful digital flight simulation was solved to the approximation needed at that time. Briefly, the mathematical result stated that the stability of simulated flight could be guaranteed to be essentially the same as real flight for all possible airplane flight conditions. In other words, the realism of the flight simulation could be guaranteed in advance, regardless of the flight path to be followed.

With the delivery of UDOFTT to the Navy Training Device Center in 1960, the opportunity was presented to demonstrate these results in a real simulator. The present study has undertaken to demonstrate the validity of the mathematical proof and to extend the result to an empirical demonstration of the accuracy of digital flight simulation of an F-100A airplane.

2. Technical Background

The mathematical proof of a priori stability of digital flight simulation rests upon the "quadrature formula stability chart." The latter is a mapping in the complex plane showing the effect of digital computer (or "numerical") solution using a specified integrating or "quadrature" formula on a set of linear ordinary differential equations. More specifically, the stability chart maps the true frequencies of the analytic solution into the corresponding frequencies of the numerical solution. The stability chart displays both the error in oscillation period and the error in damping rate. Formulas exist which permit the computation of total error in the numerical solution of linear equations at any specified time.

Stability is assured even when accuracy is poor as long as the numerical solution is positively damped. The stability chart carries a curve of zero damping, which is therefore the boundary of stability.

Actually, the frequencies referred to above are so-called "dimensionless frequencies," i.e. the actual frequencies multiplied by the quadrature interval or time-step by which the flight solution is advanced. By proper selection of the time-step and quadrature formula, it is always possible to keep the numerical solution well within the stable region of the stability chart. Unfortunately this calls for too short a time-step for some quadrature formulas and existing digital computers could not keep up in real time. Fortunately, some quadrature formulas have been found which satisfy all these conditions but at some small sacrifice in accuracy.

The stability chart applies only for linear systems. Airplane characteristics are only quasilinear, i.e., they change but the change is slow enough that the quadrature formula treats them as linear. The results of this study indicate that the assumption of quasi-linearity holds for the F-100A but not as well as might be desired by some users who require very high accuracy as well as stability. For them, the solution is faster digital simulators (or more efficient programming of UDOFTT) and/or improved quadrature formulas. Thus, although the present study has confirmed the favorable predictions of the stability chart, further effort is warranted to extend the techniques of digital flight simulation.

II. WORK PERFORMED

1. Introduction

This section describes the work performed for the evaluation of the mathematical methods for UDOFTT during the past year. A summary of previous mathematical studies along with some recent studies are presented in Section 2. Included among these recent studies are some on the meaning of stability charts for nonlinear differential equations. Section 3 discusses the experimental work performed from the viewpoint of theory and method. The maneuvers studied are listed, the initial conditions and the control positions for the maneuvers are discussed, and the computer program is brought up to date.

2. Summary of Mathematical Studies

The first Progress Report prepared under this contract was devoted to presenting a summary of the previously conducted mathematical studies which led to the development of stability charts for quadrature formulas. The summary demonstrated the applicability of the stability charts to sets of linear homogeneous differential equations. In the past Moore School reports, the manner in which forcing functions enter into the numerical solution was described only for single equations. The effect of such forcing functions on sets of equations was derived and described in Progress Report No. 2. Also presented in Progress Report No. 2 was a section on introductory comments on the meaning of stability charts for primitively nonlinear differential equations.

The following sections present a brief summary of the material referred to above:

2.1 Solution of Linear Homogeneous Differential Equations

The general constant-parameter linear system

$$\begin{aligned} \dot{x}_1 &= a_{11}x_1 + \cdots + a_{1n}x_n \\ &\vdots \\ \dot{x}_n &= a_{n1}x_1 + \cdots + a_{nn}x_n \end{aligned} \tag{1}$$

may be written in the form

$$\dot{X} = AX \tag{2}$$

where X is the column vector

$$\begin{pmatrix} x_1 \\ \vdots \\ x_n \end{pmatrix}$$

and A is the matrix

$$\begin{pmatrix} a_{11} & \cdots & a_{1n} \\ \vdots & & \vdots \\ a_{n1} & \cdots & a_{nn} \end{pmatrix}$$

2.1.1 Solution Using Jordan Canonical Form

Equation (2) shows that the derivative $\dot{X}$ is obtained from the ordinate vector X by a linear transformation T, which in the X coordinate system is represented by the matrix A. When the proper choice of coordinate system is made, the matrix representing T takes on an especially simple form; and the solution of (2) becomes quite easy.

The matrix U can be obtained so that

$$X = UY \tag{3}$$

$$Y = U^{-1}X \, . \tag{4}$$

Using (3) and (4) the relationship between A and B, the matrices of T in the X and in the Y systems, can be computed.

$$Y = U^{-1}X$$
$$\dot{Y} = U^{-1}\dot{X} = U^{-1}AX = U^{-1}AUY = BY, \tag{5}$$

Then the following theorem was established:

> Let X and Y be related by (3) and (4). Then X is a solution of $\dot{X} = AX$, if and only if Y is a solution of $\dot{Y} = BY$, where A and B are related by (5).

The objective, thus, is to find a coordinate system in which the matrix has a minimum of off-diagonal elements. An especially convenient situation occurs when T has n linearly independent eigenvectors $V_1, \ldots, V_n$ with eigenvalues $\lambda_1, \ldots, \lambda_n$. In this case matrix B is diagonal, having $\lambda_1, \ldots, \lambda_n$ as diagonal elements, and it is necessary only to consider the system

$$\begin{aligned} \dot{y}_1 &= \lambda_1 y_1 \\ &\vdots \\ \dot{y}_n &= \lambda_n y_n \, . \end{aligned} \tag{6}$$

Thus, the general solution of (2) in this case is given by

$$X = U \begin{pmatrix} c_1 e^{\lambda_1 t} \\ \vdots \\ c_n e^{\lambda_n t} \end{pmatrix} \tag{7}$$

where $\begin{pmatrix} c_1 \\ \vdots \\ c_n \end{pmatrix} = U^{-1} X(0).$

When the characteristic equation has multiple roots, the Jordan canonical form reduces the solution of system (2) to the solution of systems of the form

$$\begin{aligned} \dot{y}_1 &= \lambda y_1 \\ \dot{y}_2 &= \lambda y_2 + y_1 \\ &\vdots \\ \dot{y}_m &= \lambda y_m + y_{m-1}. \end{aligned} \tag{8}$$

Equations (8) are of such a form that, knowing $y_j(t)$, $y_{j+1}(t)$ can be obtained. Thus,

$$\begin{aligned} y_1(t) &= c_1 e^{\lambda t} \\ y_j(t) &= \left(\frac{c_1}{(j-1)!} t^{j-1} + \frac{c_2}{(j-2)!} t^{j-2} + \ldots + c_{j-1} t + c_j \right) e^{\lambda t} \end{aligned} \tag{9}$$

where $c_j = y_j(0)$ $\quad (j=1, \ldots, m).$

For additional details refer to Section II-2 and to Appendix A-2 of Progress Report No. 1, M.S.R. No. 60-23.

2.1.2 The Laplace Transform Point-of-View

Section II-4 and Appendix A-3 of Progress Report No. 1, M.S.R. No. 60-23, show that Laplace-transform techniques can also be used to solve equation (2) to reach the same solution as that obtained in Section 2.1.1.

2.1.3 Numerical Solutions

Given an O_{MN} method the numerical solution of $\dot{X} = AX$ was found to be

$$X_n = \sum_{k=1}^{M} a_k X_{n-k} + h A \sum_{k=1}^{N} b_k X_{n-k} \quad . \tag{10}$$

Replacing X_n by UY_n and multiplying by U^{-1} gave

$$Y_n = \sum_{k=1}^{M} a_k Y_{n-k} + h U^{-1} AU \sum_{k=1}^{N} b_k Y_{n-k} \quad . \tag{11}$$

When A is diagonalisable, only the following system needs to be considered:

$$\begin{aligned} \dot{y}_1 &= \lambda_1 y_1 \\ &\vdots \\ \dot{y}_m &= \lambda_m y_m \end{aligned} \qquad \text{Refer to Eq. (6)}$$

These are the equations for which stability charts were first studied; and so it was known that

$$y_i(nh) = \sum_{k=1}^{r} c_k \left(e^{\mu_{ik} h}\right)^n \qquad (i=1, \ldots, m) \tag{12}$$

where $\mu_{i1}h, \ldots, \mu_{ir}h$ are the dimensionless frequencies which the numerical method associates with the dimensionless frequencies $\lambda_i h$.

For the system

$$\begin{aligned} \dot{y}_1 &= \lambda y_1 \\ \dot{y}_2 &= \lambda y_2 + y_1 \\ &\vdots \\ \dot{y}_m &= \lambda y_m + y_{m-1} \end{aligned} \qquad \text{Refer to Eq. (8)}$$

the same assumptions as above on λh gave

$$y_k(nh) = \sum_{j=1}^{r} P_{jk}(n) \left(e^{\mu_{jk} h}\right)^n \tag{13}$$

where all $P_{jk}(n)$ are polynomials in n of degree m-1 or lower.

Appendix A-4 in Progress Report No. 1, M.S.R. No. 60-23, and

Progress Report No. 2, M.S.R. No. 61-07, describes the use of O_{33} mod Gurk to solve a 3x3 system of linear homogeneous differential equations, and gives the O_{33} mod Gurk quadrature formula in closed form.

2.2 Numerical Solution of Linear Inhomogeneous Differential Equations

It was the purpose of this phase of the work to study the numerical solution of linear equations with time-dependent forcing functions which are slowly varying with a view to determining the value of stability charts in predicting the stability and the accuracy of such solutions. Preliminary results indicated that both the stability and the relative accuracy of the solution of inhomogeneous equations can be predicted from the stability chart; and whenever the homogeneous solution is stable, the inhomogeneous will also be stable.

2.2.1 Solution of Single Equations

Application of a given open quadrature formula O_{MN}* to the homogeneous equation $\dot{x} = \lambda x$ yielded

$$x_{s+p} = \sum_{j=1}^{s} \alpha_j \, x_{s-j+p} \tag{15}$$

where $s = \max(M,N)$, $\alpha_k = a_k + h\lambda b_k$, and the a_k for $k > M$ and the b_k for $k > N$ are set equal to zero. The closed-form solution to (15) is

$$x(nh) = \sum_{k=1}^{s} c_k \, r_k^n \triangleq \sum_{k=1}^{s} c_k \, e^{h\mu_k n} \triangleq \sum_{k=1}^{s} c_k \, e^{w_k n} \tag{16}$$

where the r_k are the roots of the characteristic polynomial of O_{MN}, i.e.,

$$r^s - \sum_{j=1}^{s} a_j \, r^{s-j} = 0, \tag{17}$$

and the c_k are constants determined from the s initial values.

Application of one of the open-closed formulas having the same stability chart as the O_{MN} formula to $\dot{x} = \lambda x$ led to the same equation (15) when the proper conditions held for the α_k (Refer to p.1-14 of M.S.R. No. 57-02).

---

* O_{MN}: $x_{s+p} = \sum_{j=1}^{M} a_j \, x_{s-j+p} + h \sum_{j=1}^{N} b_j \, \dot{x}_{s-j+p}$ (14)

To determine the effect of a forcing function on the solution, Q_{MN} was applied to

$$\dot{x} = \lambda x + f(t) \, . \tag{18}$$

This yielded

$$x_{s+p} = \sum_{j=1}^{s} a_j \, x_{s-j+p} + f_{s+p} \tag{19}$$

where

$$f_m \triangleq \sum_{j=1}^{s} h \, b_j \, f\left[(m-j)h\right] . \tag{19a}$$

In closed-form the solution is

$$x_n = \sum_{k=1}^{s} c_k \, r_k^{\,n} + \sum_{k=1}^{s} \sum_{j=s}^{n} \frac{f_j \, r_k^{\,n-j}}{\prod_{i \neq k} \left(1 - \frac{r_i}{r_k}\right)} \tag{20}$$

Note that if $|r_1| >> |r_k|$, $k = 2, 3, \ldots, s$, almost the entire term f_q is applied to r_1 (or μ_1) while the other frequencies $\mu_2, \mu_3, \ldots, \mu_s$ are only slightly excited. Moreover, even these small excitations damp out much more rapidly than the r_1 term. In fact, in this special case

$$x_n \approx c_1 \, r_1^{\,n} + \sum_{j=s}^{n} f_j \, r_1^{\,n-j} \, . \tag{21}$$

It follows that the numerical solution of the inhomogeneous equation (18) has the following characteristics:

1. The solution is the sum of two components.
2. One component of the solution (the complementary term) is identical with the solution of the corresponding homogeneous equation.
3. The other component of the solution (the particular solution) is composed of the sum of the separate contributions of the forcing function at each step of the solution, the contribution at each step being independent of all the other contributions and of the complementary term.
4. At the n'th step of the solution, the new contribution of the forcing function f_n depends not only on the stability chart

but also on the particular quadrature formula used. This is the only difference between O_{MN} and $O_{PQ}\,C_{RT}$ formulas with the same stability chart.

5. Each contribution f_n propagates exactly as the complementary solution. All of the frequencies $\mu_k (k=1,2,\ldots,s)$ are excited and no others. In particular, if the complementary term is stable in the sense that its contribution decays asymptotically to zero regardless of starting conditions x_0, x_1, ..., x_{s-1}, then the particular solution is also stable in the sense that it does not grow without bound. Moreover, accuracy late in the solution is not affected by errors introduced early in the solution.

6. If one root r_1 greatly exceeds all the other roots in absolute magnitude, the corresponding frequency μ_1 will be the only one excited to any appreciable extent and almost the full effect of the forcing function will be applied to this excitation.

7. A quadrature formula with a good stability chart will have $\mu_1 \approx \lambda$ and $|r_1| >> |r_k|$ for all $k > 1$. The quadrature solution of the inhomogeneous equation will, therefore, be determined by the "natural resonant frequency" of the corresponding homogeneous equation.

For additional details refer to Section II-5 of Progress Report No. 1, M.S.R. No. 60-23.

2.2.2 Solution of a System of Equations

The general constant-coefficient inhomogeneous system

$$\begin{aligned} \dot{x}_1 &= a_{11}x_1 + \ldots + a_{1m}x_m + f_1(t) \\ &\vdots \\ \dot{x}_m &= a_{m1}x_1 + \ldots + a_{mm}x_m + f_m(t) \end{aligned} \tag{22}$$

may also be written in vectorial form as

$$\dot{X} = AX + F(t) \tag{23}$$

where X is the column vector

$$\begin{pmatrix} x_1 \\ \cdot \\ \cdot \\ \cdot \\ x_m \end{pmatrix},$$

F(t) is the column vector

$$\begin{pmatrix} f_1(t) \\ \cdot \\ \cdot \\ \cdot \\ f_m(t) \end{pmatrix},$$

and A is the matrix

$$\begin{pmatrix} a_{11} & \cdots & a_{1m} \\ \cdot & & \cdot \\ \cdot & & \cdot \\ \cdot & \cdots & \cdot \\ a_{m1} & \cdots & a_{mm} \end{pmatrix}.$$

Applying Q_{MN} to equation (23) with s = max (M,N) yields

$$X_n = \sum_{k=1}^{s} a_k X_{n-k} + h \sum_{k=1}^{s} b_k AX_{n-k} + h \sum_{k=1}^{s} b_k F_{n-k} \quad . \tag{24}$$

Any m dimensional vector V can be written in the form $\sum_{j=1}^{m} y_j X^{(j)}$ where the $X^{(j)}$ are the eigenvectors of an arbitrary m by m constant matrix and the y_j are linear combinations of the components of V. Let the eigenvectors of A be $X^{(1)}, X^{(2)}, \ldots, X^{(m)}$ where $X^{(j)}$ is associated with eigenvalue λ_j.

Equation (24) can thus be written for the first quadrature step as

$$\begin{aligned} X(sh) = &\sum_{k=1}^{s} a_k \left(\sum_{j=1}^{m} y_j [(s-k)h] X^{(j)} \right) \\ &+ \sum_{k=1}^{s} h b_k A \left(\sum_{j=1}^{m} y_j [(s-k)h] X^{(j)} \right) \\ &+ \sum_{k=1}^{s} h b_k F [(s-k)h] \quad . \end{aligned} \tag{25}$$

Assume that the matrix A has m distinct eigenvalues. Then there is a matrix χ such that

$$\chi^{-1} A \chi = D$$

where

$$D = \begin{pmatrix} \lambda_1 & & 0 \\ & \lambda_2 & \\ & & \ddots \\ 0 & & & \lambda_m \end{pmatrix}$$

Consider the transformation $Y = \chi^{-1} X$. χ is known to be the matrix $(X^{(1)} \ldots X^{(m)})$. Hence $\chi^{-1} X^{(q)} = 1^{(q)}$,

where $1^{(1)} = \begin{pmatrix} 1 \\ 0 \\ \vdots \\ 0 \end{pmatrix}$, $1^{(2)} = \begin{pmatrix} 0 \\ 1 \\ 0 \\ \vdots \\ 0 \end{pmatrix}$, etc.

Also $\chi^{-1} A X^{(q)} = \lambda^{(q)}$

where $\lambda^{(1)} = \begin{pmatrix} \lambda_1 \\ 0 \\ \vdots \\ 0 \end{pmatrix}$, $\lambda^{(2)} = \begin{pmatrix} 0 \\ \lambda_1 \\ 0 \\ \vdots \\ 0 \end{pmatrix}$, etc.

Hence equation 25 can be transformed to

$$\begin{aligned} Y(sh) = \chi^{-1} X(sh) = & \sum_{k=1}^{s} a_k \left(\sum_{j=1}^{m} y_j \left[(s-k)h \right] 1^{(j)} \right) \\ & + \sum_{k=1}^{s} h\, b_k \left(\sum_{j=1}^{m} y_j \left[(s-k)h \right] \lambda^{(j)} \right) \\ & + \sum_{k=1}^{s} h\, b_k \, \bar{\Phi} \left[(s-k)h \right] \end{aligned} \qquad (26)$$

where $\Phi\left[(s-k)h\right] = \chi^{-1} F\left[(s-k)h\right]$.

Equation (26) may be separated into the components $y_j(sh)$

where $Y(sh) = \left(y_1(sh),\ y_2(sh),\ \ldots,\ y_m(sh)\right)^T$.

Iteration then produces that

$$y_j(nh) = \sum_{k=1}^{s} (a_k + h\,\lambda_j\,b_k)\, y_j\left[(n-k)h\right] + \sum_{k=1}^{s} h\,b_k\,\Phi\left[(n-k)h\right] . \tag{27}$$

where $\Phi\left[(n-k)h\right] = \left(\Phi_1\left[(n-k)h\right],\ \ldots,\ \Phi_m\left[(n-k)h\right]\right)^T$

$= \chi^{-1} F\left[(n-k)h\right]$; and $j = 1,\ \ldots,\ m$

Equation (27) can be written in the simpler form

$$y_j(nh) = \sum_{k=1}^{s} a_{jk}\, y_j\left[(n-k)h\right] + \Phi_{jn} \tag{28}$$

where $a_{jk} = a_k + h\,\lambda_j\,b_k$

and $\Phi_{jn} = \sum_{k=1}^{s} h\,b_k\,\Phi_j\left[(n-k)h\right]$.

The solution of equation (28) in closed-form is

$$y_j(nh) = \sum_{k=1}^{s} c_{jk}\, r_{jk}^{\,n} + \sum_{k=1}^{s} \sum_{q=s}^{n} \frac{\Phi_{jq}\, r_{jk}^{\,n-q}}{\prod_{i \neq k} \left(1 - \frac{r_{ji}}{r_{jk}}\right)} \tag{29}$$

Hence the final solution to equation (23) is

$$X(nh) = \chi Y(nh) = \chi\left(y_1(nh),\ \ldots,\ y_m(nh)\right)^T \tag{30}$$

where the $y_j(nh)$ are determined by (29).

For additional details refer to Section II-1 of Progress Report No. 2., M.S.R. No. 61-07.

For the results of applying this method to a 3 by 3 system of equations refer to Appendix B of M.S.R. No. 61-07.

2.3 Introductory Comments on the Meaning of Stability Charts for Primitively Nonlinear Differential Equations

A study was initiated to determine the extent to which the mathematical work done in the past with linear differential equations applies to nonlinear differential equations. Work was performed using a primitively nonlinear equation and a simple numerical method.

The nonlinear equation considered was

$$\dot{x} = \lambda x + \epsilon x^{p+1} \quad . \tag{31}$$

It is easily verified that the analytic solution of this equation is

$$x(t) = \frac{x_o\, e^{\lambda t}}{\left[1 + \frac{\epsilon}{\lambda}\, x_o^{\,p}(1 - e^{p\lambda t})\right]^{1/p}} \quad . \tag{32}$$

For sufficiently small ϵ, the solution can be approximated as

$$x(t) \approx x_o\, e^{\lambda t} \left[1 - \frac{\epsilon}{p\lambda}\, x_o^{\,p}(1 - e^{p\lambda t})\right] . \tag{33}$$

The O_{11} quadrature formula was used for the numerical solution. The n^{th} value of x as given by O_{11} was

$$\begin{aligned} x_n &= x_{n-1} + h\lambda x_{n-1} + h\epsilon x_{n-1}^{p+1} \\ &= r x_{n-1} + E x_{n-1}^{p+1} \quad , \end{aligned} \tag{34}$$

where $r \triangleq 1+h\lambda \triangleq e^{\mu h}$ and $E \triangleq h\epsilon$. Note that the definitions of r and μ are identically those that appear in the derivation of the stability charts.

The next step was to obtain an expression for the solution at any point in terms of x_o. Based on equation (34) and the assumption that $E^2 \ll 1$, it was proved by induction that

$$x_n \approx r^{n-1} \left[r\, x_o + E\, x_o^{p+1} \left(\frac{1 - r^{np}}{1 - r^p} \right) \right]. \qquad (35)$$

For $E << 1$ and with $e^{\mu h}$ substituted for r, equation (35) can be written as

$$x(nh) \approx x_o\, e^{\mu nh} \left(1 + \frac{h\epsilon}{e^{\mu h}}\; x_o^p\; \frac{1 - e^{p\mu nh}}{1 - e^{p\mu h}} \right). \qquad (36)$$

For sufficiently small μh equation (36) is approximated by

$$x(nh) \approx x_o\, e^{\mu nh} \left[1 - \frac{\epsilon}{p\mu}\; x_o^p \left(1 - e^{p\mu nh} \right) \right]. \qquad (37)$$

Comparison of equation (37) with equation (33) shows that, with the restrictions stated above, the solution of a first-order slightly nonlinear differential equation obtained by the numerical method O_{11} bears an interesting similarity to the analytical solution of the equation. The two solutions differ only in that (33) is in terms of λ and (37) is in terms of μ.

It was conjectured that stability charts can be used to indicate the conditions for accuracy of the numerical solution by noting the regions where there is close agreement between μh and λh. The results of two computations using equations (33) and (37) are given to illustrate the accuracy of O_{11} as applied to a nonlinear differential equation.

Example 1.

$x_o = 1,\ \lambda = -1,\ \epsilon = 0.01,\ p = 0.1,\ t = 1,\ h = 0.1$

From equation (33) $x = 0.370$
From equation (37) $x = 0.352$

Example 2.

$x_o = 1,\ \lambda = -1,\ \epsilon = 0.01,\ p = 2,\ t = 1,\ h = 0.1$

From equation (33) $x = 0.370$
From equation (37) $x = 0.350$
By O_{11} (10 iterations) $x = 0.350$

This work was, of course, concerned with a simple equation and a simple numerical method. However, the indication is that more complex situations should be investigated in the hope that similarly gratifying results may be obtained.

For additional details refer to Section II-2 of Progress Report No. 2, M.S.R. No. 61-07.

2.4 Comments on a Runge-Kutta Formula

Motivated by the findings relating to O_{33} mod Gurk computations presented in MIT Final Demonstration Report 45-2, January, 1959, "An Exporimental Analog-Digital Flight Simulator," a preliminary study was conducted relative to the significance of the stability-chart criteria as applied to the accuracy of solutions of nonlinear differential equations. The following Runge-Kutta type formula was first considered:

$$x_1 = x_o + x_1^{i} + x_1^{ii} + x_1^{iii} + x_1^{iv} \tag{38}$$

where $x_1^{i} = h\dot{x}_o$

$$x_1^{ii} = \frac{1}{2} h \dot{x}_1^{i}$$

$$x_1^{iii} = \frac{1}{3} h \dot{x}_1^{ii}$$

$$x_1^{iv} = \frac{1}{4} h \dot{x}_1^{iii}$$

This formula was used to obtain the solution for the linear equation

$$\dot{x} = \lambda x. \tag{39}$$

The true solution of this equation is known to be

$$x(t) = x_o e^{\lambda t} = x_o e^{\lambda h n} = x_o e^{zn} \tag{40}$$

where $z \triangleq \lambda h$, $h = \Delta t$, and $t = hn$.

The solution using formula (38) is obtained as follows:

$$x_1^{i} = h\dot{x}_o = h\lambda x_o = zx_o$$

$$x_1^{ii} = \frac{1}{2} h\dot{x}_1^{i} = \frac{1}{2} h\lambda x_1^{i} = \frac{1}{2!} z^2 x_o$$

$$x_1^{iii} = \frac{1}{3} h\dot{x}_1^{ii} = \frac{1}{3} h\lambda x_1^{ii} = \frac{1}{3!} z^3 x_o$$

$$x_1^{iv} = \frac{1}{4} h\dot{x}_1^{iii} = \frac{1}{4} h\lambda x_1^{iii} = \frac{1}{4!} z^4 x_o.$$

$$x_1 = x_0 + sx_0 + \frac{1}{2!} s^2 x_0 + \frac{1}{3!} s^3 x_0 + \frac{1}{4!} s^4 x_0$$

$$= x_0 \left(1 + s + \frac{s^2}{2!} + \frac{s^3}{3!} + \frac{s^4}{4!}\right) \qquad (41)$$

$$\approx x_0 e^s = x_0 e^{\lambda h} .$$

Let $\lambda = -1$. Then (39) becomes

$$\dot{x} = -x,$$

and with $x_0 = 1$ and $h = 1$ (41) gives

$$x_1 = 1 \left(1 - 1 + \frac{1}{2!} - \frac{1}{3!} + \frac{1}{4!}\right)$$

$$= 0.3750.$$

The true solution given by (40) is

$$x(1) = e^{-1}$$

$$= 0.3679.$$

The percent error is 1.9%.

Next the nonlinear equation,

$$\dot{x} = -x + \frac{1}{2} x^2, \qquad (42)$$

was considered.

The true solution for (42) with $x_0 = 1$ is

$$x(t) = \frac{2}{1+e^t} . \qquad (43)$$

From the Taylor series expansion for $f(x,t)$, it follows that for the first interval

$$\lambda = f'(x_0,t_0) = \frac{\partial}{\partial x} f(x,t) \Big|_{t=t_0} \qquad (44)$$

Hence, for equation (42) with $x_0 = 1$ and $h = 1$

$\lambda = -1 + x_0 = 0$ initially

$\lambda \approx -0.5$ at the end of the interval

Using the Runge-Kutta type formula (38) to obtain the solution for (42)

$$x_1^{i} = h\dot{x}_o = -1 + \frac{1}{2}(1)^2 = -0.5000$$

$$x_1^{ii} = \frac{1}{2} h\dot{x}_1^{i} = \frac{1}{2}\left[.5000 + \frac{1}{2}(-.5000)^2\right] = 0.3125$$

$$x_1^{iii} = \frac{1}{3} h\dot{x}_1^{ii} = \frac{1}{3}\left[-.3125 + \frac{1}{2}(.3125)^2\right] = -0.0879$$

$$x_1^{iv} = \frac{1}{4} h\dot{x}_1^{iii} = \frac{1}{4}\left[.0879 + \frac{1}{2}(-.0879)^2\right] = 0.0229$$

$$x_1 = 1 - .5000 + .3125 - .0879 + .0229$$

$$= 0.7475$$

The true solution for t=1 as given by (43) is

$$x(1) = 0.5379.$$

The percent error is 39%.

Since $\lambda h=0$ initially, a more accurate solution might have been expected based on the Runge-Kutta stability chart. Apparently the large change in λh over the interval, i.e., the strong nonlinearity, causes serious error in this Runge-Kutta type formula.

The classical Runge-Kutta formula for solving an equation of the form $\dot{x} = f(x)$ is

$$x_1 = x_o + \Delta x \tag{45}$$

where $$\Delta x = \frac{1}{6}(k_1 + 2k_2 + 2k_3 + k_4)$$

with

$$k_1 = f(x_o)h$$

$$k_2 = f\left(x_o + \frac{k_1}{2}\right) h$$

$$k_3 = f\left(x_o + \frac{k_2}{2}\right) h$$

$$k_4 = f(x_o + k_3)\, h.$$

For equation (42) this gave

$k_1 = -0.5000$

$k_2 = -0.46875$

$k_3 = -0.472534$

$k_4 = -0.388356$

$\Delta x = -0.461821$

$x_1 = 1 - 0.4618$

$= 0.5382.$

The percent error is 0.06%.

The classical Runge-Kutta gives a much better result than does formula (38) when applied to equation (42) even though the two formulas have the same stability chart. The reason for the difference is not as yet fully understood.

For comparison the O_{33} mod Gurk quadrature formula was used to obtain a solution for (42) over the same interval. It gave

$x_1 = 0.4667$

when the proper past values were used. The percent error is 13%, which is higher than what might have been expected based on the O_{33} mod Gurk stability chart.

The results of this preliminary study point out the need for determining the significance of the stability-chart criteria when applied to the accuracy of the solution of nonlinear differential equations.

3. Experimental Work

3.1 Theory and Method

The quadrature methods used in UDOFTT were studied and evaluated by comparing results obtained from programmed autopilot maneuvers using various quadrature intervals. Several flight maneuvers were selected for study and for demonstration of the properties of digital flight simulation. On the one hand, maneuvers were selected which would demonstrate the advantages of digital simulation; and on the other hand, maneuvers were sought which would display the limitations of digital simulation.

Each maneuver was started from one of four in-air positions. Each position was defined by a set of initial conditions, i.e., the information needed to initialize flight. Autopilot programs were generated to provide repeatable control positions as a function of time. Each maneuver was flown with several different quadrature intervals using the O_{33} mod Gurk and the $O_{30}C_{31}$ mod Gurk quadrature formulas. The quadrature intervals used were 10 msec., 20 msec., 50 msec., 70 msec., and 100 msec. (It should be noted that the duration of the computation cycle was held constant while the quadrature intervals were changed. While this increased the computation time with the shorter quadrature intervals, it had no effect on the results.)

In order to use the above quadrature intervals, certain quantities which depend upon the quadrature interval had to be changed for each interval. These quantities included the O_{33} mod Gurk coefficients d, e, and f, and the $O_{30}C_{31}$ mod Gurk coefficient d_c. (A list of the constants with their values for the various quadrature intervals can be found in Appendix E presented in Progress Report No. 3, MSR No. 61-13 and this report.)

While the maneuver was being run, analog-output recordings were made of the following quantities: u, v, w, p, q_1, l_3, n_3, and H (an exception to this occurred during the short-period-oscillation-in-yaw maneuver where r replaced H and ψ replaced w). During the flight these quantities were monitored, and at its end the minimum and the maximum values of the quantities were printed out to provide a scale for the tracings. In addition, values for the quantities to be studied were periodically stored in the number memory and then printed out in a block at the end of the maneuver. The frequency with which the values were stored depended upon the maneuver.

3.2 Discussion of Work and Approach

3.2.1 Maneuvers Studied

The maneuvers that were studied fall into three groups as follows:

Group 1: These maneuvers involve essentially steady-state flight.

a. Steady level flight

b. Steady rate of climb.

Group 2: These maneuvers involve two-dimensional transient motion.

a. Phugoid oscillation.

b. Short period oscillations in yaw introduced by applying a pulse to the rudder.

c. Short period oscillations in pitch introduced by applying a pulse to the elevators.

d. Snap roll.

e. Stall

Group 3: These maneuvers involve three-dimensional motion.

a. Immelman turn.

b. Split S.

The maneuvers were started from "in-flight" initial conditions. The four initial conditions required were classified by the altitudes and the indicated air speeds as follows:

Initial Condition I	30,000 feet 365 knots
Initial Condition II	30,000 feet 200 knots
Initial Condition III	20,000 feet 150 knots
Initial Condition IV	10,000 feet 500 knots

The maneuvers classified by initial conditions are

I. 1. Steady level flight.

2. Short period oscillations in yaw.

3. Short period oscillations in pitch

4. Snap Roll.

5. Phugoid oscillation.

II. 1. Split S

III. 1. Stall.

IV. 1. Steady rate of climb.

2. Immelman turn.

3.2.2 Obtaining Initial Conditions for the Maneuvers

In order to evaluate the numerical methods used, it was necessary to start each maneuver from identical conditions for each flight with the different quadrature intervals so that they could be realistically compared. If the initial conditions had not been identical for each execution of a maneuver, there could be little useful comparison of the results.

A set of initial conditions is the information needed to continue computations from a given point in time. Each of the four sets of initial conditions was obtained as follows:

A pilot took off in the trainer. The discrete-input switches, which could not be set while the trainer was on the ground, were set to their pre-determined positions.* As soon as all the discrete-input switches were properly set the trainer was flown to what seemed, from information observed on the instruments, to be a steady level flight at the specified altitude and indicated air speed. When this condition was attained, the controls were released. Because there are no control forces in the F-100A trainer, releasing the controls was equivalent to placing constant control positions in the memory and using them to fly the trainer. The flight was continued with these constant control positions for about one minute. During this test flight, the instruments on the instructor's console were observed to determine whether a steady level flight had been attained. If it had not, the pilot took over control and tried to bring the trainer to a better position; and the above test was repeated. If steady level flight had been attained, the FREEZE switch was turned on and a "print-out" program was read into the instruction memory. This print-out program consisted of CLA instructions calling for the contents of the number-memory

*Discrete-input switches were set so that the flights would be flown with a "clean" airplane with low weight.
Refer to Appendix C in Progress Report No. 3, MSR. No. 61-13, for a list of the proper switch positions.

locations that are of interest. The computer was then put in CONT PRINT, and the quantities were printed out. These quantities were then studied more closely, and the quantities considered necessary to initialize a flight from an in-air position were punched on input cards for UDOFTT. The chosen quantities were then tested by using them to initialize a steady level flight with the constant control positions that were obtained from the print-out.

3.2.3 Obtaining Control Positions for Maneuvers

The control positions for the autopilot program for the various maneuvers were obtained in the following way:

A pilot flew the trainer to a steady level flight corresponding to the proper initial condition. When the steady-level-flight condition had been attained, FREEZE was turned on and the proper set of initial conditions was read into the number memory. The controls were then set to the proper positions to agree with the values in the initial conditions. The analog-output recorder was started, FREEZE was turned off, and the maneuver was executed. While the maneuver was being executed, the control-position inputs were monitored by the program and then multiplexed out to the analog-output recorder. The analog-output recorder produced tracings of the control positions, and the min.-max. monitor program provided the minimum and maximum values of the recorded functions from which scales were determined. The control positions were then approximated by straight lines and thus made available for use in the autopilot program. (A sample approximation is shown in Appendix D in Progress Report No. 3, MSR No. 61-13)

3.2.4 Test Program

3.2.4.1 Introduction

The test program was written to fly the trainer from an "in air" condition through a predetermined maneuver at any one of several quadrature intervals using one of two quadrature formulas while monitoring several of the variables in the flight equations. In order to do this, the autopilot program provides the control positions as a function of time and provides analog and digital outputs for the monitored variables. It would have been desirable to have one complete program to perform these tasks for each maneuver at each quadrature interval. However, consideration of the large number of cards which would be needed for these programs prompted the division of the programs into four groups which could be used in many combinations to form the large number of programs needed.

The four parts of the autopilot program were called:

1. Initial Conditions
2. Basic Program
3. Maneuver Programs
4. Corrections for Quadrature Intervals

The autopilot program used in the investigation is listed, in Appendix G which starts in Progress Report No. 3,MSR No. 61-13, and is continued in Interim Technical Report MSR 61-19. This appendix contains the complete listing of the Basic Program, the Maneuver Program (except for the scaling values) for each of the nine maneuvers, and two examples of the Corrections-for-Quadrature-Interval programs. These programs are listed in preliminary and in final code. The preliminary code is given in terms of the mnemonic code for the instructions and the symbol for the number-memory address. A discussion of the instructions and their mnemonic codes can be found in PROGRAMMING MANUAL FOR THE UDOFIT COMPUTER, August 1959. Appendix F, which was started in Progress Report No. 3, MSR No. 61-13, and is continued in Interim Technical Report, MSR 61-19, contains a list of the symbols which have been introduced in these programs and their definitions are given in terms of the variable represented by the symbol; however the symbol is also used to designate the number-memory location where this variable is stored. Other symbols used are taken from UDOFTT SIMULATION PROGRAM, FINAL REPORT, MAY 1960 VOLUMES I and II.

The autopilot program is entered from the permute portion of the F-100A program, and the F-100A program is re-entered via the usual permute exit which has been placed at the end of the autopilot program. It was necessary to eliminate some of the F-100A program to provide instruction-memory locations for the autopilot program. Because the maneuvers are flown in the air with the No-Fuel-Deplation Look ON, the Land- Air- Crash Decisions and the Mass of Fuel portions of the F-100A programs were removed with no resulting effect on the computations.

3.2.4.2 Initial Conditions

Group 1 of the autopilot program, Initial Conditions, contains four sets of flight variables which are used to initialize the simulator to the flight condition from which the maneuver is to start. Each set contains those variables needed to determine a given in-flight condition. A discussion of these conditions and the methods for obtaining them can be found in Section 3.2.1 and 3.2.2.

3.2.4.3 Basic Program

Group 2 of the autopilot program, the Basic Program, contains those parts of the autopilot program which are common to all of the maneuvers to be performed. Thus group 2 contains one program which is used for all maneuvers. This program provides the analog outputs, the digital outputs, and the timer, as well as various routing and control instructions.

The autopilot program provides eight analog outputs for the analog recorder. During each computation cycle eight variables were scaled and multiplexed out. The scaling was performed to obtain a magnification of the variation of the variables. To obtain the proper

scaling a trial maneuver was executed, and the digital outputs from this maneuver provided the maximum and the minimum values that the variables attained during the maneuver. The maximum and the minimum values for each variable were then averaged to find the midpoint of the variation for that variable. The difference between the maximum and the minimum provided the magnitude of the variation which was used to determine the amount of shifting needed to bring this variation to the most significant portion of the output. The midpoints and shifts were then added to the Maneuver Program so that in all subsequent flights the midpoint for each variable was subtracted from the variable and the difference was then shifted left to a more significant position and multiplexed out.

The digital outputs, which were provided by the autopilot program, were: 1) a list of maximum values attained by each of eight variables, 2) the times associated with these maximums, 3) the minimum values attained, 4) the times associated with the minimums, and 5) a list of values of these variables. The maximums, the minimums, and their associated times were provided by the Maximum-Minimum recorder in the Basic Program. During each computation cycle the Maximum-Minimum recorder compared the present value of each variable with the number stored as the maximum value for that variable, and the larger of the two was stored as the new maximum. If the present value was as large as, or larger than, the past maximum, the present time was stored as the time that the maximum occurred, replacing the time previously recorded. Similar comparisons were made to determine the minimum values and their associated times.

The list of values was obtained by periodically storing the values of the variables in a block of memory. An index and the Tally Register were used to increase the storage addresses in forming the list. A print-out program was provided to enable the removal of this list and the lists from the Maximum-Minimum recorder.

A timer was needed in the autopilot program because the control positions were obtained as functions of time. The timer used 10 msec. (scaled B14) as the unit of time (i.e., 1 in the 14th binary position from the left was equal to 10 msec.) for all maneuvers except the Phugoid, where 20 msec. was used. During each computation cycle the timer added the quadrature interval being used to the time for the previous cycle and stored the result as the time for the present cycle. The end of the desired flight was determined by comparing the time calculated in this manner with a predetermined number. When the flight was over the autopilot program set the crash flag so that the trainer entered the FREEZE mode of computation.

The Basic Program also contained clear-add orders which replaced the multiplex-in orders for the control positions in the F-100A program. The clear-add orders called for the control positions from memory locations rather than from the cockpit controls; this enabled the autopilot program to provide the control positions necessary to perform a maneuver.

3.2.4.4 Maneuver Programs

Group 3 of the autopilot program, the Maneuver Programs, contains a program for each of the nine maneuvers to be performed. For a list of these maneuvers refer to Section 3.2.1. Each of the programs contains a list of the breakpoints, the slopes, and the intercepts for the control functions used to give that maneuver. The method used to obtain these functions is described in Section 3.2.3. The control positions are calculated in the Function Generator with time as the independent variable. They are then scaled and stored for later use by the F-100A program. As a result of the scaling used the control positions were stored with the same precision, 10 bits, as if they were provided via the analog-to-digital converters used in the trainer.

The Maneuver Programs also contain the list of midpoints and shift-left orders for the analog-output scaling. Although these orders are contained in the Basic Program, their magnitudes were set according to the maneuver being performed. They were, therefore, stored with each maneuver.

3.2.4.5 Corrections for Quadrature Intervals

Group 4 of the autopilot program, Corrections for Quadrature Intervals, contains a program for each maneuver at each quadrature interval used, or fifty-four programs in all. Each program is a small group of numbers and instructions which had to be changed when the quadrature interval was changed. These include constants which involve the quadrature interval such as the weighting coefficients in the integration formula, the time increment for the timer, and shift orders for scaling made necessary by changes in these constants. For a list of the quadrature intervals used and a discussion of the constants which depend on them refer to Section 3.1.

3.2.4.6 O_{30} C_{31} Flight Program

The test autopilot program described above was based on and used with the F-100A simulation program which used the O_{33} mod Gurk quadrature formula. The additional program used during the study was a modification for the F-100A simulation program. This modification, when used in conjunction with the F-100A program, provided a simulation program using the $O_{33}C_{31}$ mod Gurk quadrature formula.

The classical $O_{30}C_{31}$ integration formula is formed by the cyclic combination of the classical O_{30} prediction formula and the classical C_{31} closure formula. In this manner each new value of the variable is estimated by the O_{30} formula, the corresponding derivative is computed, and the improved estimate of the variable is found using the C_{31} formula. The $O_{30}C_{31}$ mod Gurk quadrature formula, which was used for the study, is an improvement over the classical $O_{30}C_{31}$. The $O_{30}C_{31}$ mod Gurk formula is given in detail in Apendix E.

To obtain an F-100A simulation program that used the $O_{30}C_{31}$ mod Gurk quadrature formula, modifications were made on the existing simulation program which uses the O_{33} mod Gurk quadrature formula. The O_{33} integration routine was replaced by the $O_{30}C_{31}$ routines. The program was then passed through twice, the first time using O_{30} and the second time using C_{31}, for each $O_{30}C_{31}$ cycle. Since two sets of values for each variable were involved in each cycle, i.e., the first and second estimates, new variable storage locations and provisions for determining which value was needed were added. It was found that all the computations needed for the manuvers could be run in this way in the 50-msec. interval provided.

III. RESULTS

In this section the results obtained for the quantities of primary interest for each maneuver will be discussed. A list of these quantities and their symbols are given below:

- u: velocity vector along the airplane X-axis
- w: velocity vector along the airplane Z-axis
- p: roll rate
- q_1: pitch rate
- l_3: cosine of the angle between the X-axis of the airplane and the fixed Z-axis of the earth
- n_3: cosine of the angle between the Z-axis of the airplane and the fixed Z-axis of the earth
- ψ: sideslip angle
- H: altitude above ground

The maneuvers were flown using the O_{33} mod Gurk and $O_{30}C_{31}$ mod Gurk quadrature formulas with quadrature intervals of 10, 20, 50, 70, and 100 msec. The results thus obtained are presented in drawings (in Appendix H) where each drawing shows the results with one of the two quadrature formulas and the appropriate quadrature intervals. When there is little difference between the results obtained with the various quadrature intervals, some of the results are omitted from the drawing in order to preserve clarity.

The comparison of the results for a given maneuver with one of the quadrature formulas is based upon the magnitude of the difference between the results obtained with each quadrature interval. The percent error, or percent difference, figures are not given since they depend to a large degree upon the magnitude of the solution as well as upon the magnitude of the error. The frequency of the solution in those maneuvers which involve oscillations, such as the oscillations in pitch, is noted so that comparisons can be made between the various frequencies obtained and the frequencies predicted by the stability-chart criteria.

The comparisons between the results with the O_{33} quadrature formula and the $O_{30}C_{31}$ quadrature formula are also based on the magnitude of the differences in the results. For these comparisons the results for each of several selected maneuvers at the 50-msec. quadrature interval are given on the same Figure for direct comparison of the simulations. For some maneuvers the difference curve for these two simulations is also shown. The maneuvers for which such figures are given were selected to indicate the type and magnitude of the differences encountered.

1. Steady Flight

For the Steady-Flight maneuver u was selected as the variable of primary interest; therefore evaluation of the data obtained was directed toward u. The results are displayed in Figures 1-2.

The steady flight maneuver was obtained by simulating flight for 50 seconds with constant control positions. Digital samplings were taken at one second intervals during the flight. The O_{33} formula was used with two quadrature intervals, 50 and 100 msec. The data from the 100-msec. run indicates inaccurate results; however the solution was marginally stable and the inaccuracies are not sufficient to rule it out as a possible simulation. The data from the 50-msec. run indicates a stable, acceptable flight. There were indications that underflow was effecting the results at 50 msec.; thus the smaller intervals were not used. The $O_{30}C_{31}$ formula was used with the five intervals, and there was very good agreement among the results obtained with all intervals. The maximum deviation between the results with 10 msec. and 100 msec. is less than 1 in the fourth octal place, and the results with the other intervals fall between these two. The effects of underflow on the results is quite apparent, particularly at h = 10 msec. where no variation is present. The difference between the results obtained with the two quadrature formulas is very small, except for those at 100 msec. where the $O_{30}C_{31}$ simulation gave considerably better results.

2. Short Period Oscillations in Yaw

For the Oscillations- in-Yaw maneuver Ψ was selected as the variable of primary interest; therefore evaluation of the data obtained was directed toward Ψ . It should be noted that Ψ itself is not obtained directly by O_{33} (or $O_{30}C_{31}$) computations; but it is obtained from the ratio kv/u, where k is a constant and u and v are obtained directly by O_{33} ($O_{30}C_{31}$) computations. The results are displayed in Figures 3-7.

The maneuver was performed by applying a triangular pulse to the centered rudder-control position at time t=5 seconds during a steady level flight at 30,000 feet and Mach 0.98. The flight duration was 50 seconds, but digital samplings were obtained only over the time interval t=4.2 to 14 seconds. Two types of pulses, one of moderate and the other of large amplitude, were used. Early studies indicated that the maximum amplitude of Ψ obtained with the moderate pulse was considerably less than that reported in the MIT report, Final Demonstration Report 45-2, January, 1959, "An Experimental Analog-Digital Flight Simulator." Since approximating the MIT condition was of interest, the Oscillations-in-Yaw maneuver using the large pulse was added to the test maneuvers.

The moderate pulse had a duration of 1 second and an amplitude of approximately 1/4 of the allowable deflection from the centered rudder-control position. It produced a damped oscillation in ψ with an average period of approximately 2.5 seconds and a damping factor of about 0.2, giving a μ of approximately $-0.2 \pm 2.5i$. The solutions with both quadrature formulas at all quadrature intervals were stable and similar. The principal variation among the results is a slight increase in the period with decreasing amplitude; this is most apparent with the 10-msec.-interval data. It was suspected that underflow and round off were responsible for the change in period for the simulations with h = 10 msec., so difference methods were used to approximate the effects of round off for the O_{33} simulation. Because $\psi = kv/u$ and u is essentially constant during this flight, the estimation was based on the integration of $\dot{v}$. The portion of the curve studied, i.e., in the vicinity of t = 11.8 sec., was selected because it is a part of the curve with a relatively large derivative and would provide a conservative estimate for the round-off error. It was found that for this portion of the flight approximately 9% of the contribution of the contribution of the derivative to the integral was lost because of round off. A much higher percentage was lost near the top of the curves where the derivatives were smaller. The presence of underflow is clearly shown by the flattening of the final peak of the O_{33} simulation with h = 10 msec. The absence of change in period for the maneuver with the larger pulse also tends to confirm that the problem is related to underflow.

The large pulse had a duration of 2 seconds and an amplitude which was approximately equal to the allowable deflection from the centered rudder-control position. It produced a damped oscillation in ψ with an average period of approximately 2.4 seconds and a damping factor of about 0.26, giving a μ of about $-0.26 \pm 2.6i$. The solutions with both quadrature formulas at all quadrature intervals were stable and similar. There is such close agreement among the results with the different quadrature intervals that only the results with 10, 50, and 100 msec. are shown. This close agreement indicates that the simulation with the 50-msec. quadrature interval is fairly accurate and certainly meets the requirements for a satisfactory simulation.

For a given quadrature interval the O_{33} simulation and the $O_{30}\ C_{31}$ simulation were in close agreement for the oscillation in yaw excited by the moderate pulse and by the large pulse. The two simulations for ψ and their difference with the large pulse and the 50-msec. quadrature interval are shown in Figure 7. The difference curve indicates that the two formulas gave a slightly different phase response to the forcing function but that the simulations of the unforced portions of the oscillation differed only in the magnitude of the oscillations. The scales for Figure 7 show that the amplitude difference for the two simulations was about 5% with $O_{30}\ C_{31}$ having the larger magnitude.

As a whole the results obtained are in close agreement. Nowhere was difficulty of the nature reported by MIT encountered, and no explanation can be deduced for their difficulty. It is noted that for our maneuver the moderate rudder pulse produced a max $|\psi| \approx 1.4$ degrees and the large pulse produced a max $|\psi| \approx 12$ degrees, while that for the group solution in the MIT report is about 17 degrees. It is also noted that 17 degrees exceeds the limit of 15.9 degrees placed on $|\psi|$ in the F-100A program.

3. Short Period Oscillations in Pitch

For the Oscillations-in-Pitch maneuver q_1 was selected as the variable of primary interest; therefore evaluation of the data obtained was directed toward q_1 . The results are displayed in Figures 8-11

The maneuver was performed by applying a triangular pulse at time t = 5 seconds to that elevator position required to maintain steady-level flight at 30,000 feet and Mach 0.98. The pulse had a duration of 1 second and an amplitude of $(-.0200000)_8$* . The flight duration was 24 seconds, but digital samplings were obtained only over the time interval t = 4.2 to 9.1 seconds. The pulse produced an oscillation in q_1 with an average period of approximately 1 second, and a μ of approximately $\sim$0.7 + 6.5i

The results with the O_{33} formula are displayed in Figures 8-9. The results with 100 msec. show amplitudes which are much greater than those with the other quadrature intervals; however the envelope of the curve indicates that the oscillation is growing in a linear manner instead of the exponential growth encountered with an unstable solution. This, together with the fact that the minimum and maximum values occurred at approximately 11-12 seconds, indicates that although the solution is unsatisfactory because of the large oscillations, it is stable. The results with 10, 20, 50, and 70 msec. are displayed in Figure 8 and are similar to each other.

The results with the $O_{30}C_{31}$ formula using 10, 50, and 100 msec. are displayed in Figure 10. The three tracings are similar; however, as with O_{33}, there is a slight decrease in the period as the quadrature interval is increased. This variation is expected in part from stability-chart criteria, but it seems to be present to a greater degree here because of the nonlinearity of the F-100A flight equations. There is also more damping with the $O_{30}C_{31}$ than there is with the O_{33}. However, the most notable variation from the O_{33} results is that the 100-msec. results track the others quite well with the $O_{30}C_{31}$ while with the O_{33} the 100-msec. results are wild. This difference seems to indicate that the $O_{30}C_{31}$ formula gives better solutions to the slightly nonlinear equations when the larger values of μh are reached.

If λ for the oscillations in q_1 is determined by assuming close agreement between the true solution and the numerical solution, i.e., between λh and μh, with h = 50 msec., a λ of approximately -0.7 + 6.5i is obtained. The locus of λh for all h on the O_{33}-mod-Gurk stability chart

---

*Subscript 8 denotes octal representation of numbers.

is a straight line from the origin through the point $\lambda h = .1(-0.7 + 6.5i)$, i.e., for h = 100 msec. Figure 1 (in this section) shows the O_{33}-mod-Gurk stability chart (and the $O_{30}C_{31}$-mod-Gurk stability chart since it is the same as that for the O_{33}) with this line drawn and λh for h = 100 msec., 70 msec., and 50 msec. marked. It is quite apparent that the λh for h = 100 msec. is close enough to the branch contour for inaccurate results to be expected. For h = 70 msec., however, the λh is sufficiently far away from the branch contour for relatively good results to be expected. Note also that an increase in frequency with increase in h is indicated by the chart. Such a shift is present in the results obtained; however for the O_{33} simulation it is slightly greater than that indicated by the stability chart. The stability chart predicts a solution with a μh of approximately $-0.12 + .75i$, and Figure 9 indicates that the imaginary part of the μh for the actual simulation using O_{33} at h = 100 msec. was approximately 0.83. However, the agreement between the predicted and the actual frequency for the 70-msec. simulation is much closer, i.e., 0.47 vs. 0.474. This difference may be caused by the effects of nonlinearity becoming significant near the branch contour. The solution with the $O_{30}C_{31}$ is not wild for h = 100 msec., and the frequency obtained from the graph is quite close to that predicted by the stability chart. This indicates that the $O_{30}C_{31}$ simulation is not effected as much by the nonlinearities of the system as is the O_{33} simulation.

The results with 50 msec. for both of the quadrature formulas are displayed in Figure 11. The main variations are that there is more damping with the $O_{30}C_{31}$ and there is a slight increase in the period with the $O_{30}C_{31}$ toward the end.

O_{33} MOD GURK

$X_o = 1.1462X_{-1} - 0.2011X_{-2} + 0.0549X_{-3} + h(1.6416X_{-1} - 1.0080X_{-2} + 0.2751X_{-3})$

FIGURE 1

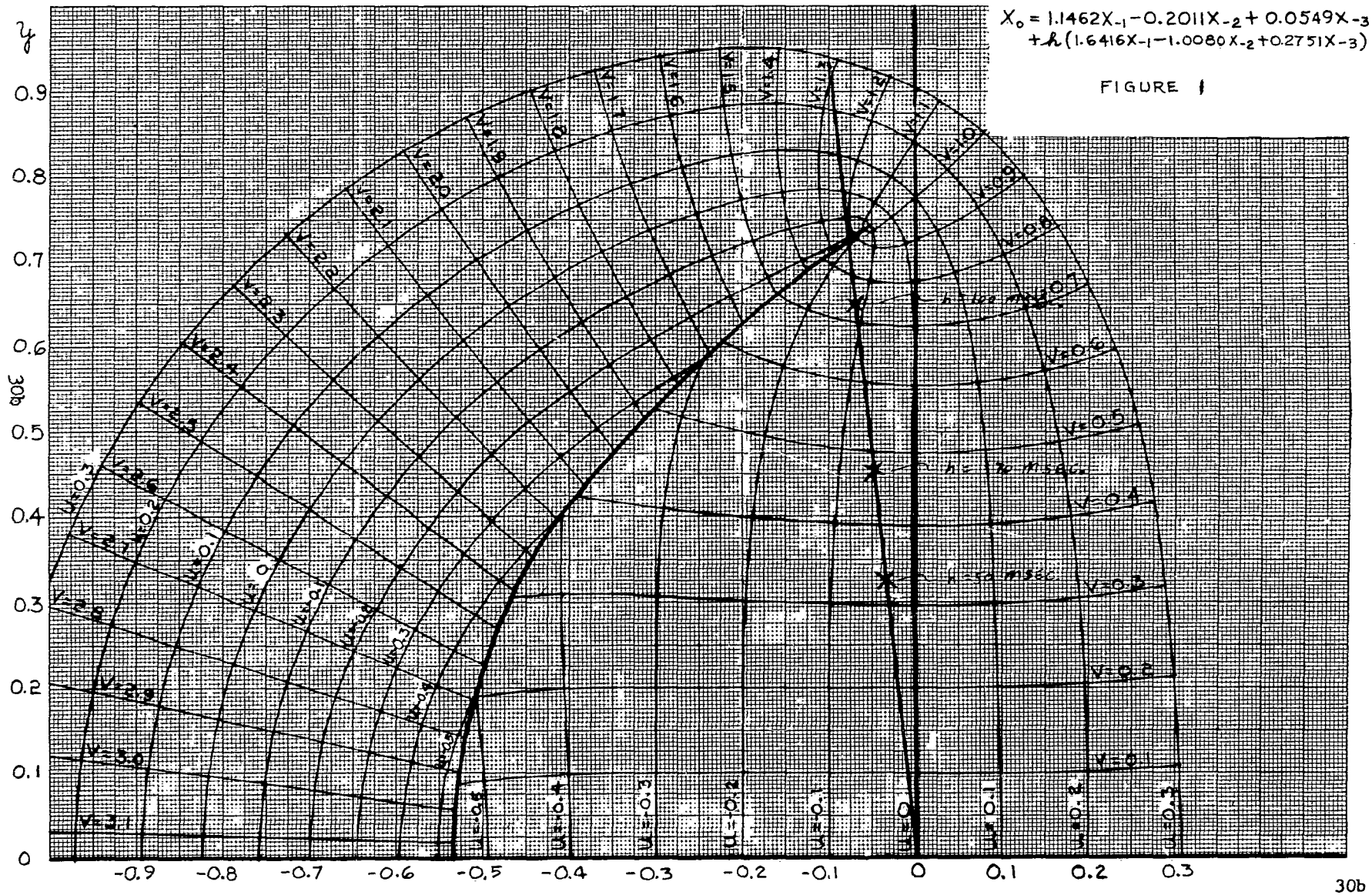

4. Snap Roll

For the Snap-Roll maneuver p and n_3 were selected as the variables of primary interest; therefore evaluation of the data obtained was directed toward p and n_3. The results are displayed in Figures 12-15.

It took about 5 seconds to perform the roll, after which the simulator was allowed to continue flight with the initial control positions for about 15 seconds. During the "steady flight" portion, the results for both p and n_3 with the various quadrature intervals and both quadrature formulas are so nearly equal that only the 50-msec. points are shown. During the roll portion of the maneuver, the results are also in close agreement -- with tracking a little better for n_3 with the $O_{30}C_{31}$. This is particularly so with the 100-msec. interval where it is again noted that the $O_{30}C_{31}$ seems to give slightly better results through a violent maneuver.

5. Phugoid Oscillation

The phugoid oscillation is one in which there is a large amplitude variation of air speed, pitch, and altitude, but during which the variation of angle of attack is slight. Because the periods are relatively long, the effects of inertia forces and damping forces are small. The phugoid can be thought of as a slow interchange of kinetic and potential energy about some equilibrium energy level, i.e., the phugoid can be considered as a long-period oscillation of the airplane's velocity as it attempts to re-establish the equilibrium condition from which it has been disturbed. The period of the phugoid is sufficiently long and the response of the airplane is such that negative damping of this oscillation has little bearing on the pilot's opinion of the flying qualities of the airplane. For this reason the military often has no requirements on the damping of the phugoid, and as a result many military airplanes will exhibit unstable phugoid characteristics within some range of their operating conditions.*

Included with the various maneuvers run during earlier phases of the project was one for phugoid oscillation. The phugoid maneuvers were performed by incrementing the integral of the rate of climb or the air speed a few seconds after the start of a steady flight using Initial Condition I and allowing the flight to continue for a few minutes. With small changes the trainer quickly resumed a steady flight (but not necessarily at the original altitude). This effect was apparently the result of underflow in the calculation of u and H. When the change was large enough to produce an oscillation, the trainer went into an unstable phugoid oscillation. Figure 16 indicates the types of results obtained. A stable phugoid was not

---

* The discussion in this paragraph is based on material in Perkins, C.D., and Hage, R.E., Airplane Performance Stability and Control. New York, New York: John Wiley and Sons, Inc., 1949 (30), Chapter 10.

obtained with this initial condition; however as was pointed out above the presence of an unstable phugoid for some flight conditions of a military airplane is not unusual, so it was assumed that these results were consistent with the characteristics of the airplane.

There are several changes in the airplane's parameters that can be made to increase the damping of a phugoid. These include increasing the mass, increasing the parasitic drag, or moving the center of gravity to a more favorable position. Therefore, as an endeavor to obtain a stable phugoid oscillation the phugoid tests were run from a new condition which incorporated the above changes in the airplane parameters. To insure high drag the condition was taken at a moderate altitude, 12,000 feet, with the tip tanks on and the speed brakes out. The addition of the tip tanks, which were full, and an increase in the fuel load provided an increase in the mass of the airplane and a shift in the center of gravity. The condition was obtained at full throttle with the afterburner off which produced a flight at Mach 0.5.

For this test the phugoid was initiated by decreasing u by 40 knots at time t = 14 seconds during a steady flight using the phugoid condition described above. The duration of the flight was 322 seconds during which several of the flight variables were sampled at seven-second intervals. Of primary interest were u and H, which were selected as the variables that would best exhibit the characteristics of the phugoid oscillation. The results, as shown in Figures 17A and 17B, indicate the presence of a stable phugoid oscillation superimposed on a gradual climb. The period of the oscillation was approximately one minute, and the damping was positive and appreciable.

The results for H indicate a large amount of disagreement between the simulations with various quadrature intervals. If the results for u are considered, however, we see that there are increasing amounts of round off leading to underflow, indicated by the flattening of the curves, as the quadrature intervals were reduced. It is also of interest that there is close time-agreement between the points where the H curves diverge and the points where the u curves become dominated by underflow. It was decided to run further tests to substantiate the statement that the poor agreement in the simulations was caused by the presence of underflow rather than the characteristics of the quadrature formula used.

In an attempt to reduce the effects of underflow modifications were made for the computation of the derivatives, $\dot{u}$, $\dot{w}$, $\dot{l}_3$, $\dot{m}_3$, $\dot{n}_3$, and the rate of climb and the integration of these quantities. These modifications involved the change of scale factors and the use of two words per variable in order to increase precision. The increase in precision for

these computations ranged from two to six bits with a six-bit increase for u and H.

The phugoid tests described above were then run with these changes in the program. The results obtained, Figures 17C and 17D show very good agreement for all quadrature intervals; and there is also close agreement between these results and the results with h = 100 msec. without the increased precision. This shows quite clearly that the difficulties encountered in obtaining phugoids and that the poor agreement among the simulations at various quadrature intervals were caused by the effects of round off and underflow. The good results obtained with increased precision and the phugoid maneuver demonstrates the ability of the O_{33} mod Gurk formula to handle low-frequency oscillations of the type encountered in the Phugoid-Oscillation maneuver.

The $O_{30}C_{31}$ mod Gurk formula was not used for the Phugoid-Oscillation maneuver since it had already been shown, for example in the Steady-Rate-of-Climb maneuver, that for nonviolent maneuvers the $O_{30}C_{31}$ mod Gurk and the O_{33} mod Gurk formulas give very similar results. Thus, the inclusion of an $O_{30}C_{31}$ test for this maneuver would not have provided any information that had not already been obtained. The main objective was to investigate the behavior of the O_{33} mod Gurk formula during the simulation of a maneuver whose dimensionless frequency falls near the origin and slightly to the left of the x = 0 line on the stability chart.

6. Split S

For the Split-S maneuver w and p were selected as the variables of primary interest; therefore evaluation of the data obtained was directed toward w and p. The results are displayed in Figures 18-22.

For w with O_{33} the results with 10, 20, and 50 msec. are in close agreement, and the 100-msec. results track these fairly well. With the $O_{30}C_{31}$ the agreement is somewhat better. With the 50-msec. quadrature interval the results with the two formulas are nearly equal, as can be seen in Figure 20. The larger variations at the two places, 6-7 seconds and 18-20 seconds, are probably caused by the discrete sampling of ringing functions with slight phase shifts.

For p all of the results with both formulas are in very close agreement.

7. Stall

For the Stall maneuver u and l_3 were selected as the variables of primary interest; therefore evaluation of the data obtained was directed toward u and l_3. The results are displayed in Figures 23-27.

The elevator function which was applied to the simulator to produce the stall was analogous to continuously pulling back on the "stick" in the trainer while flying steady flight at 20,000 feet and Mach 0.33. Stall occurred at approximately 8 seconds after starting the maneuver, but the flight was continued until t=50 seconds.

The results for u with the O_{33} formula and quadrature intervals of 10, 20, 50, 70, and 100 msec. are in close agreement for the first 18 seconds. After that the results begin to diverge. The $O_{30}C_{31}$ results are quite similar to those from the O_{33} except that the pattern of divergence is different. Most notable is the decrease in the value with the 10-msec. interval toward the end. As can be seen from Figure 25 the 50-msec. results for both formulas are in quite close agreement.

The results for l_3 with the O_{33} formula and all five quadrature intervals are in close agreement during the first 18 seconds, and then they begin to diverge. The $O_{30}C_{31}$ results are quite similar to the O_{33} ones except that the pattern of divergence is different. With the 50-msec. quadrature interval the results with both formulas are in quite close agreement.

Since the point of divergence of the results seems to correspond to the point of minimum velocity, it is felt that the variations are caused by the effects of small differences in the flights as the plane slides into a dive with the nose up.

8. Steady Rate of Climb

For the Steady-Rate-of-Climb maneuver l_3 and H were selected as the variables of primary interest; therefore evaluation of the data obtained was directed toward l_3 and H. The results are displayed in Figures 28-31.

The results for l_3 with quadrature intervals of 10, 20, and 50 msec. are displayed in the figures. The 70-msec. results track the 50-msec. ones so closely that they are not shown. The 100-msec. results oscillate and go positive, but the minimum and maximum values indicate that the results are stable. While there is close agreement among the displayed results, the results with a smaller interval slightly lead those with a larger one. There is close agreement between the results with the two formulas.

The results for H with quadrature intervals of 10, 20, 50, and 100-msec. are displayed in the figures; the 70-msec. results track the 50-msec. ones. There is close agreement among the various results except for those with 100-msec. With the 100-msec. quadrature interval the simulator went into a dive instead of climbing and crashed at about 20 seconds with the 0_{33} and at about 38 seconds with the $0_{30}C_{31}$. This difference in crash-times is the principal variation between the results with the two quadrature formulas. This again shows tendencies for better behavior with the $0_{30}C_{31}$.

The start of the erratic behavior of l_3 for the simulation with h = 100 msec. was coincident with the application of the stick motion to the simulation. As has been mentioned before, the oscillations in q_1 and l_3 encountered during the tests have frequencies such that the simulation with h = 100 msec. sends λh close to the branch contour on the 0_{33}-mod-Gurk stability chart. The effects of the subdominant roots are prominent in this region; and, even for a linear system, accurate solutions could not be expected. The erratic behavior of q_1 and l_3, in particular the swings of l_3 into positive regions, appears to lead to a change in the altitude of the airplane which results in a dive and crash since no corrective control action is taken.

As a whole the flights with all of the quadrature intervals are satisfactory except those with the 100-msec. interval.

9. Immelman Turn

For the Immelman-Turn maneuver p and q_1 were selected as the variables of primary interest; therefore, evaluation of the data obtained was directed toward p and q_1. The results are displayed in Figures 32-35.

The results for p with quadrature intervals of 10, 50, and 100 msec. are displayed in the figures. The 20- and 70-msec. results are not displayed, but they are in close agreement with those with 50 msec. The results with 100 msec. deviate from the others during the period 34 to 42 seconds. Note that p goes down to -0.3 at t = 34 seconds with the O_{33}. The deviation is less with the $O_{30}C_{31}$ formula, again showing its tendency to give slightly better results for a violent maneuver.

The results for q_1 with quadrature intervals of 10, 50, and 70 msec. are displayed in the figures. The results with 20 msec. are near those with 50 msec.; and the results with all four intervals are in close agreement -- the agreement being a little better with the $O_{30}C_{31}$ than with the O_{33}. The results with 100 msec. are too large to show. They oscillate wildly and reach both of the limit stoppers with O_{33} and the positive limit stopper with $O_{30}C_{31}$ during the early portion of the maneuver. The subsequent decrease in amplitude indicates stability, however.

IV. CONCLUSIONS AND RECOMMENDATIONS

In connection with the evaluation of the accuracy of the mathematical procedures used in digital airplane flight simulation, selected maneuvers were run on UDOFTT by means of an autopilot program. During the execution of a maneuver, digital print-outs and analog tracings were obtained for the variables of primary interest. The digital samplings were plotted with the same time scale so that direct comparison of the simulation with different quadrature intervals, or quadrature formulas, could be made.

The results obtained with some of the maneuvers indicate that the accuracy of the solutions obtained was being limited by underflow. It appears that some of the problem was caused by overly conservative scaling in the F-100A program. In particular it was noticed that underflow made it difficult to perform a phugoid oscillation and caused the steady-flight maneuver to have essentially no variation of flight conditions. This made it difficult to obtain information about the integration formulas themselves with these maneuvers, particularly at the smaller quadrature intervals.

As a whole the results of the tests are very good. The close agreement between the sets of results for each maneuver indicates accuracy in the solutions by both O_{33} and $O_{30}C_{31}$ mod Gurk quadrature formulas at quadrature intervals of 10 msec., 20 msec., 50 msec., and 70 msec. The stability and good accuracy of these results had been predicted by the stability-chart criterion. The poorer results at a quadrature interval of 100 msec. had also been predicted by the stability-chart criterion. However, the accuracy and stability obtained, particularly at h = 70 msec., was somewhat better than was expected.

The O_{33} mod Gurk quadrature formula gave stable results for all maneuvers at all quadrature intervals, with the simulations for all intervals except 100 msec. being acceptable and reasonably accurate. The results with h = 100 msec. gave large, but stable, oscillations in q_1 and l_3 for some maneuvers. These oscillations usually resulted in a poor simulation or a crash. Some of the wildness in the solutions with h = 100 msec. can be attributed to the effects of the subdominant roots of μh whose presence are indicated by the proximity of μh to the branch contour with this quadrature interval. The increase in frequency can also be attributed in part to the increase in μh; however it was noticed that the increase in frequency was greater than was indicated by the stability chart.

The $O_{30}C_{31}$ mod Gurk quadrature formula also gave good results for all quadrature intervals except, in some cases, h = 100 msec. The $O_{30}C_{31}$ and the O_{33} solutions were very close in most cases giving further indications of accuracy. However, the $O_{30}C_{31}$ formula seems to give somewhat better results with h = 100 msec., particularly during the violent

portions of a maneuver and for the high frequency pitch oscillations. This indicates that $O_{30}C_{31}$ gives somewhat better results for violent maneuvers.

It had been expected that the numerical solutions for strongly nonlinear systems would differ from the solutions predicted by the use of stability-chart criteria since stability charts were developed using linear theory. (Refer to Section II - 2. 4, particularly the discussion relating to solution by O_{33} mod Gurk.) Thus the good, and predictable, results obtained in the majority of maneuvers indicates that both of the formulas used are not affected to any great degree by nonlinearities of the type encountered in the F-100A equations. However, as was pointed out in the discussion of the Oscillations-in-Pitch maneuver, the frequency of the results with the $O_{30}C_{31}$ formula at h = 100 msec. was predictable by stability-chart criteria whereas the frequency of the results with the O_{33} formula at h = 100 msec. was larger than the predicted value. The results with the O_{33} formula at h = 100 msec. were also much larger in amplitude than had been expected. This indicates that O_{33} mod Gurk formula is affected by the nonlinearities in the F-100A simulation equations if a quadrature interval is used which brings the "dimensionless frequencies" near the branch contour. The $O_{30}C_{31}$ formula does not seem to be as greatly affected by the nonlinearities, for the results were still predictable.

The results obtained using the O_{33} and the $O_{30}C_{31}$ mod Gurk formulas seem to show that when formulas of this type are applied to slightly nonlinear systems, such as the F-100A flight equations, the stability-chart criteria hold. This includes the limiting condition that where the effects of the subdominant roots are expected to become significant the nonlinearities will also begin to affect the solution.

The experiments performed, particularly the Phugoid-Oscillation maneuver, show that the O_{33} mod Gurk quadrature formula gives good results for systems whose dimensionless frequencies lie near the origin of the stability chart. This was expected from stability-chart criteria, but it is of particular interest because of the difficulty often encountered when using analog devices for such systems. The experiments performed, particularly the Oscillations-in-Pitch maneuvers and the Oscillations-in-Yaw maneuvers, also demonstrated conclusively that both quadrature formulas used give good results for systems with frequencies as high as one cycle per second (i.e., periods as small as 1 second) with quadrature intervals as large as 50 msec. It was also shown conclusively that for systems with periods of two seconds, such as were present in the Oscillations-in-Yaw maneuver, good simulations will be obtained with quadrature intervals as large as 100 msec. This agrees with the behavior predicted by the stability charts.

The presence of underflow in some of the maneuvers (in particular the clear demonstration of its presence and effects in the phugoid maneuver) brings up the question of sufficient precision in UDOFTT. It should be noted that the existing F-100A simulation program is conservatively scaled. The scaling in the program is such that the truncation feature built into the machine as protection against overflow is not used. Until tests are performed with a less conservatively scaled program, it is difficult to say whether or not the appearance of underflow indicates a need for more precision in future simulators of this type. The problems involved in scaling the program to allow both violent maneuvers and accurate phugoids would indicate, however, that the use of floating-point arithmetic in future simulators would be an advantage.

V. BIBLIOGRAPHY

KENNEDY, O. W., Jr; MORONEY, R; MORSE, H., III. An Experimental Analog-Digital Flight Simulator, Final Demonstration Report 45-2. Cambridge, Massachusetts: Massachusetts Institute of Technology, 1959.

THE MOORE SCHOOL OF ELECTRICAL ENGINEERING. Progress Report No. 1, Investigation and Evaluation of UDOFTT Mathematical Procedures, Summary of Moore School Reports on Mathematical Studies for Real-Time Simulation. Philadelphia, Pa.: University of Pennsylvania, 1960 (MSR No. 60-23).

THE MOORE SCHOOL OF ELECTRICAL ENGINEERING. Progress Report No. 2, Investigation and Evaluation of UDOFTT Mathematical Procedures, Outline of Experimental Program. Philadelphia, Pa.: University of Pennsylvania, 1960 (MSR No. 61-07).

THE MOORE SCHOOL OF ELECTRICAL ENGINEERING. Progress Report No. 3, Investigation and Evaluation of UDOFTT Mathematical Procedures, Computer Program. Philadelphia, Pa.: University of Pennsylvania, 1960 (MSR No. 61-13)

THE MOORE SCHOOL OF ELECTRICAL ENGINEERING. Interim Technical Report, Investigation and Evaluation of UDOFTT Mathematical Procedures. Philadelphia, Pa.: University of Pennsylvania, 1961 (MSR No. 61-19).

PERKINS, C. D., and HAGE, R. E. Airplane Performance Stability and Control. New York, New York: John Wiley and Sons, Inc., 1949 (50), Chapter 10

SYLVANIA ELECTRONIC SYSTEMS. UDOFTT Programming Manual. Needham, Massachusetts: Sylvania Electric Products, Inc., 1959.

SYLVANIA ELECTRONIC SYSTEMS. UDOFT Simulation Program, Final Report, Volumes I and II. Needham, Massachusetts: Sylvania Electric Products, Inc., 1960.

VI. APPENDICES

E. Quadrature Formulas

The $O_{30}C_{31}$ mod Gurk quadrature formula is

$$\dot{x}_n = \sum_{j=1}^{3} a_{oj} \ddot{x}_{n-j} \qquad O_{30}$$

$$\ddot{x}_n = \sum_{j=1}^{3} a_{cj} \ddot{x}_{n-j} + h b_{c0} \dot{x}_n \qquad C_{31}$$

Where $\ddot{x}_{n-1}$, $\ddot{x}_{n-2}$, and $\ddot{x}_{n-3}$ are the three past ordinates; $\dot{x}_n$ is the present time derivative computed by using the value obtained with the O_{30} (x_n); h is the quadrature interval; and

$$a_{o1} = 1.8065805$$
$$a_{o2} = -1.1093273$$
$$a_{o3} = 0.3027468$$
$$a_{c1} = 1.1462084$$
$$a_{c2} = -0.2010870$$
$$a_{c3} = 0.0548787$$
$$b_{c0} = 0.9086705$$

For use in the computer program the $O_{30}C_{31}$ mod Gurk quadrature formula is written

$$\dot{x}_n = 2(a_o \ddot{x}_{n-1} + b_o \ddot{x}_{n-2} + c_o \ddot{x}_{n-3})$$

$$\ddot{x}_n = 2(a_c \ddot{x}_{n-1} + b_c \ddot{x}_{n-2} + c_c \ddot{x}_{n-3} + d_c \dot{x}_n)$$

where

$$a_o = \frac{1}{2} a_{o1}$$

$$b_o = \frac{1}{2} a_{o2}$$

$$c_o = \frac{1}{2} a_{o3}$$

$$a_c = \frac{1}{2} a_{c1}$$

$$b_c = \frac{1}{2} a_{c2}$$

$$c_c = \frac{1}{2} a_{c3}$$

$$d_c = \frac{1}{2} h b_{c0}$$

Thus, d_c is the only coefficient which has to be changed when the quadrature interval is changed. The values of d_c for the various quadrature intervals are given in Table 1.

Quad. Interval	d_c
10 msec.	0022470
20 msec.	0045160
50 msec.	0135030
70 msec.	0202210
100 msec.	0272060

Table 1

Values of d_c for the various quadrature intervals (values are in octal and the units point is at the extreme left).

H. Results

This appendix contains the tracings for the results discussed in Section III. The values for the quantities are plotted in octal scaled as obtained from the computer. The notation Bn ($n = 0, 1, 2, \ldots, 20$) indicates that the number shown must be multiplied by 2^n to obtain the true value.

NOTES:

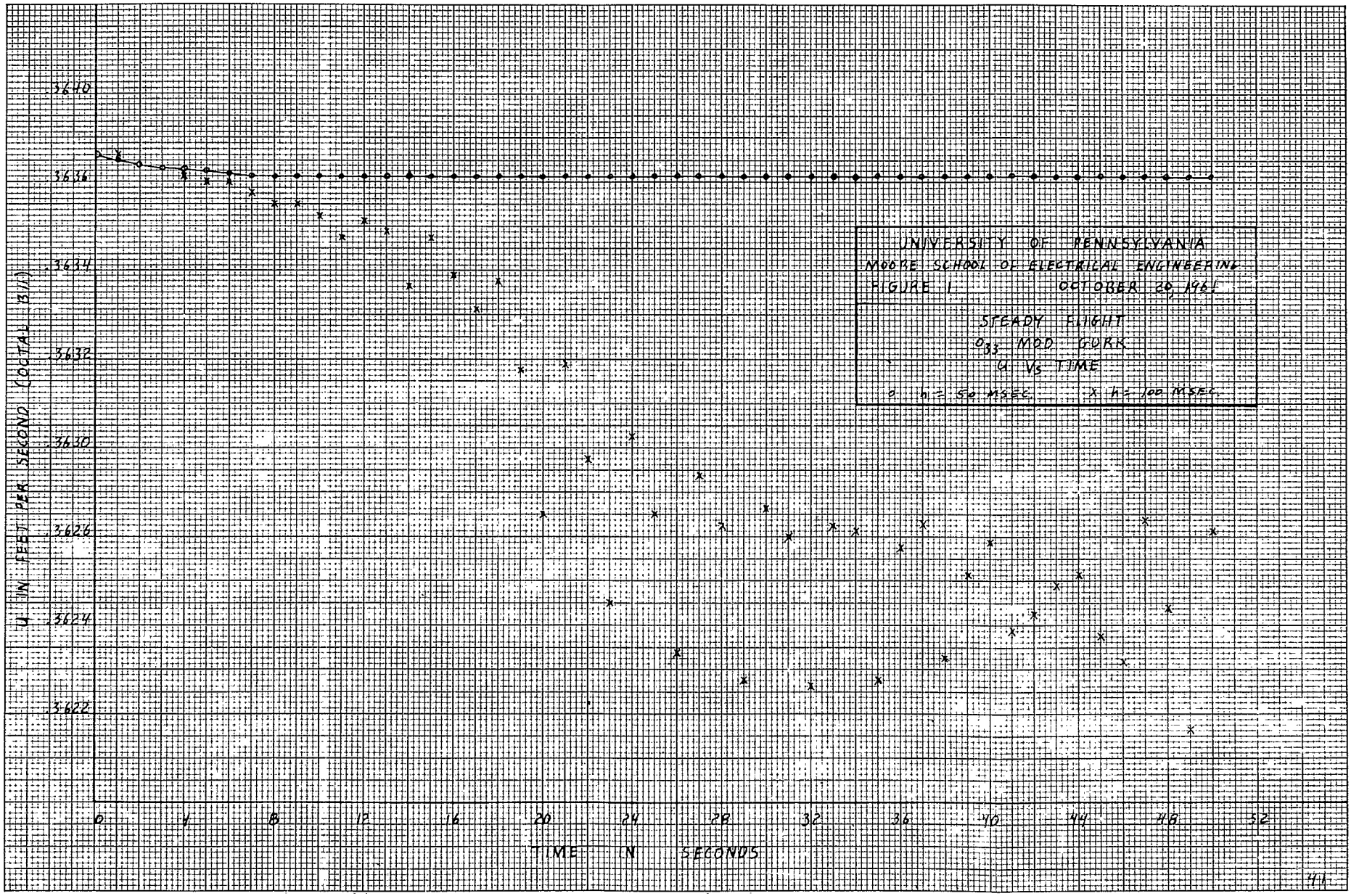
UNIVERSITY OF PENNSYLVANIA
MOORE SCHOOL OF ELECTRICAL ENGINEERING
FIGURE 1 OCTOBER 20, 1961
STEADY FLIGHT
σ_{33} MOD GUST
Q VS TIME
o h = 50 MSEC x h = 100 MSEC
Q IN FEET PER SECOND (OCTAL B/U)
3640
3636
3634
3632
3630
3626
3624
3622
0 4 8 12 16 20 24 28 32 36 40 44 48 52
TIME IN SECONDS
41

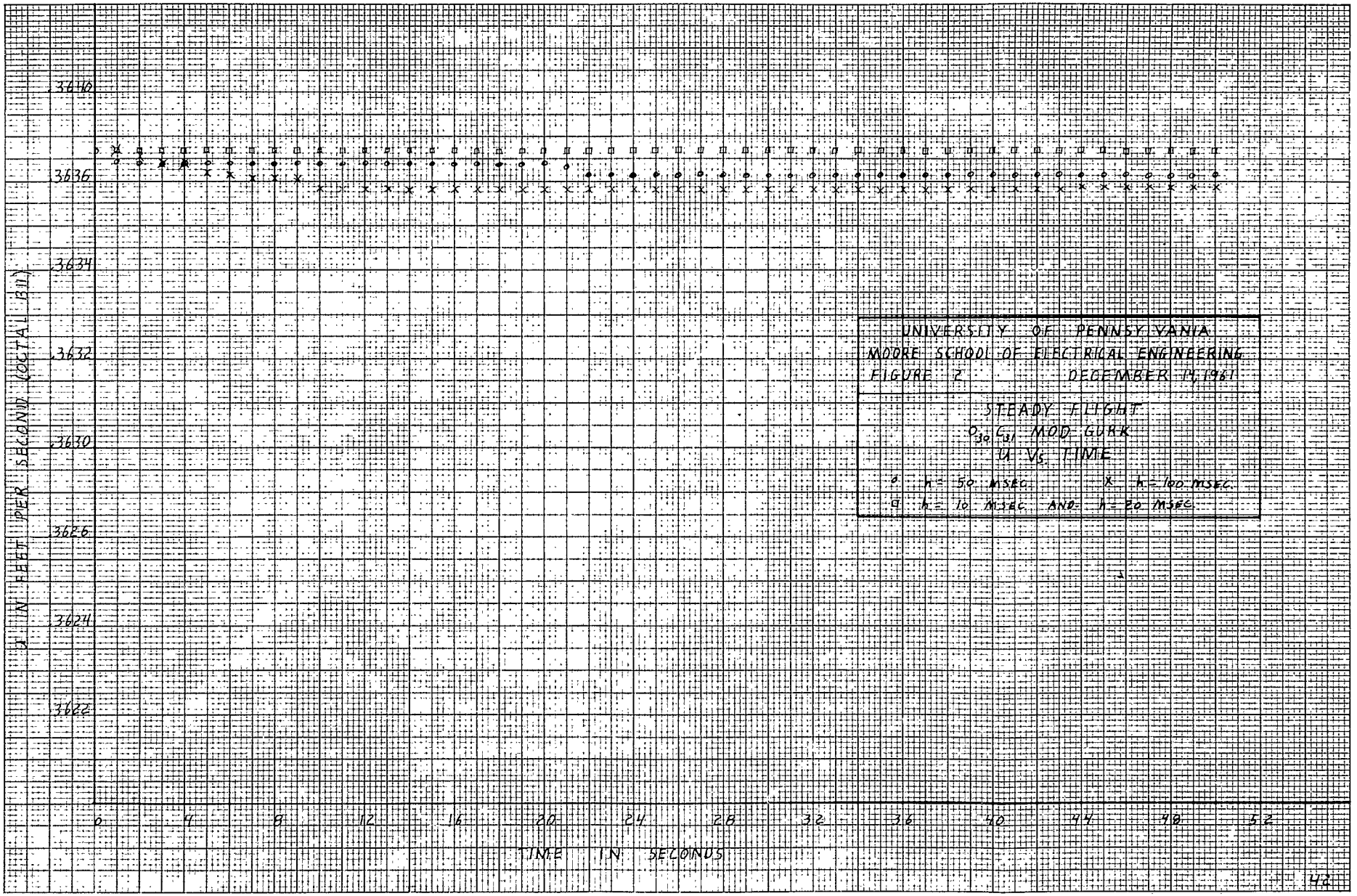
3640
3636
3634
3632
3630
3628
3624
3622
0
4
8
12
16
20
24
28
32
36
40
44
48
52
TIME IN SECONDS
U IN FEET PER SECOND (OCTAL 31)
UNIVERSITY OF PENNSYLVANIA
MOORE SCHOOL OF ELECTRICAL ENGINEERING
FIGURE 12 DECEMBER 14, 1961
STEADY FLIGHT
O_{30} G_{31} MOD GURK
U V_S TIME
o h = 50 MSEC. X h = 100 MSEC.
□ h = 10 MSEC. AND h = 20 MSEC.

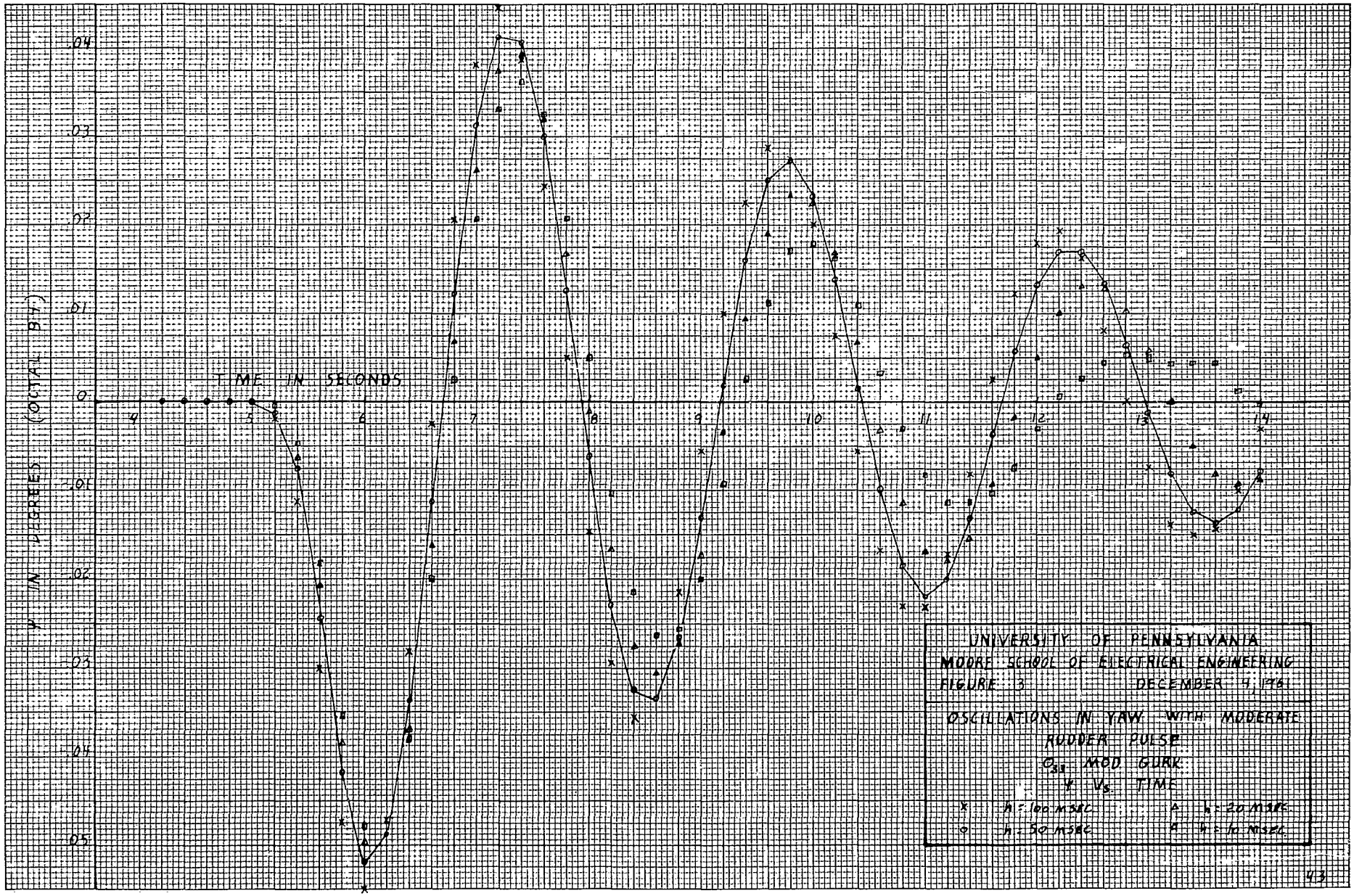
.04
.03
.02
.01
0
.01
.02
.03
.04
.05
ψ IN DEGREES (OCTAL BIT)
TIME IN SECONDS
4
5
6
7
8
9
10
11
12
13
14
UNIVERSITY OF PENNSYLVANIA
MOORE SCHOOL OF ELECTRICAL ENGINEERING
FIGURE 3 DECEMBER 4, 1961
OSCILLATIONS IN YAW WITH MODERATE RUDDER PULSE
C_{n_β} MOD GURK
ψ Vs. TIME
× h = 100 MSEC
○ h = 50 MSEC
△ h = 20 MSEC
□ h = 10 MSEC

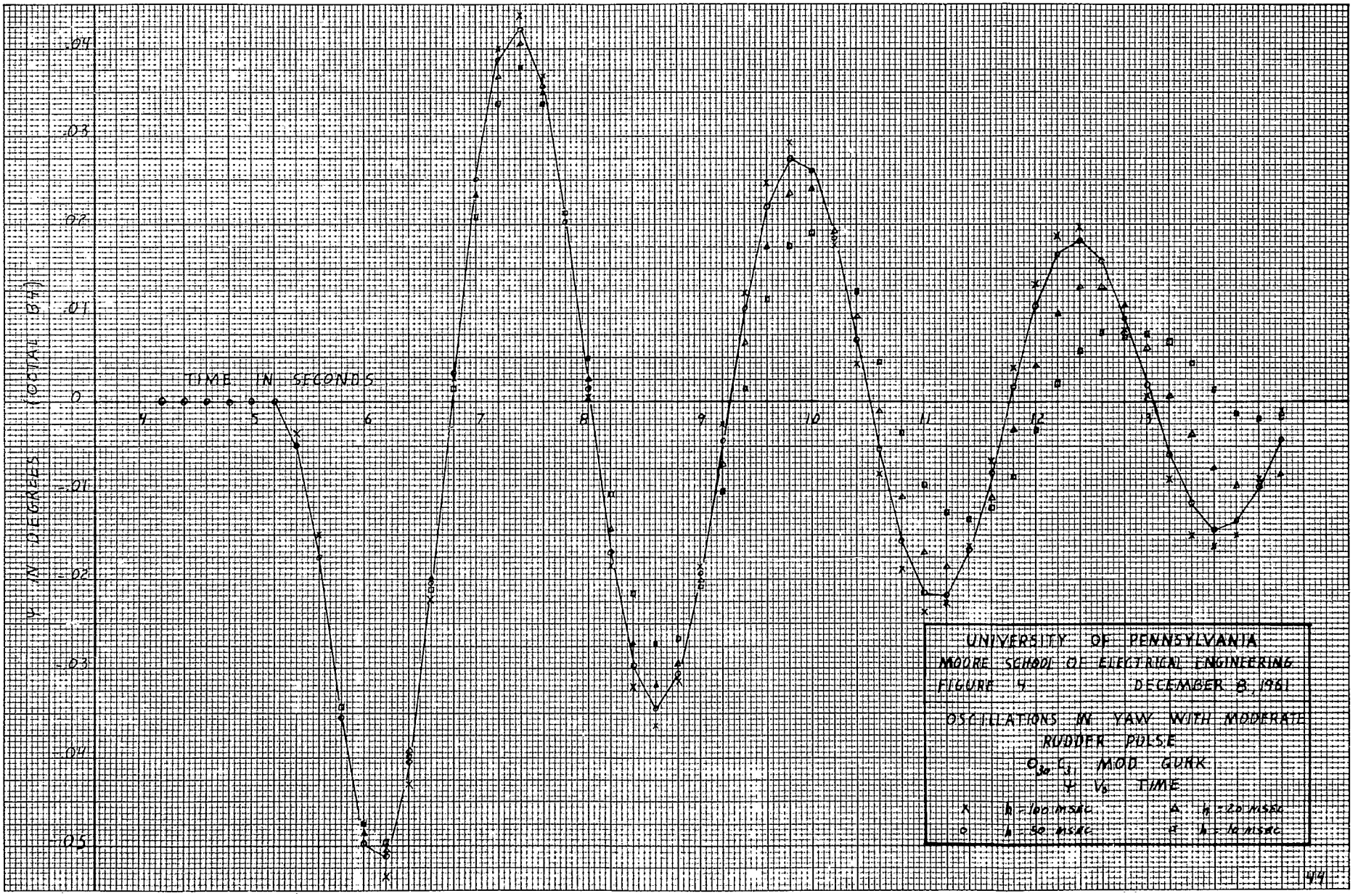
.04
.03
.02
.01
0
-.01
-.02
-.03
-.04
-.05
TIME IN SECONDS
4
5
6
7
8
9
10
11
12
3
Ψ IN DEGREES (TOTAL Ψ)
UNIVERSITY OF PENNSYLVANIA
MOORE SCHOOL OF ELECTRICAL ENGINEERING
FIGURE 4 DECEMBER 8, 1961
OSCILLATIONS IN YAW WITH MODERATE RUDDER PULSE
$C_{3\alpha}$ $C_{3\dot{\beta}}$ MOD GURK
Ψ V_0 TIME
X h = 100 msec
o h = 50 msec
Δ h = 20 msec
□ h = 10 msec

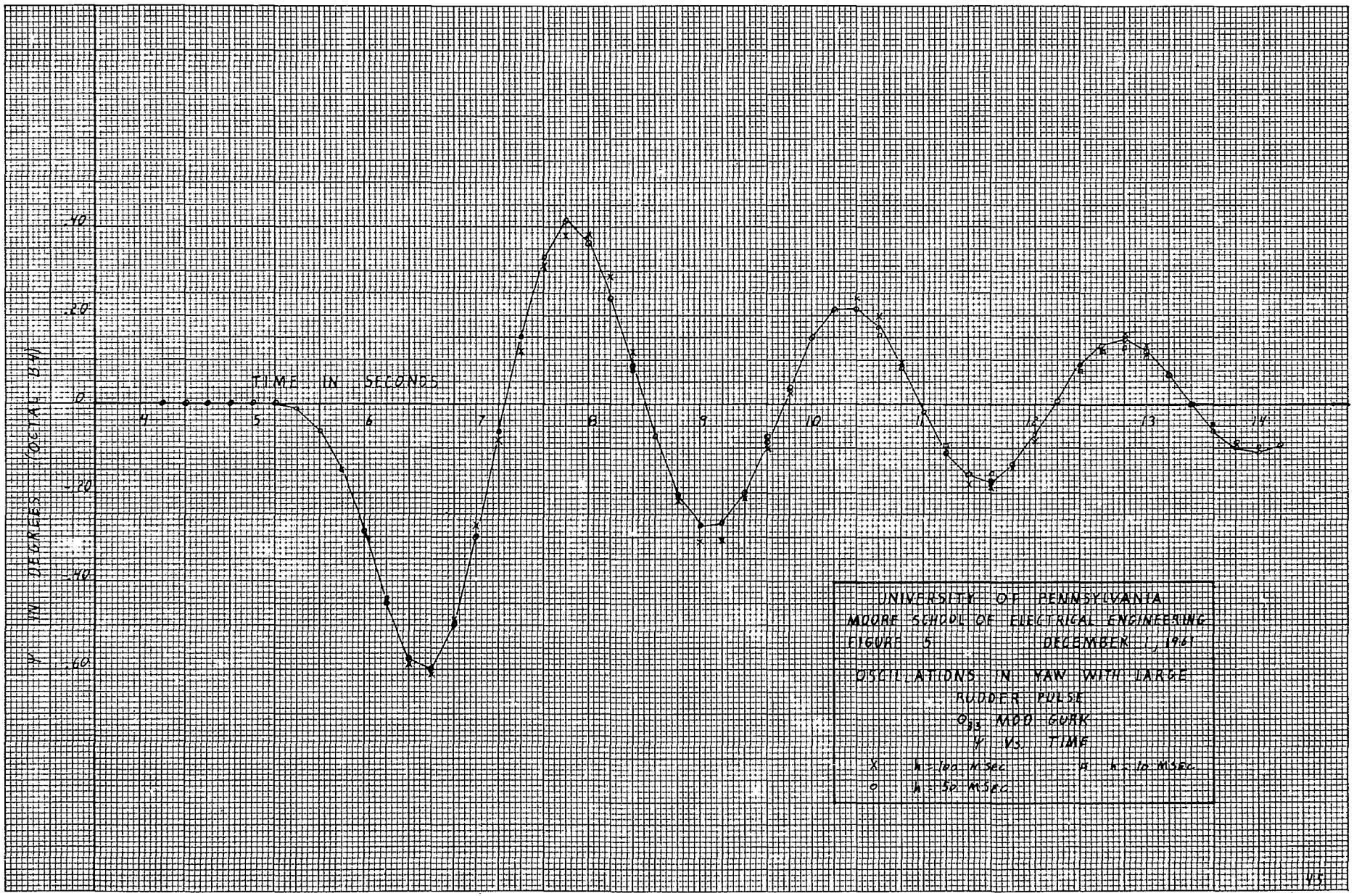
TIME IN SECONDS
4
5
6
7
8
9
10
11
12
13
14
.40
.20
0
-.20
-.40
-.60
ψ IN DEGREES (TOTAL ψ)
UNIVERSITY OF PENNSYLVANIA
MOORE SCHOOL OF ELECTRICAL ENGINEERING
FIGURE 5 DECEMBER 1, 1961
OSCILLATIONS IN YAW WITH LARGE RUDDER PULSE
O_{33} MOD GURK
Ψ Vs. TIME
X h = 100 M Sec
O h = 50 M Sec
Δ h = 10 M Sec
V5

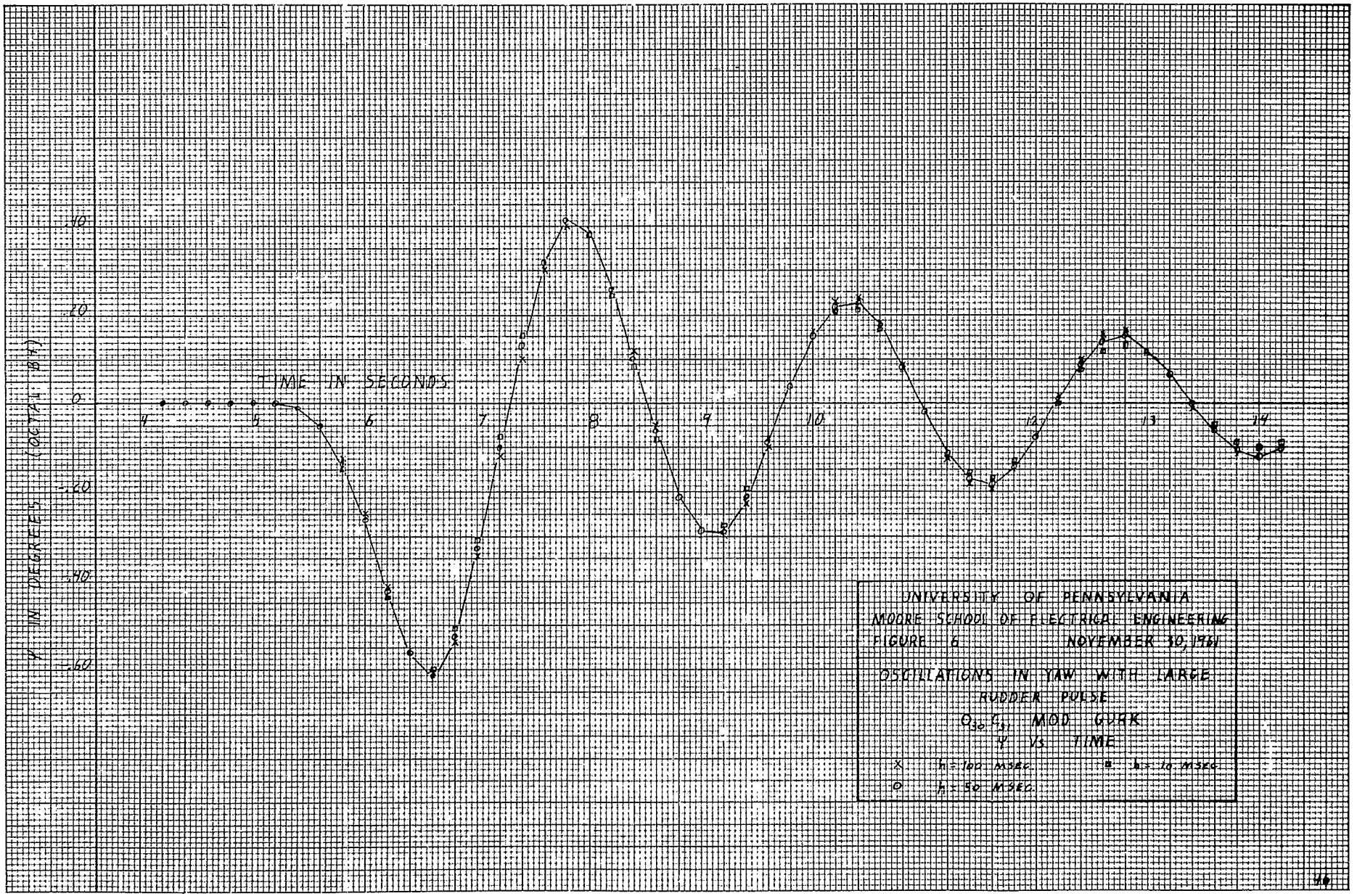
TIME IN SECONDS
Y IN DEGREES (DOTTED IN RAD.)
.40
.20
0
-.20
-.40
-.60
4
5
6
7
8
9
10
11
12
13
14
UNIVERSITY OF PENNSYLVANIA
MOORE SCHOOL OF ELECTRICAL ENGINEERING
FIGURE 6 NOVEMBER 30, 1961
OSCILLATIONS IN YAW WITH LARGE RUDDER PULSE
O_{30} C_{31} MOD GVRK
Y VS TIME
X h = 100 MSEC.
O h = 50 MSEC.
□ h = 10 MSEC.

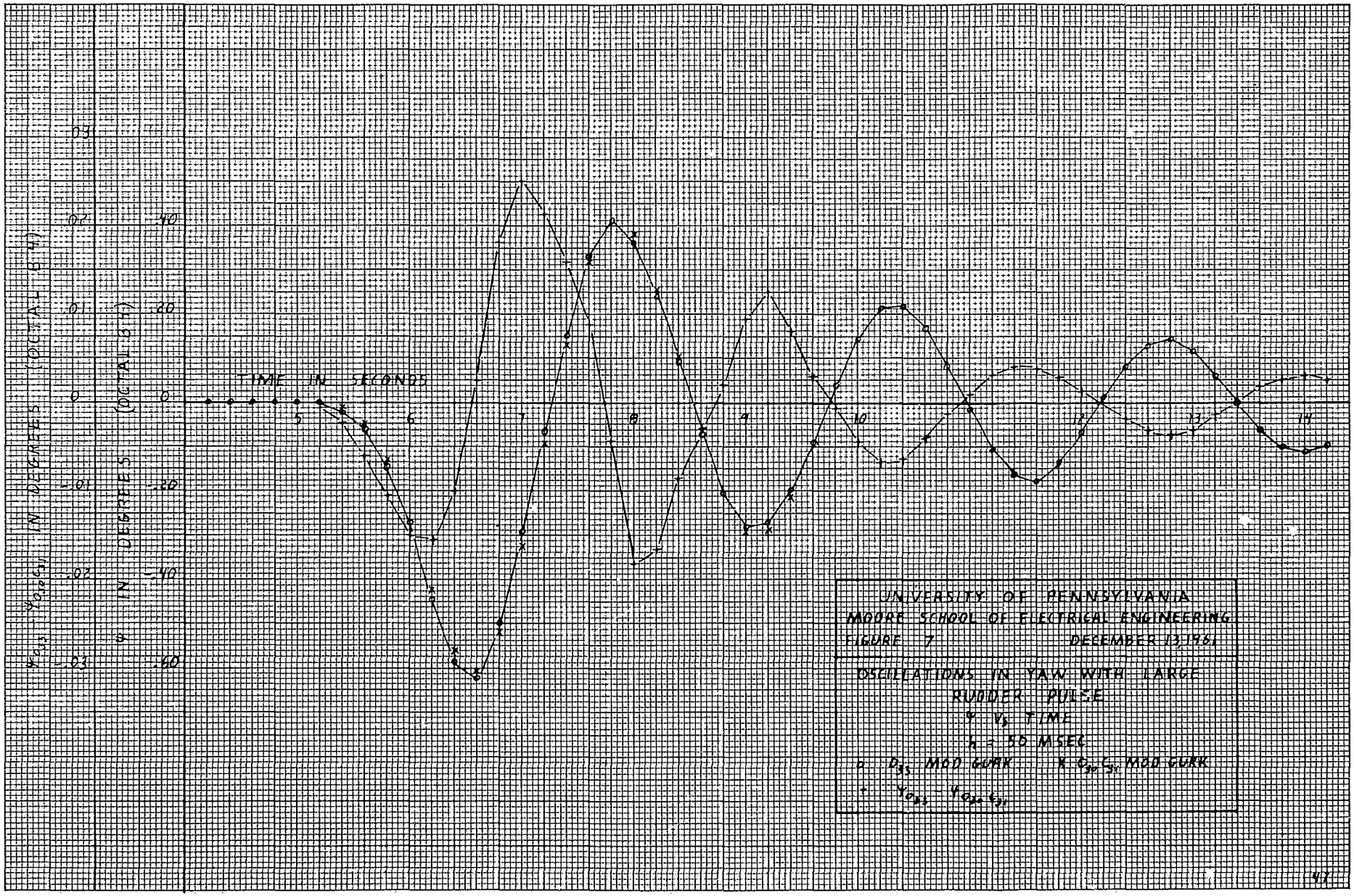
TIME IN SECONDS
IN DEGREES (OCTAL 3 4)
IN DEGREES (OCTAL 3 4)
UNIVERSITY OF PENNSYLVANIA
MOORE SCHOOL OF ELECTRICAL ENGINEERING
FIGURE 7 DECEMBER 13, 1961
OSCILLATIONS IN YAW WITH LARGE RUDDER PULSE
V_s TIME
h = 50 MSEC
D_33 MOD GURK
G_32 G_31 MOD GURK
Y_D33 Y_G32 G_31

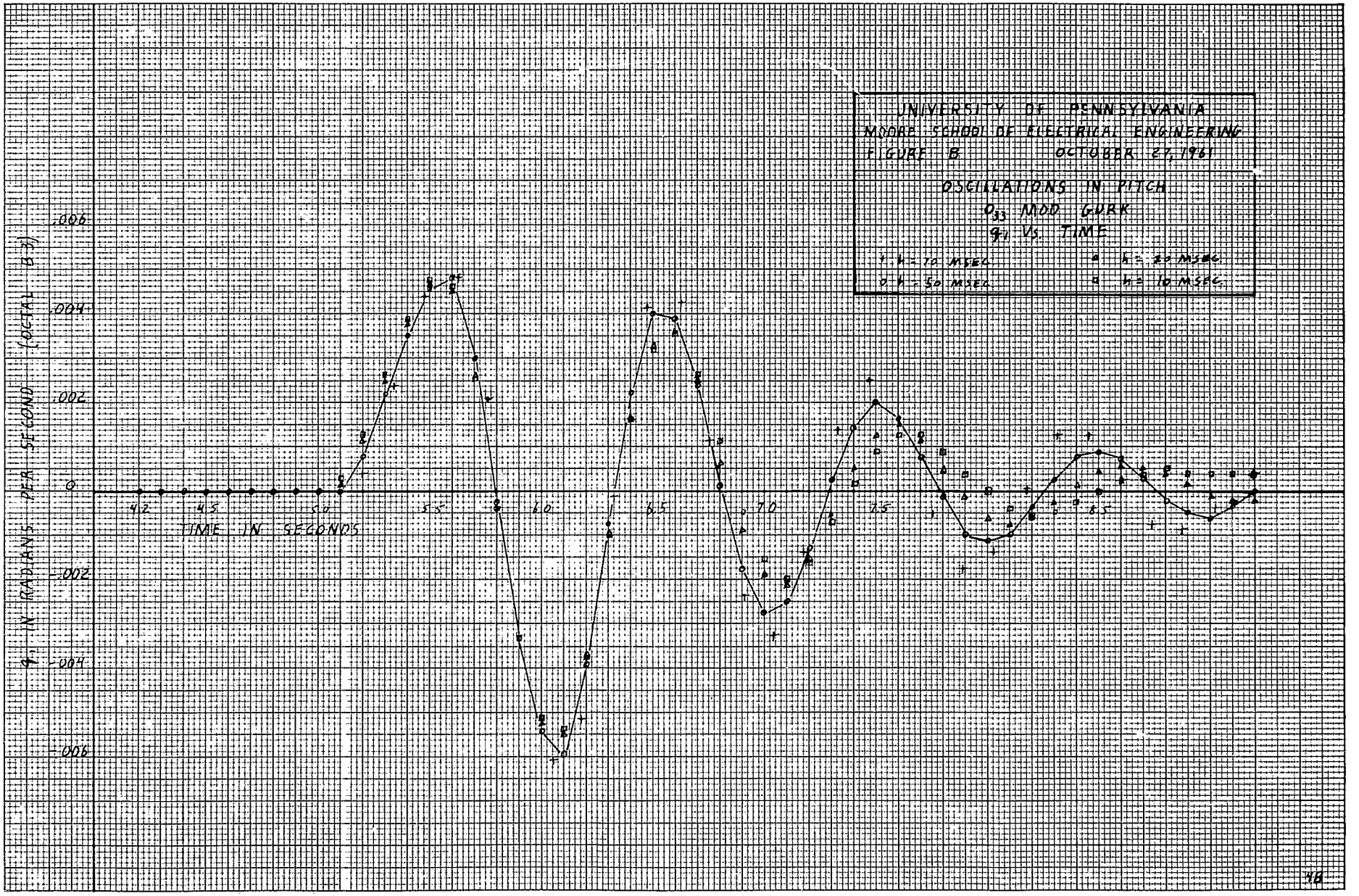
UNIVERSITY OF PENNSYLVANIA
MOORE SCHOOL OF ELECTRICAL ENGINEERING
FIGURE B OCTOBER 27, 1961
OSCILLATIONS IN PITCH
O_{33} MOD GURK
q_1 VS. TIME
+ h = 10 MSEC.
o h = 50 MSEC.
Δ h = 25 MSEC.
□ h = 10 MSEC.
.006
.004
.002
0
-.002
-.004
-.006
q_1 IN RADIANS PER SECOND (OCTAL B 3)
TIME IN SECONDS
42
45
50
55
60
65
70
75
80
85

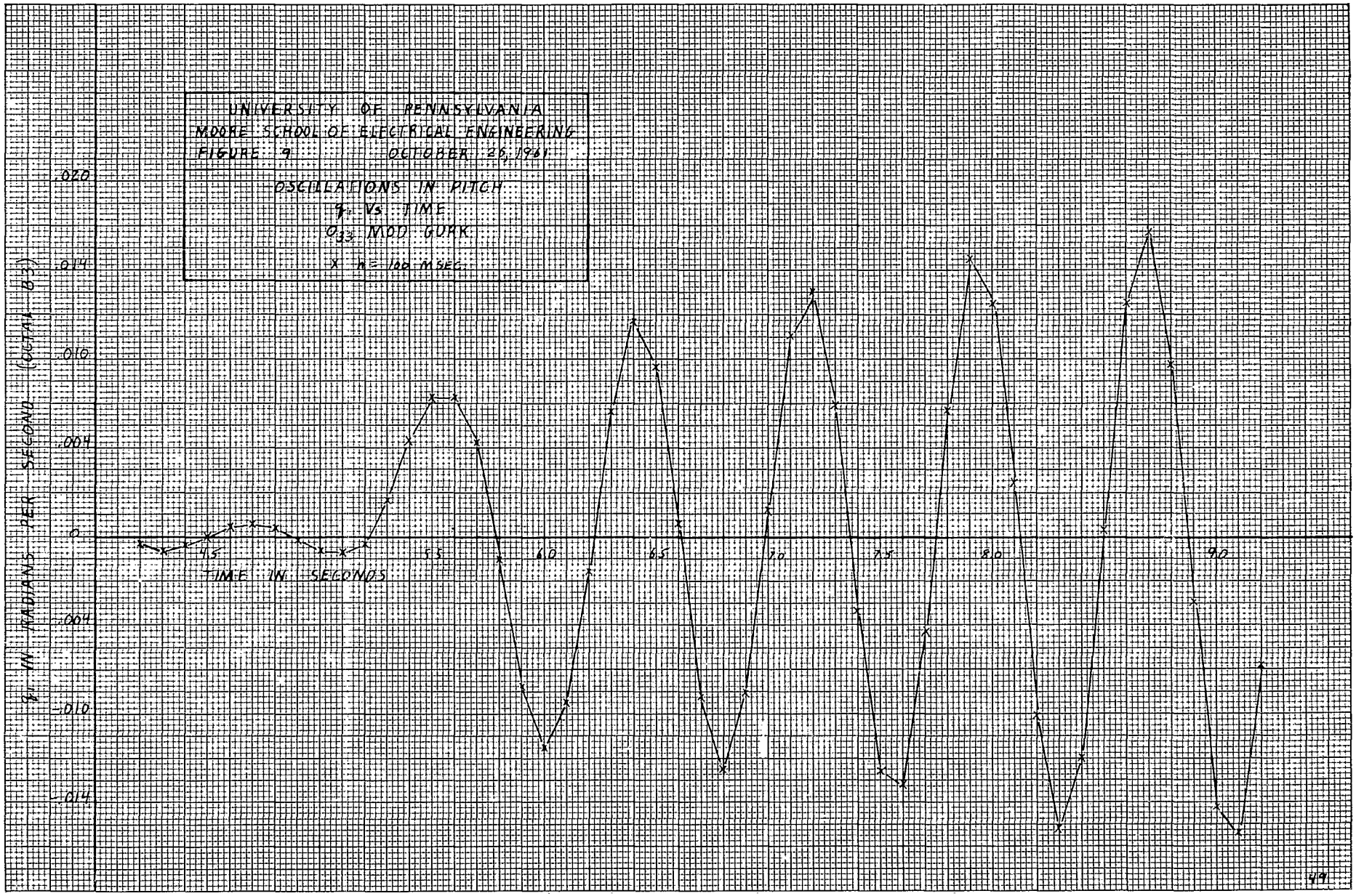
UNIVERSITY OF PENNSYLVANIA
MOORE SCHOOL OF ELECTRICAL ENGINEERING
FIGURE 9 OCTOBER 26, 1961
OSCILLATIONS IN PITCH
θ_{12} Vs TIME
Θ_{32} MOD GURK
X h = 100 MSEC.
θ_{12} IN RADIANS PER SECOND (OCTAL)
.020
.014
.010
.004
0
.004
-.010
-.014
4.5
5.0
6.0
6.5
7.0
7.5
8.0
9.0
TIME IN SECONDS

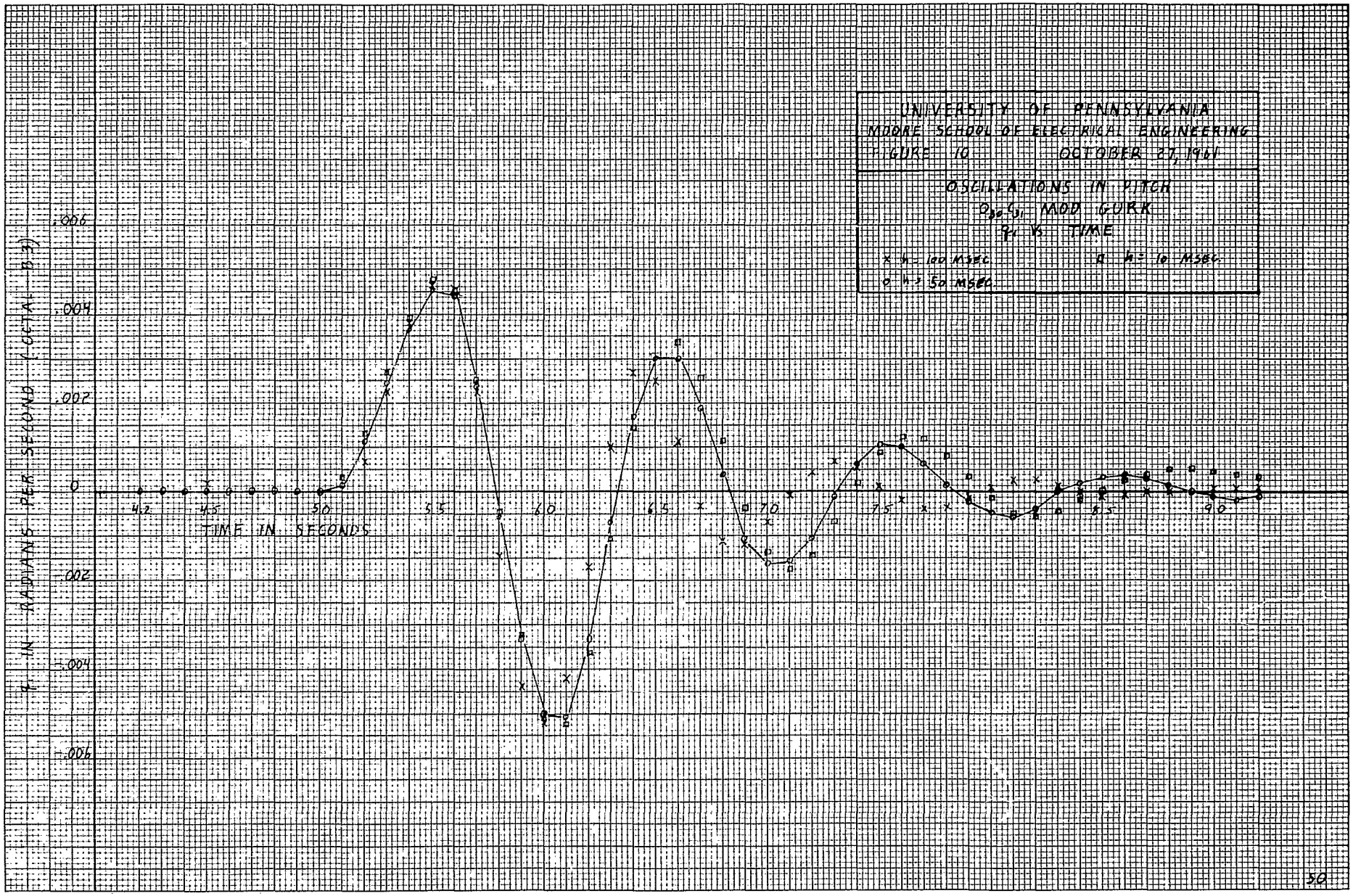
UNIVERSITY OF PENNSYLVANIA
MOORE SCHOOL OF ELECTRICAL ENGINEERING
FIGURE 10 OCTOBER 27, 1961
OSCILLATIONS IN PITCH
θ_{30} C_1 MOD GURK
θ_c VS TIME
x h = 100 MSEC
o h = 50 MSEC
□ h = 10 MSEC
θ IN RADIANS PER SECOND (OCTAL B-2)
.006
.004
.002
0
-.002
-.004
-.006
42
45
50
55
60
65
70
75
85
90
TIME IN SECONDS

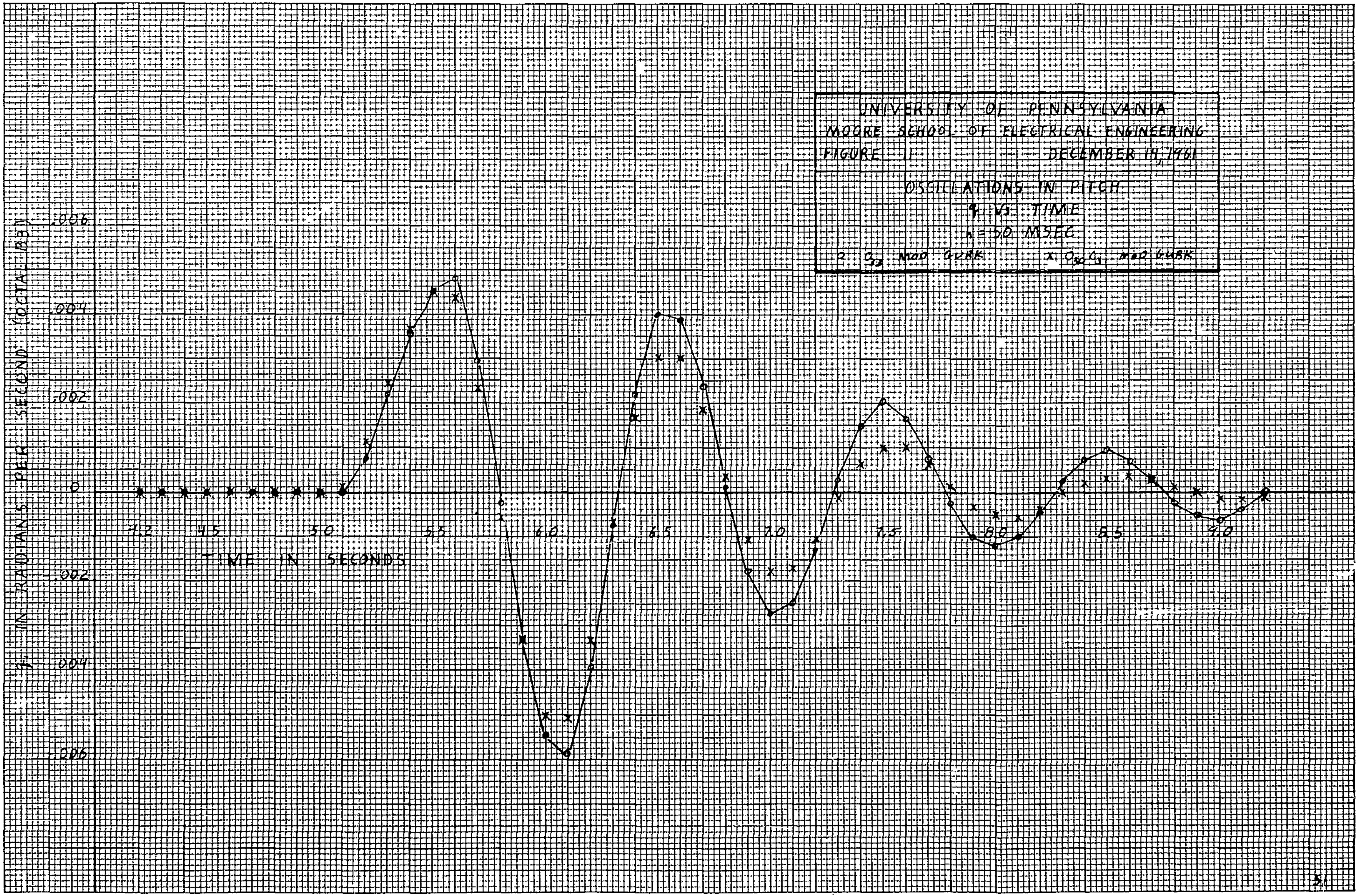
UNIVERSITY OF PENNSYLVANIA
MOORE SCHOOL OF ELECTRICAL ENGINEERING
FIGURE 11
DECEMBER 14, 1961
OSCILLATIONS IN PITCH
q VS TIME
h = 50 MSEC
o Q33 MOD GURK
x Q50 Q3 MOD GURK
q IN RADIANS PER SECOND (OCTAL B3)
.006
.004
.002
0
.002
.004
.006
4.2
4.5
5.0
5.5
6.0
6.5
7.0
7.5
8.0
8.5
9.0
TIME IN SECONDS

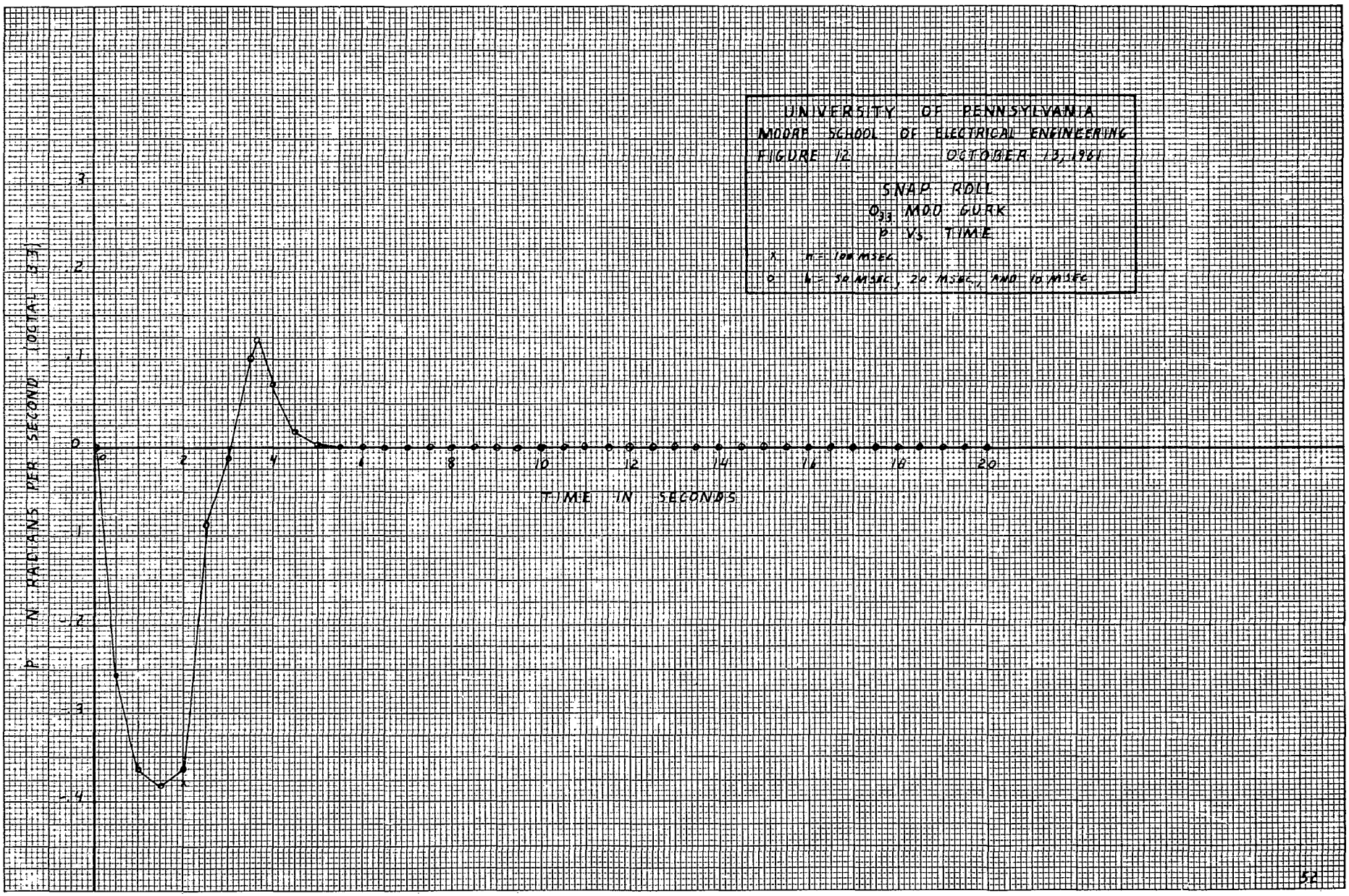
UNIVERSITY OF PENNSYLVANIA
MOORE SCHOOL OF ELECTRICAL ENGINEERING
FIGURE 12 OCTOBER 13, 1961
SNAP ROLL
O_{33} MOD GURK
P VS. TIME
X h = 100 MSEC.
O h = 50 MSEC., 20 MSEC., AND 10 MSEC.
P IN RADIANS PER SECOND (OCTAL 33)
TIME IN SECONDS
3
2
1
0
-1
-2
-3
-4
0
2
4
6
8
10
12
14
16
18
20

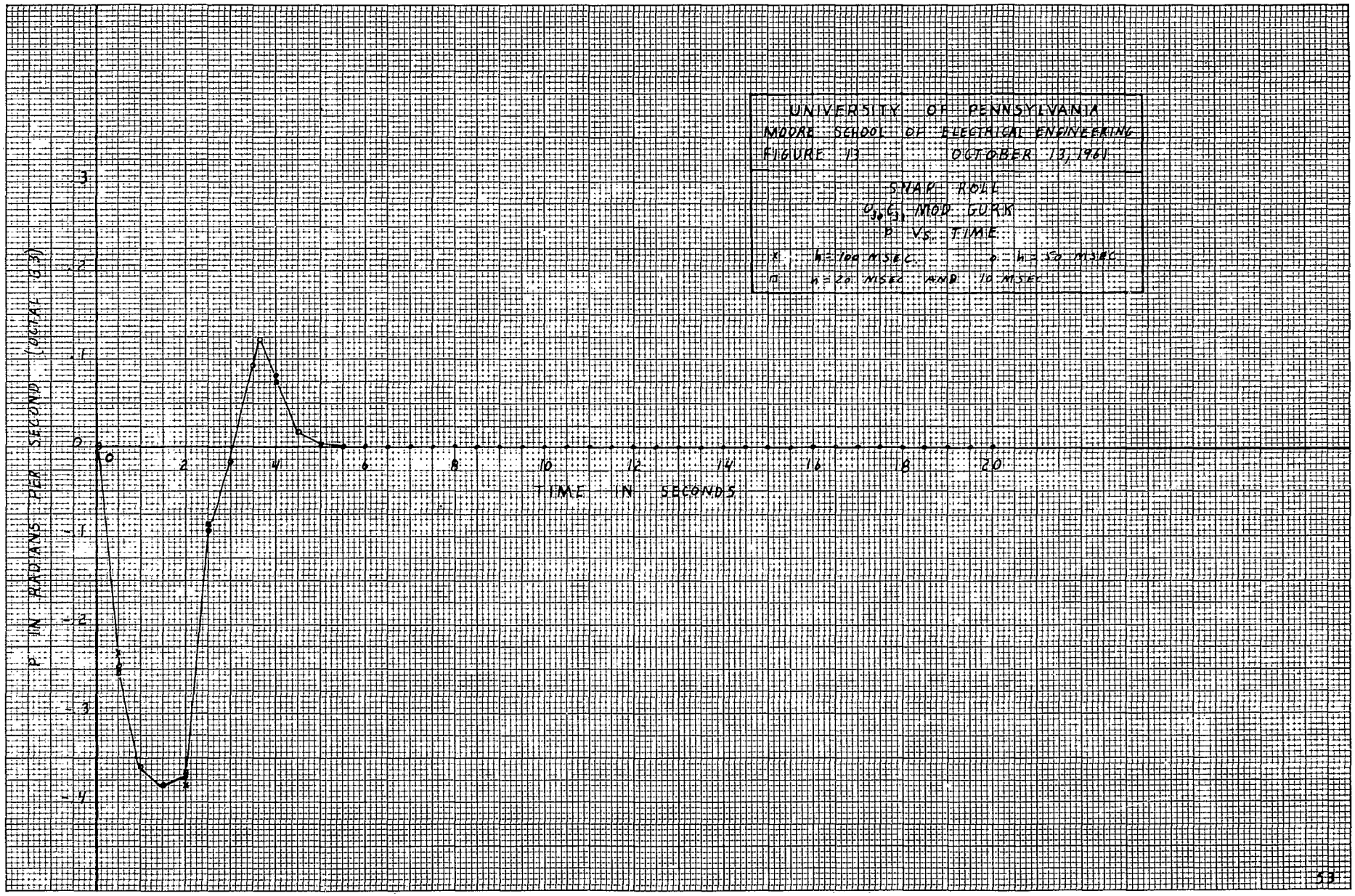
UNIVERSITY OF PENNSYLVANIA
MOORE SCHOOL OF ELECTRICAL ENGINEERING
FIGURE 13 OCTOBER 13, 1961
SNAP ROLL
$\sigma_{30} C_{31}$ MOD GURK
P VS. TIME
X h = 100 MSEC. o h = 50 MSEC
□ h = 20 MSEC AND 10 MSEC
P IN RADIANS PER SECOND (OCTAL 0.3)
TIME IN SECONDS
3
2
1
0
-1
-2
-3
-4
0
2
4
6
8
10
12
14
16
18
20

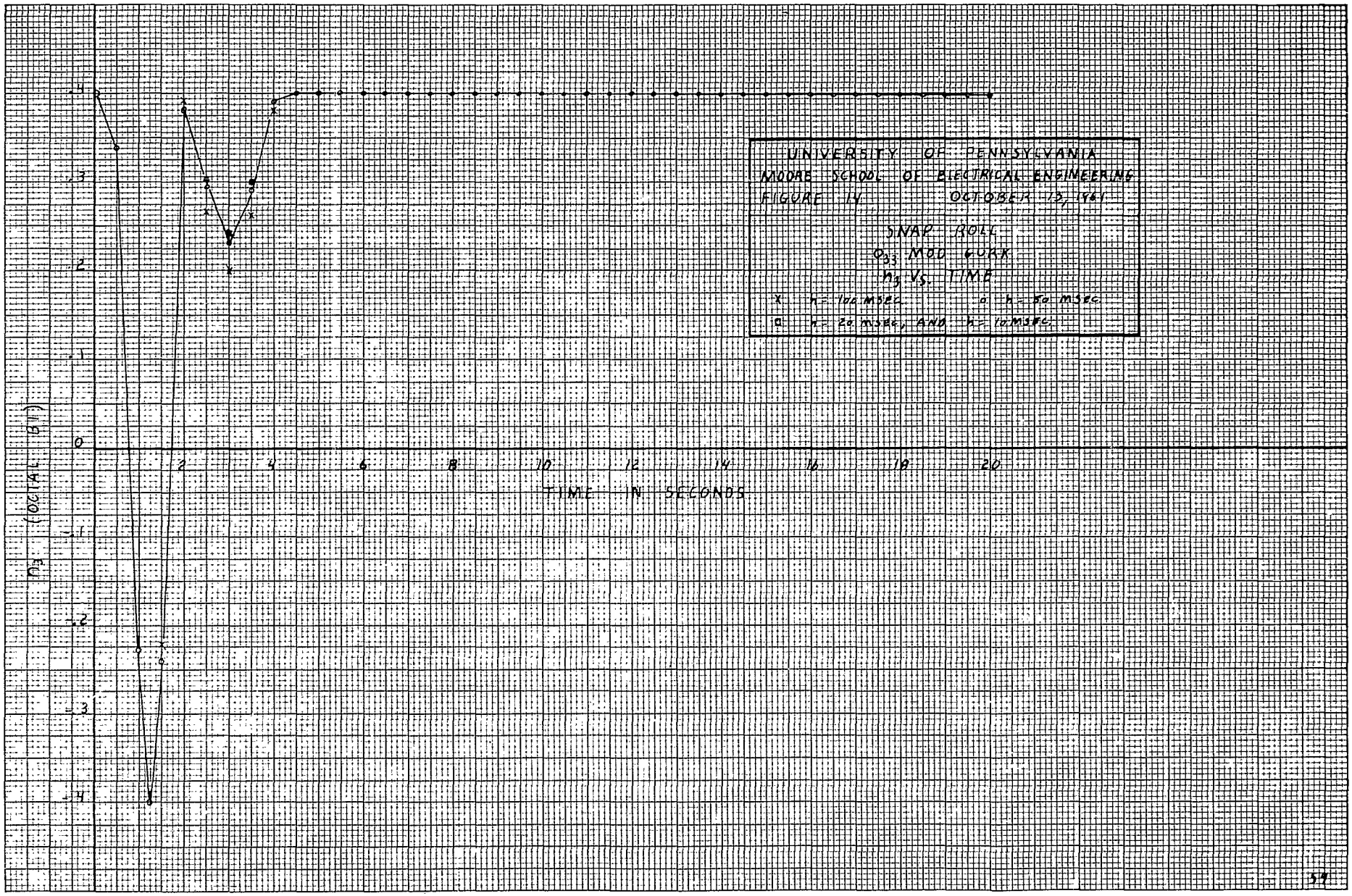
UNIVERSITY OF PENNSYLVANIA
MOORE SCHOOL OF ELECTRICAL ENGINEERING
FIGURE 14 OCTOBER 15, 1961
SNAP ROLL
O_{33} MOD WORK
h_3 VS. TIME
X h = 100 MSEC. o h = 50 MSEC.
□ h = 20 MSEC, AND h = 10 MSEC.
h_3 (OCTAL BIT)
TIME IN SECONDS
.4
.3
.2
.1
0
-.1
-.2
-.3
-.4
2
4
6
8
10
12
14
16
18
20

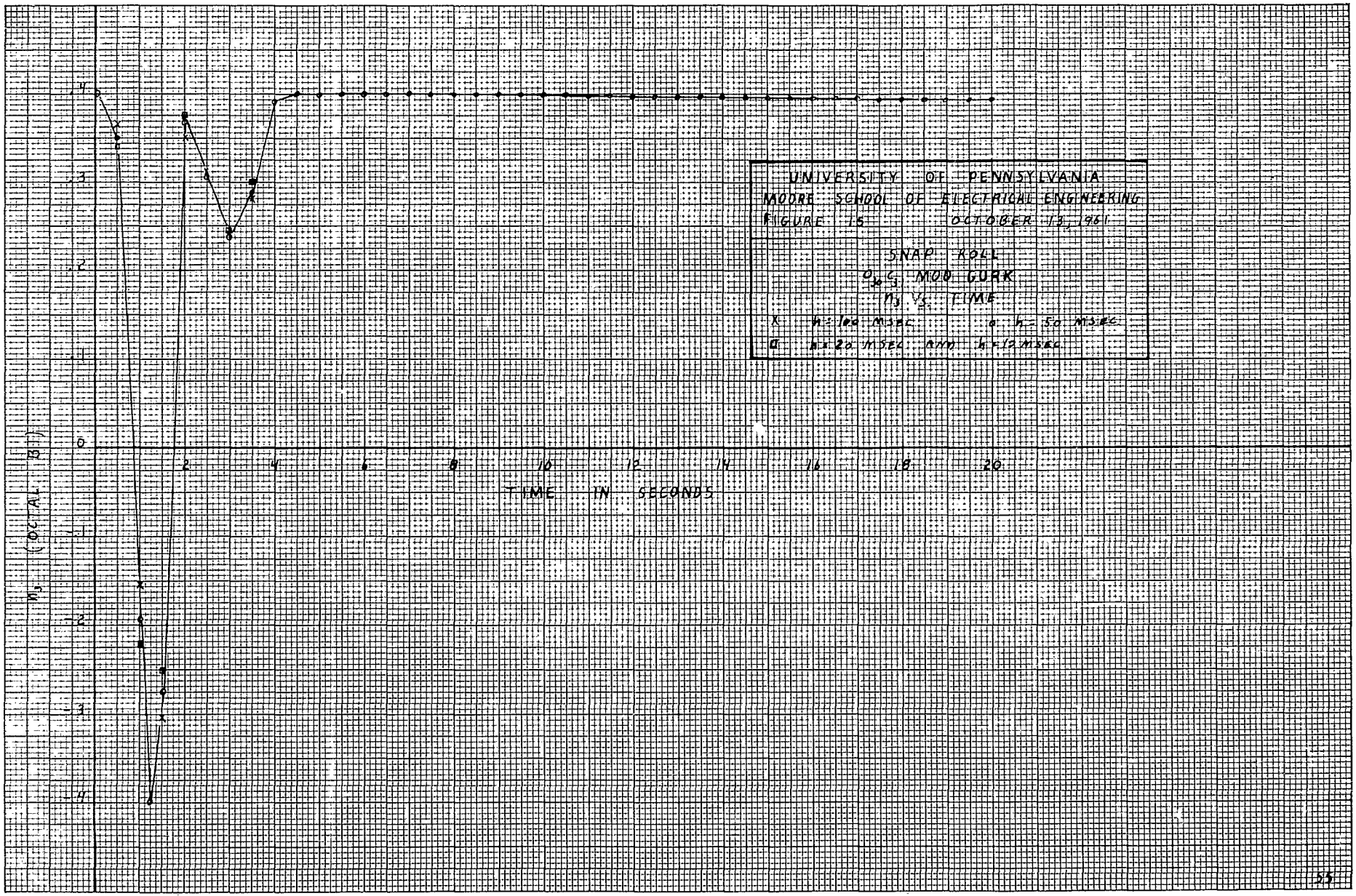
UNIVERSITY OF PENNSYLVANIA
MOORE SCHOOL OF ELECTRICAL ENGINEERING
FIGURE 15 OCTOBER 13, 1961
SNAP ROLL
θ_{ac_3} MOD GURK
n_3 V_c TIME
X h = 100 MSEC a h = 50 MSEC
a h = 20 MSEC AND h = 12 MSEC
TIME IN SECONDS
n_3 (DEGREES)

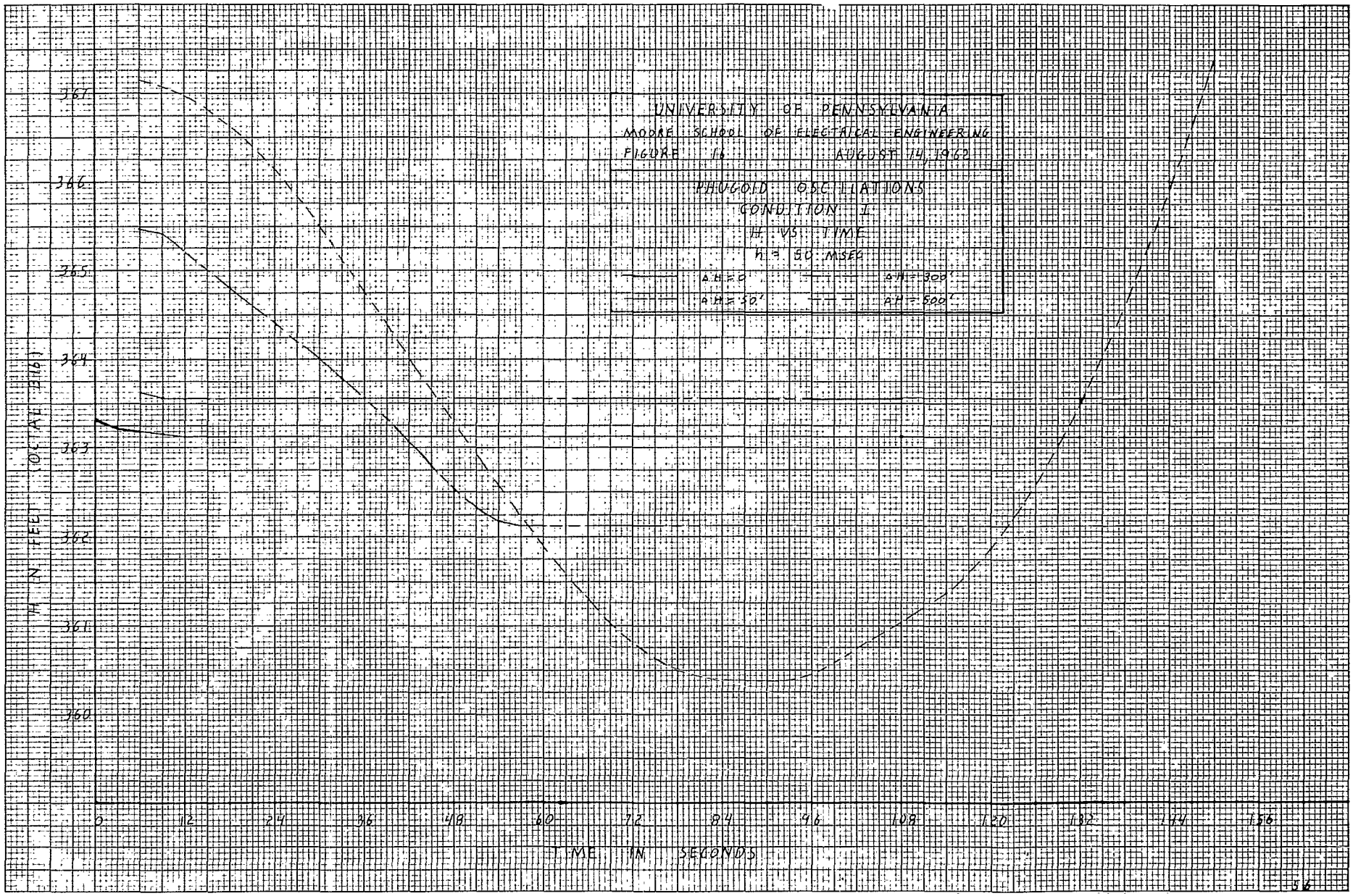
UNIVERSITY OF PENNSYLVANIA
MOORE SCHOOL OF ELECTRICAL ENGINEERING
FIGURE 16 AUGUST 14, 1962
PHUGOID OSCILLATIONS
CONDITION I
H VS TIME
h = 50 MSEC
ΔH = 0
ΔH = 30'
ΔH = 300'
ΔH = 500'
H IN FEET (OCEAN LEVEL)
361
362
363
364
365
366
367
0
12
24
36
48
60
72
84
96
108
120
132
144
156
TIME IN SECONDS

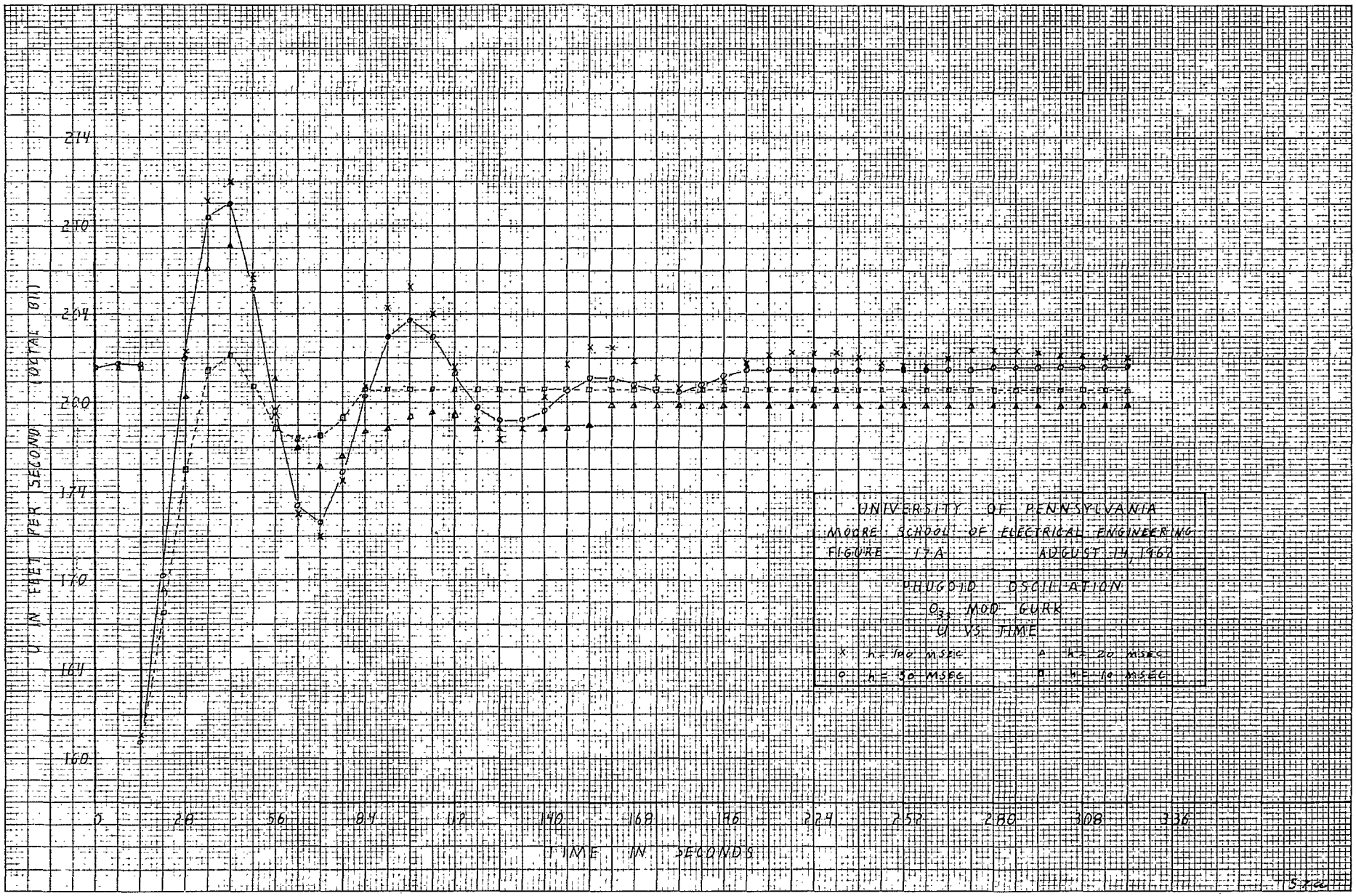
U IN FEET PER SECOND (OCTAL 811)
214
210
204
200
174
170
164
160
0
28
56
84
112
140
168
196
224
252
280
308
336
TIME IN SECONDS
UNIVERSITY OF PENNSYLVANIA
MOORE SCHOOL OF ELECTRICAL ENGINEERING
FIGURE 17A
AUGUST 14, 1962
PHUGOID OSCILLATION
O_{33} MOD GURK
U VS TIME
x h = 100 MSEC
Δ h = 20 MSEC
o h = 50 MSEC
□ h = 10 MSEC
5 Fig

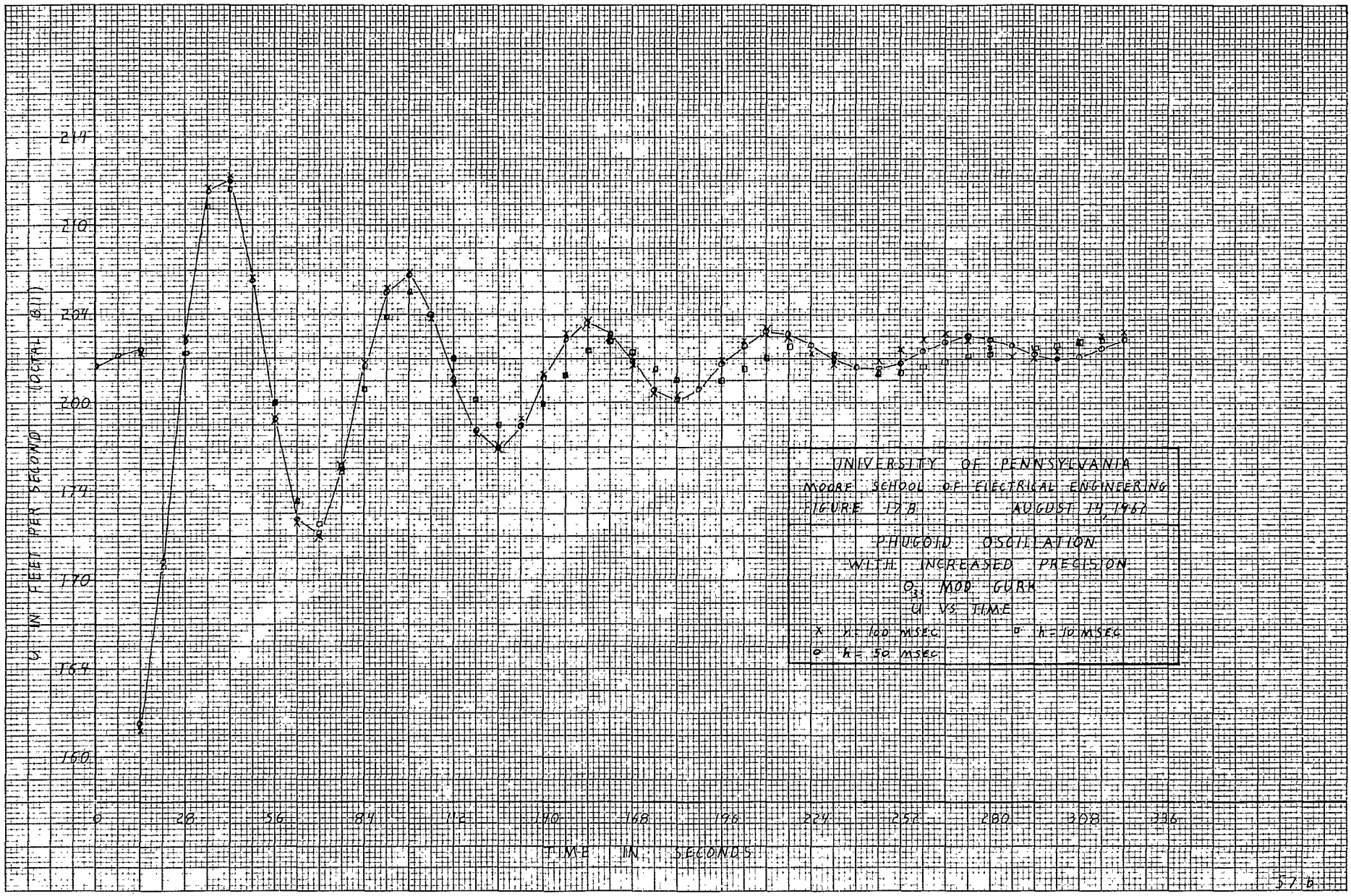
U IN FEET PER SECOND (OCTAL (B.11))
214
210
204
200
174
170
164
160
0
28
56
84
112
140
168
196
224
252
280
308
336
TIME IN SECONDS
UNIVERSITY OF PENNSYLVANIA
MOORE SCHOOL OF ELECTRICAL ENGINEERING
FIGURE 12 B
AUGUST 14, 1962
PHUGOID OSCILLATION
WITH INCREASED PRECISION
Q_{133} MOD GURK
U VS. TIME
x h = 100 MSEC
o h = 50 MSEC
□ h = 10 MSEC

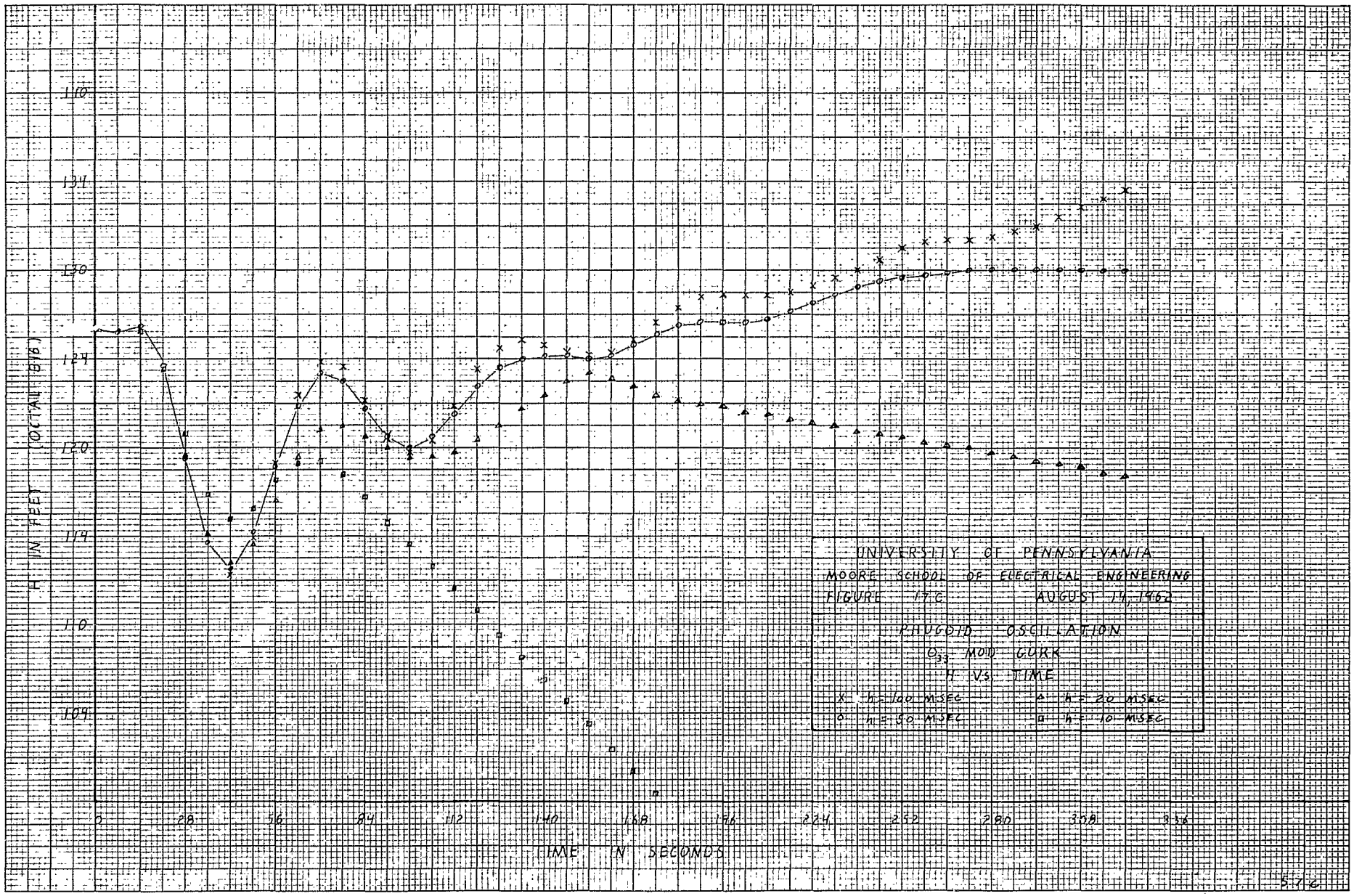
H IN FEET (OCTAL BIB)
110
124
130
124
120
114
110
104
0
28
56
84
112
140
168
196
224
252
280
308
336
TIME IN SECONDS
UNIVERSITY OF PENNSYLVANIA
MOORE SCHOOL OF ELECTRICAL ENGINEERING
FIGURE 17C AUGUST 14, 1962
PHUGOID OSCILLATION
O_{33} = MOD GURK
H VS TIME
X h = 100 M SEC
O h = 50 M SEC
Δ h = 20 M SEC
□ h = 10 M SEC
5-7-C

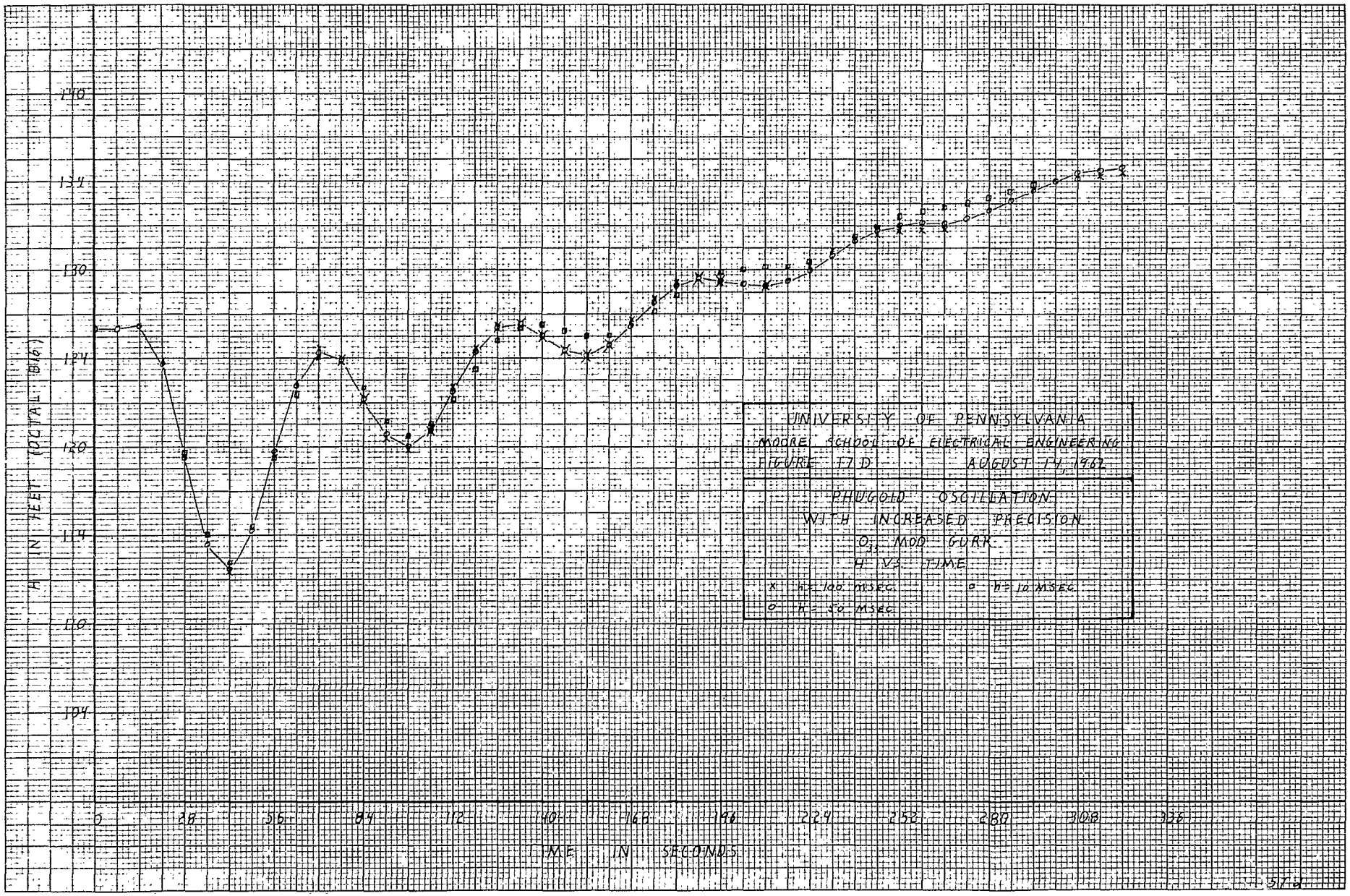
UNIVERSITY OF PENNSYLVANIA
MOORE SCHOOL OF ELECTRICAL ENGINEERING
FIGURE F7D AUGUST 14, 1962
PHUGOLD OSCILLATION
WITH INCREASED PRECISION
O_3 MOD GURK
H VS. TIME
x h = 100 MSEC. o h = 10 MSEC.
o h = 50 MSEC.
H IN FEET (OCTAL BIAS)
110
114
120
124
130
134
140
5
28
56
84
112
140
168
196
224
252
280
308
336
TIME IN SECONDS
517a

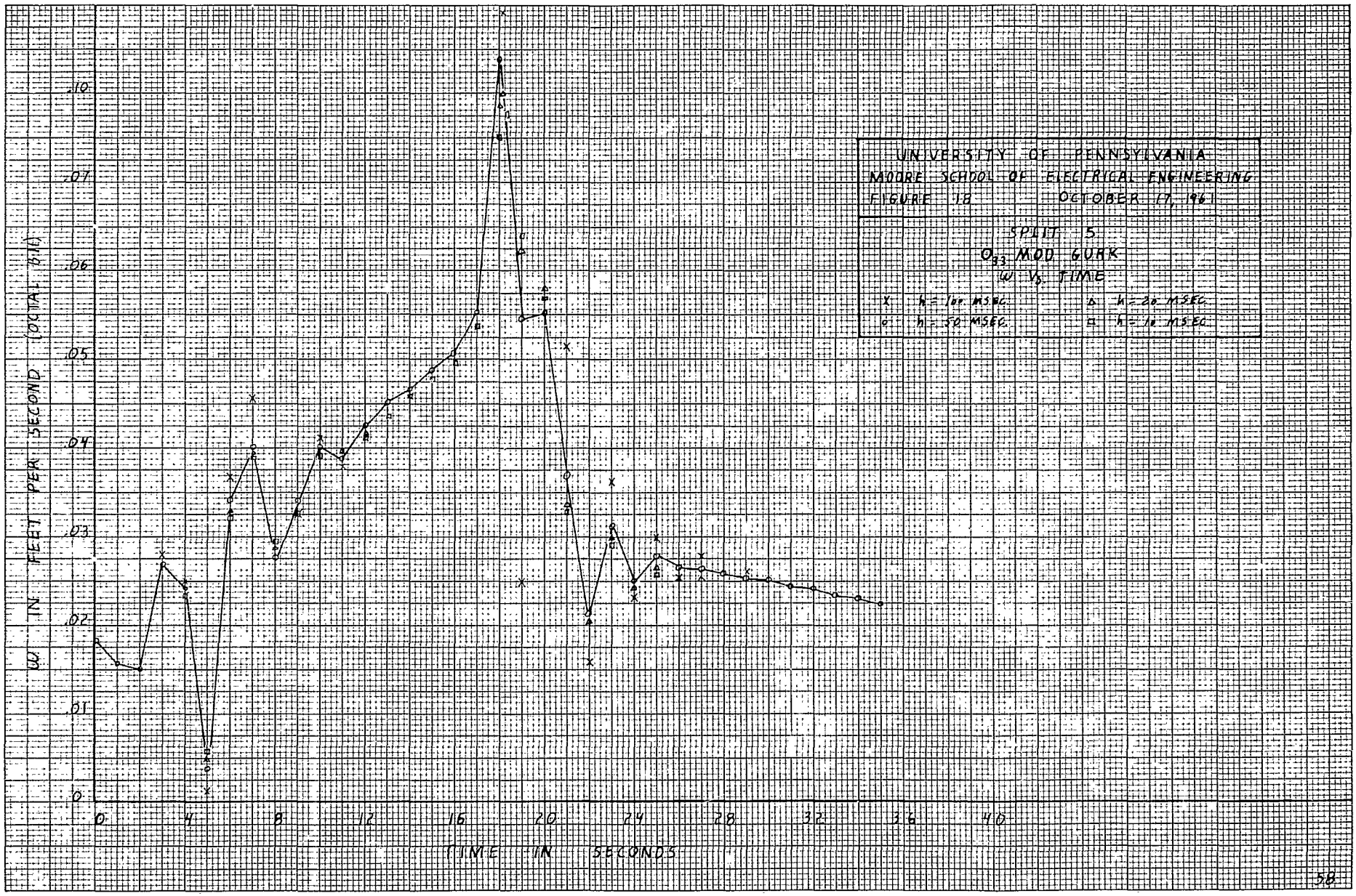
UNIVERSITY OF PENNSYLVANIA
MOORE SCHOOL OF ELECTRICAL ENGINEERING
FIGURE 18 OCTOBER 17, 1961
SPLIT 5
O_{33} MOD GURK
ω VS TIME
X h = 10T MSEC.
o h = 30 MSEC.
Δ h = 20 MSEC.
□ h = 10 MSEC.
ω IN FEET PER SECOND (OCTAL BIT)
.10
.07
.06
.05
.04
.03
.02
.01
0
0
4
8
12
16
20
24
28
32
36
40
TIME IN SECONDS

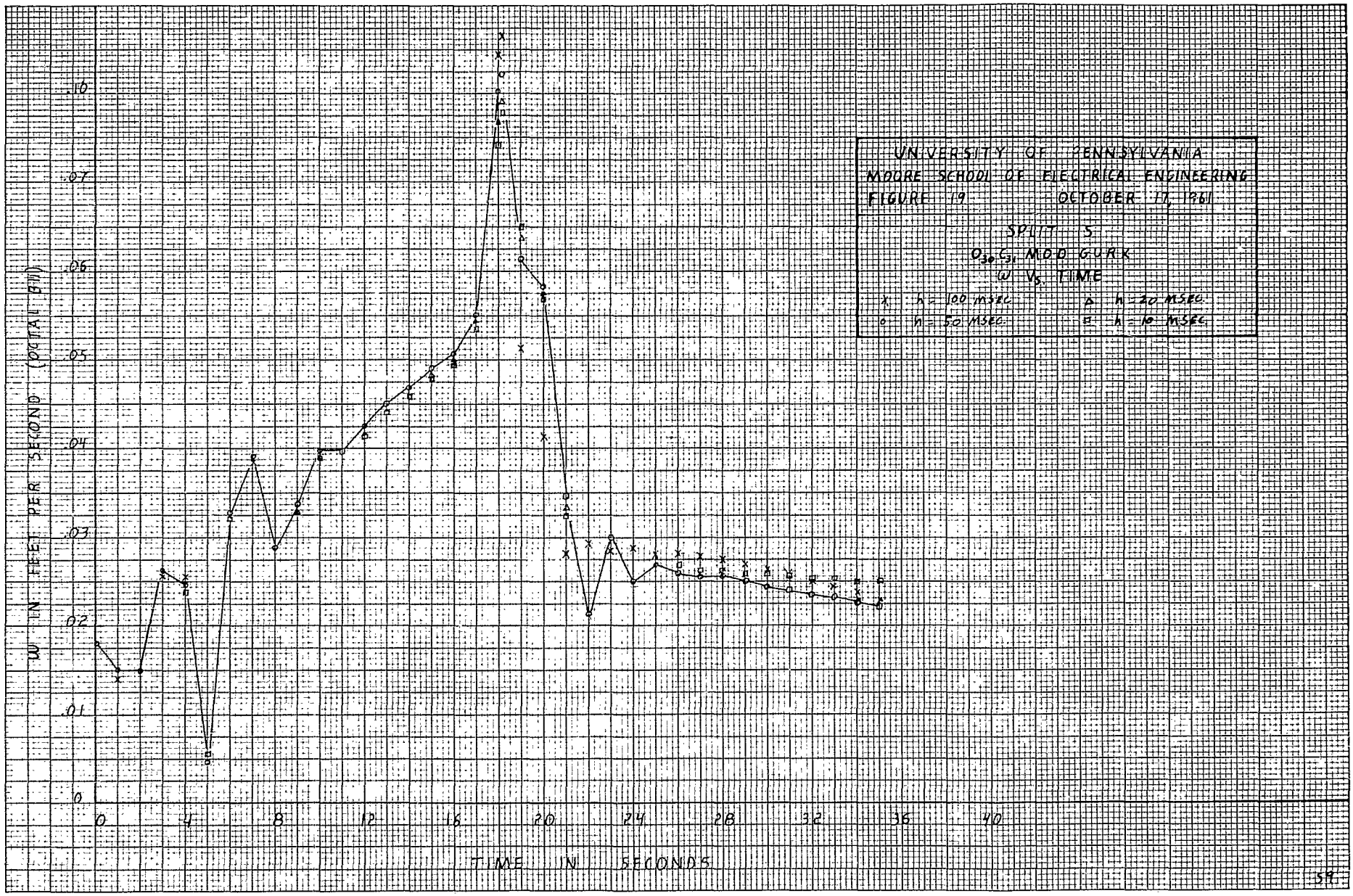
UNIVERSITY OF PENNSYLVANIA
MOORE SCHOOL OF ELECTRICAL ENGINEERING
FIGURE 19 OCTOBER 17, 1961
SPLIT S
$O_{30}C_{31}$ MOD GURK
ω VS. TIME
x h = 100 msec.
o h = 50 msec.
Δ h = 20 msec.
□ h = 10 msec.
W IN FEET PER SECOND (OCTAL 611)
.10
.07
.06
.05
.04
.03
.02
.01
0
0
4
8
12
16
20
24
28
32
36
40
TIME IN SECONDS

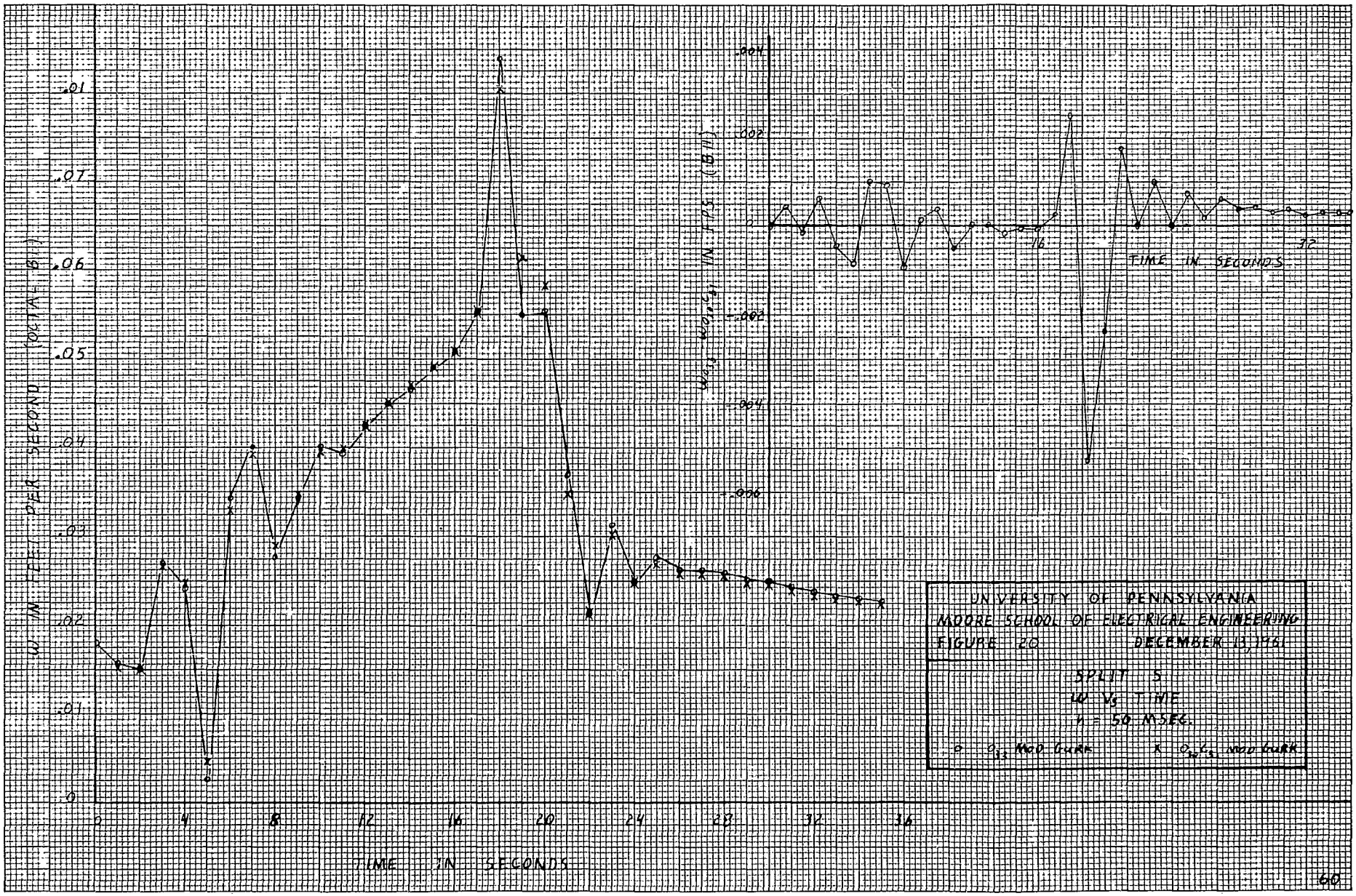
UNITS PER SECOND (OCTAL B)
.01
.07
.06
.05
.04
.03
.02
.01
0
0
4
8
12
16
20
24
28
32
36
TIME IN SECONDS
.004
.002
-.002
-.004
-.006
16
32
TIME IN SECONDS
UNIVERSITY OF PENNSYLVANIA
MOORE SCHOOL OF ELECTRICAL ENGINEERING
FIGURE 20
DECEMBER 13, 1961
SPLIT S
W VS TIME
h = 50 MSEC.
o σ_{33} MOD 64ARK
x $\sigma_{44}C_{33}$ MOD 64ARK

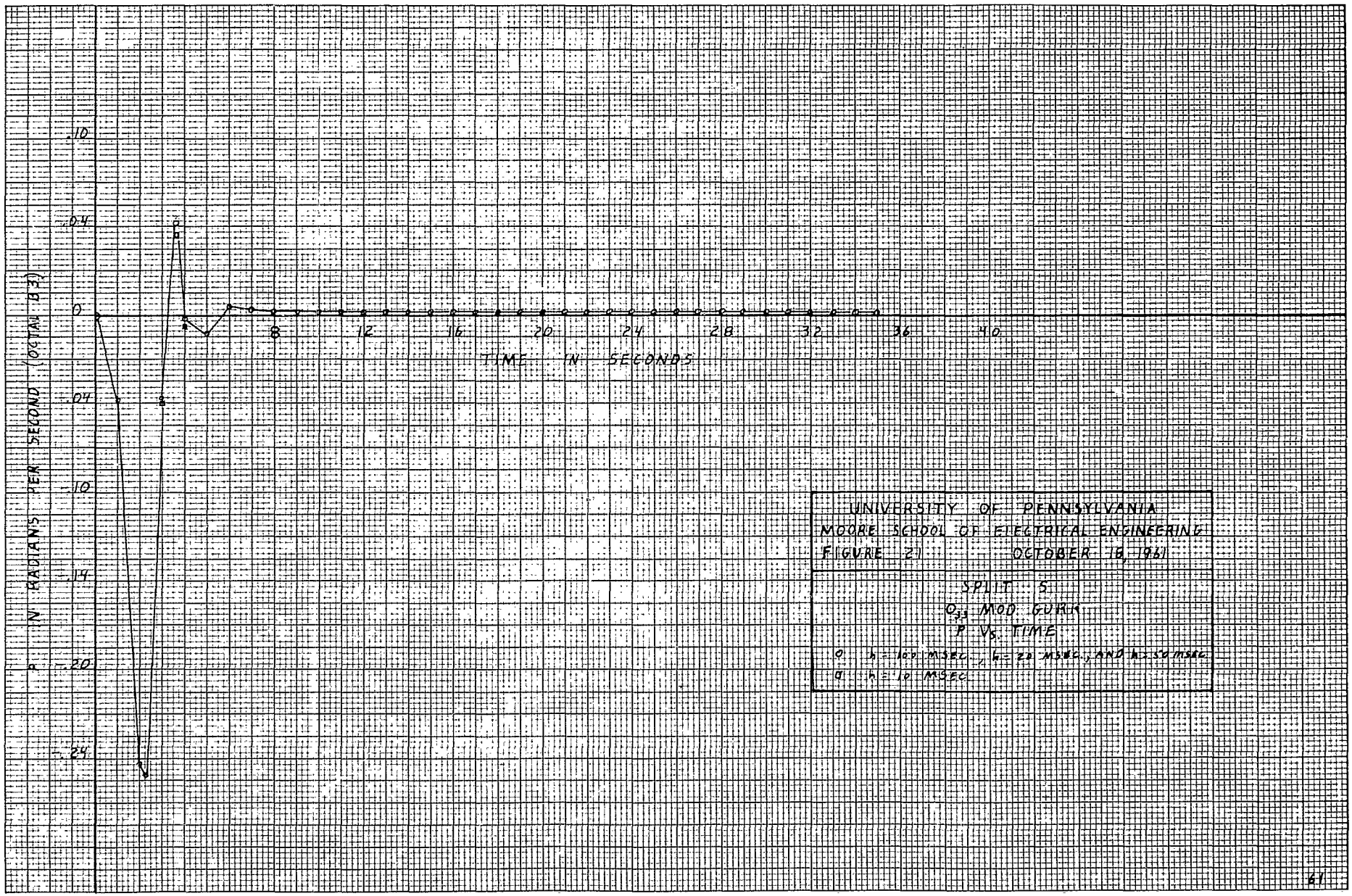

UNIVERSITY OF PENNSYLVANIA
MOORE SCHOOL OF ELECTRICAL ENGINEERING
FIGURE 21 OCTOBER 18, 1961

SPLIT S
O_{33} MOD GURK
P Vs TIME

a h = 100 MSEC, b = 20 MSEC, AND h = 50 MSEC
a h = 10 MSEC

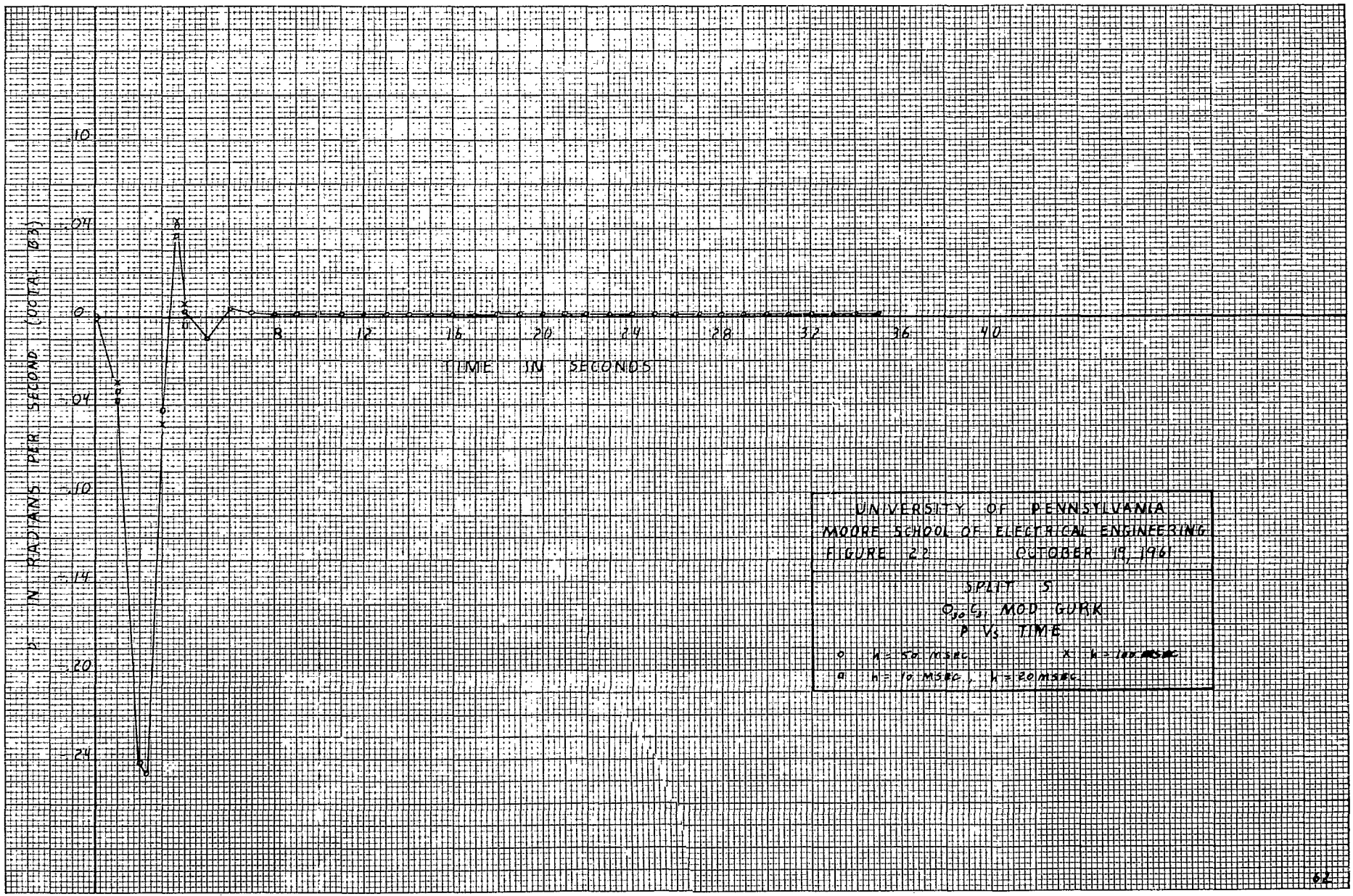
P IN RADIANS PER SECOND (OCTAL 83)
.10
.04
0
.04
.10
.14
.20
.24
8
12
16
20
24
28
32
36
40
TIME IN SECONDS
UNIVERSITY OF PENNSYLVANIA
MOORE SCHOOL OF ELECTRICAL ENGINEERING
FIGURE 22 OCTOBER 19, 1961
SPLIT S
Q_{50} G_5 MOD GURK
P VS. TIME
o h = 50 MSEC x h = 100 MSEC
a h = 10 MSEC , h = 20 MSEC

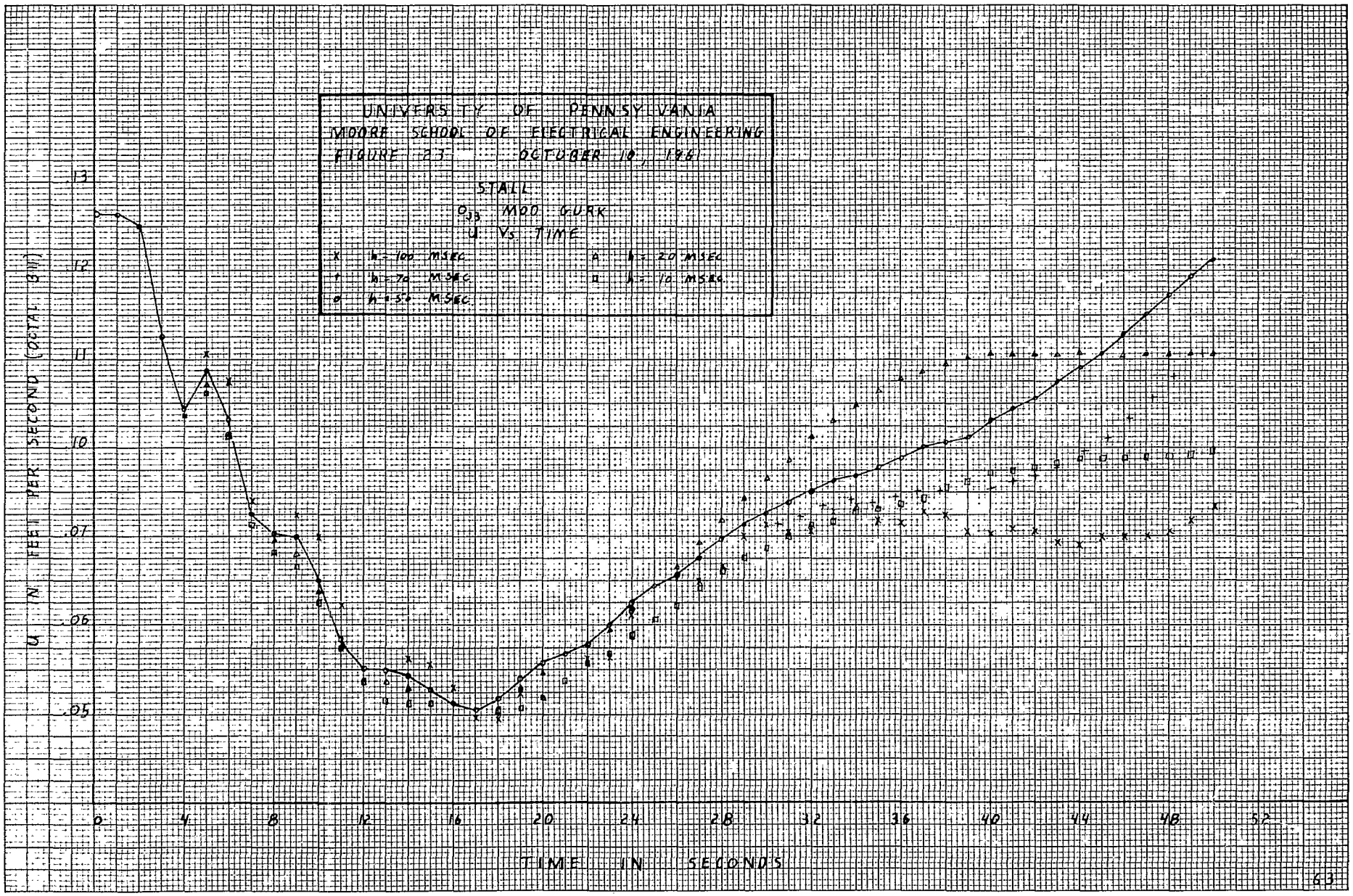
UNIVERSITY OF PENNSYLVANIA
MOORE SCHOOL OF ELECTRICAL ENGINEERING
FIGURE 23 OCTOBER 10, 1946
STALL
O_{33} MOD GURK
U Vs TIME
x h = 100 MSEC
↑ h = 70 MSEC
o h = 50 MSEC
Δ h = 20 MSEC
□ h = 10 MSEC
U IN FEET PER SECOND (OCTAL)
13
12
11
10
07
06
05
0
4
8
12
16
20
24
28
32
36
40
44
48
52
TIME IN SECONDS

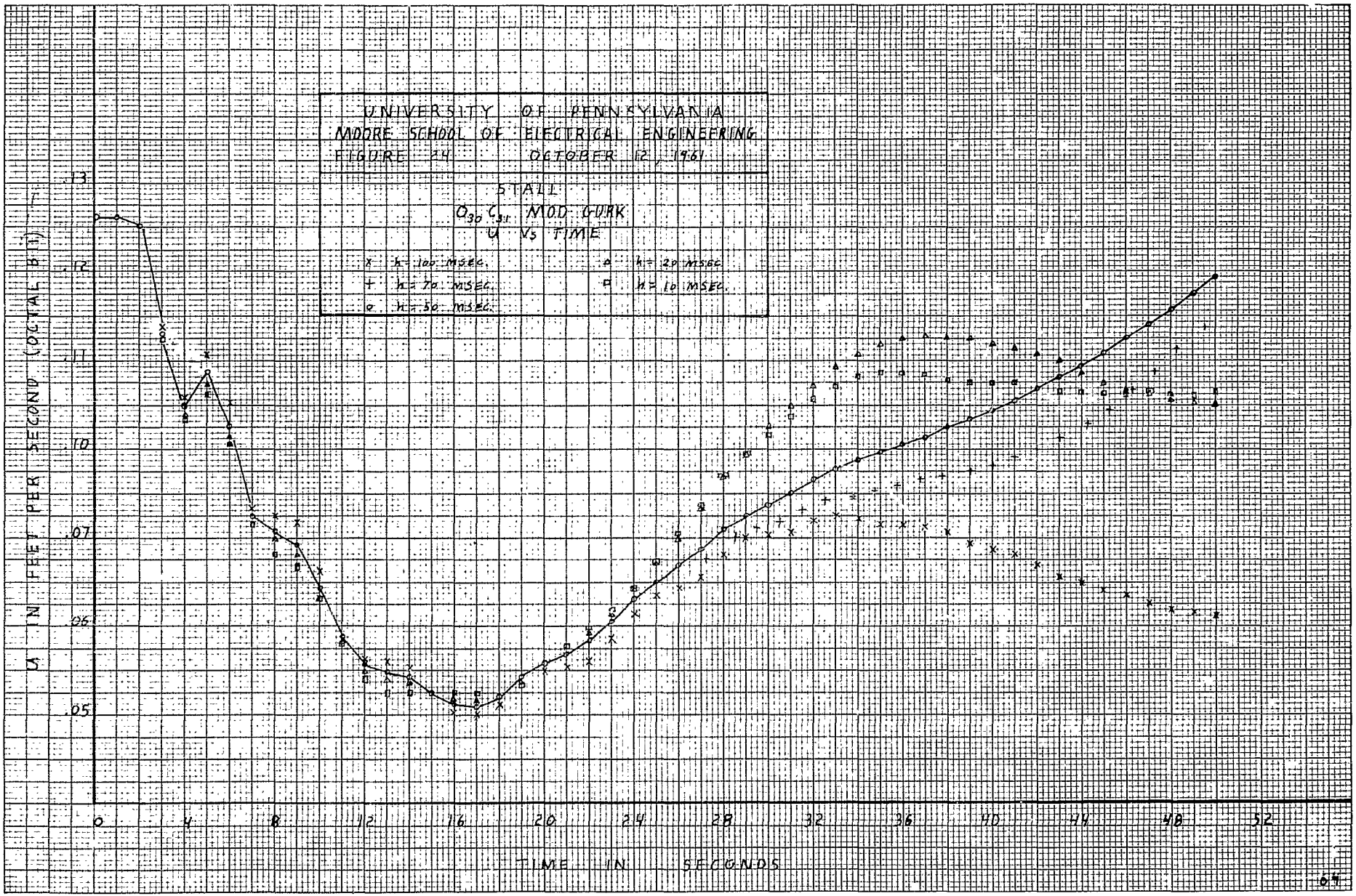
UNIVERSITY OF PENNSYLVANIA
MOORE SCHOOL OF ELECTRICAL ENGINEERING
FIGURE 24 OCTOBER 12, 1961
STALL
O_{30} C_{31} MOD QUAK
U VS TIME
x h=100 MSEC.
+ h=70 MSEC.
o h=50 MSEC.
Δ h=20 MSEC.
□ h=10 MSEC.
U IN FEET PER SECOND (OCTAL BIT)
.13
.12
.11
.10
.07
.06
.05
0
4
8
12
16
20
24
28
32
36
40
44
48
52
TIME IN SECONDS

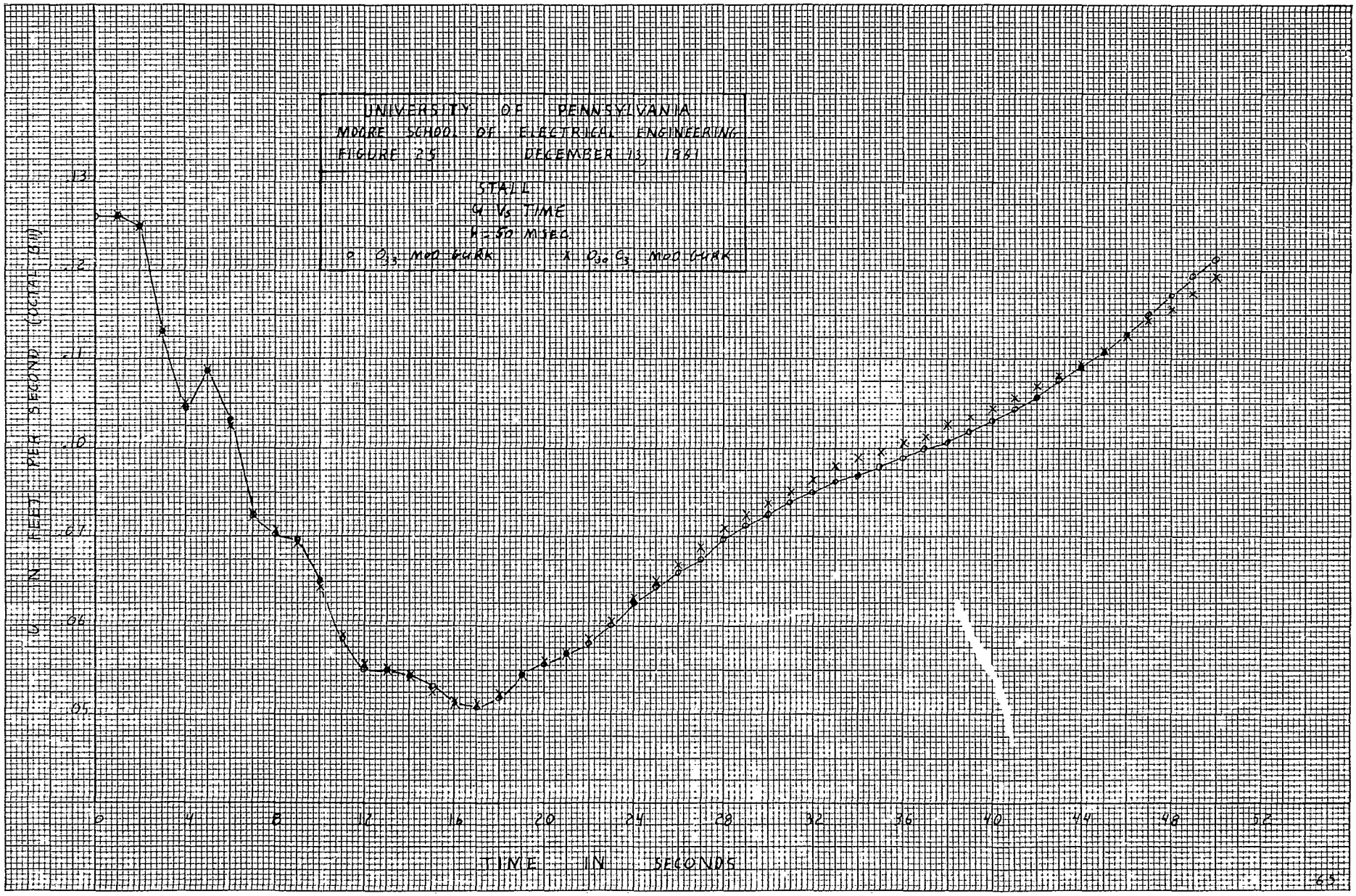
UNIVERSITY OF PENNSYLVANIA
MOORE SCHOOL OF ELECTRICAL ENGINEERING
FIGURE 25 DECEMBER 13, 1951
STALL
Q Vs TIME
h = 50 M SEC.
o Q_{33} MOD GUARK
x Q_{30} C_3 MOD GUARK
Q IN FEET PER SECOND (LOCAL STALL)
.13
.12
.11
.10
.09
.08
.07
.06
.05
0
4
8
12
16
20
24
28
32
36
40
44
48
52
TIME IN SECONDS

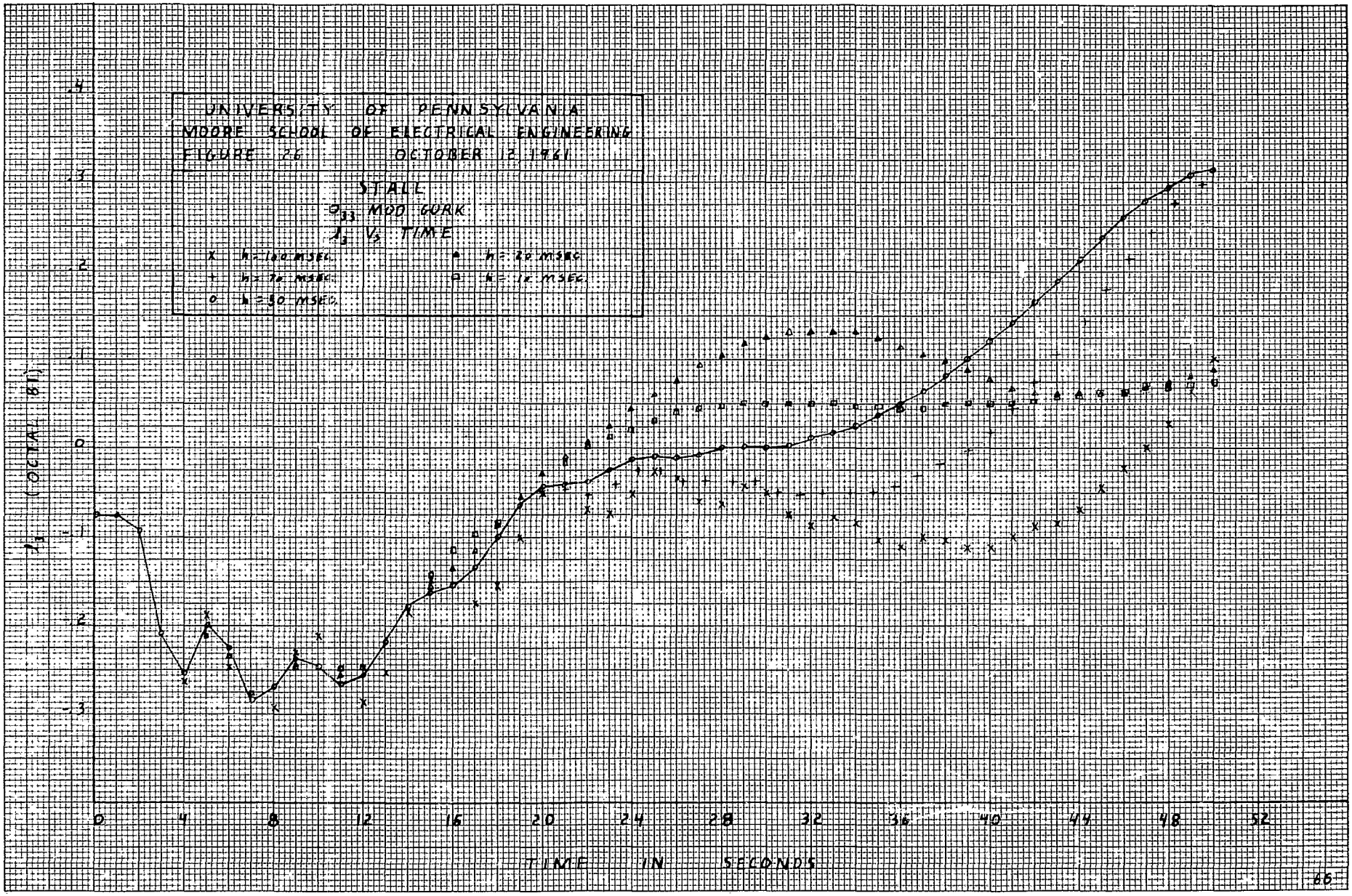
UNIVERSITY OF PENNSYLVANIA
MOORE SCHOOL OF ELECTRICAL ENGINEERING
FIGURE 26 OCTOBER 12, 1961
STALL
θ_{33} MOD GORK
λ_3 VS TIME
x h=100 MSEC.
+ h=75 MSEC.
o h=50 MSEC.
▲ h=25 MSEC.
□ h=12.5 MSEC.
λ_3 (OCTAVES)
4
3
2
1
0
-1
-2
-3
0
4
8
12
16
20
24
28
32
36
40
44
48
52
TIME IN SECONDS

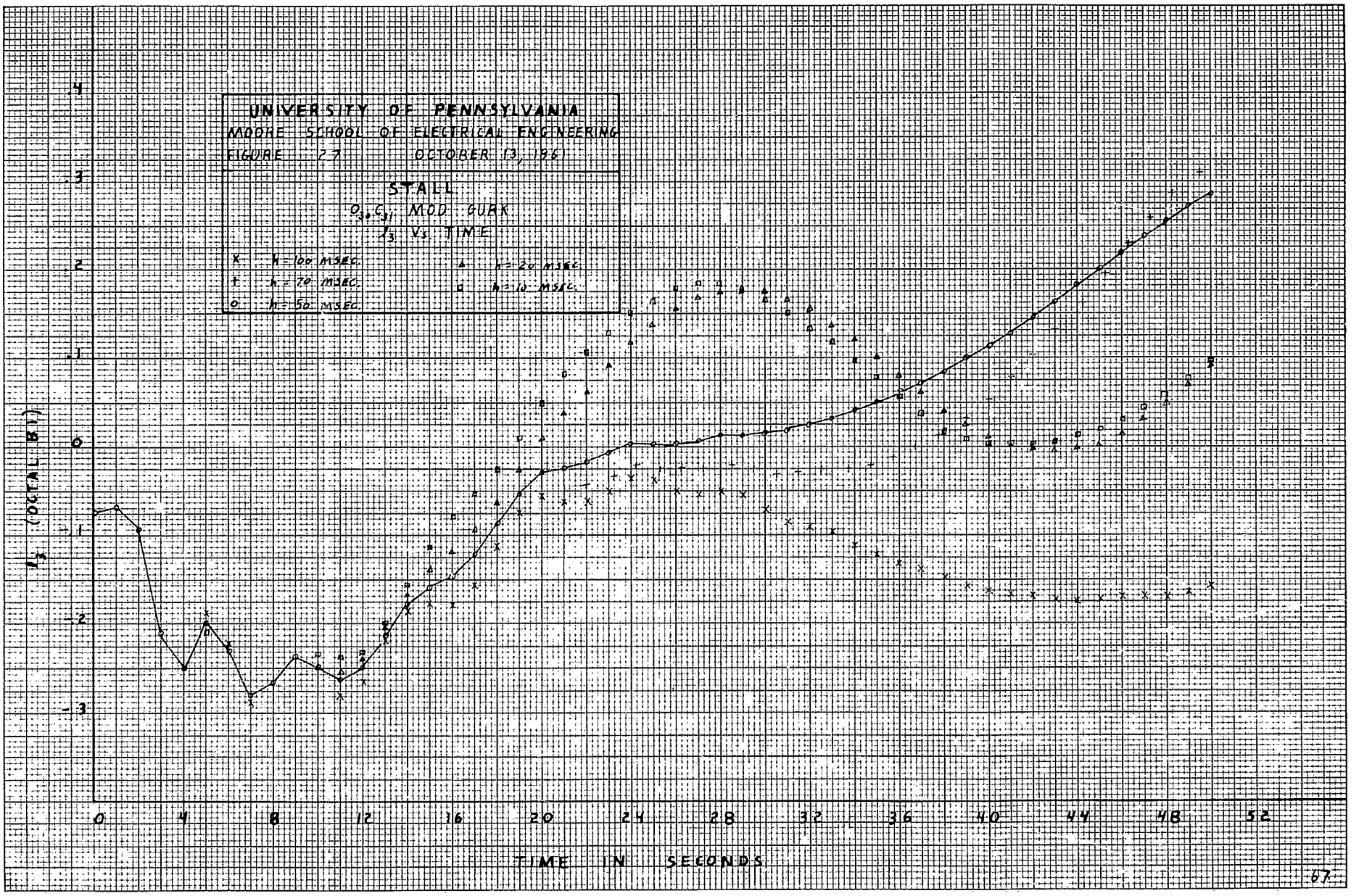
UNIVERSITY OF PENNSYLVANIA
MOORE SCHOOL OF ELECTRICAL ENGINEERING
FIGURE 27 OCTOBER 13, 1966
STALL
$O_{30}C_{31}$ MOD GUAK
I_3 Vs TIME
X h = 100 MSEC.
+ h = 70 MSEC.
o h = 50 MSEC.
Δ h = 20 MSEC.
□ h = 10 MSEC.
I_3 (LOCAL B.U.)
4
3
2
1
0
-1
-2
-3
0
4
8
12
16
20
24
28
32
36
40
44
48
52
TIME IN SECONDS

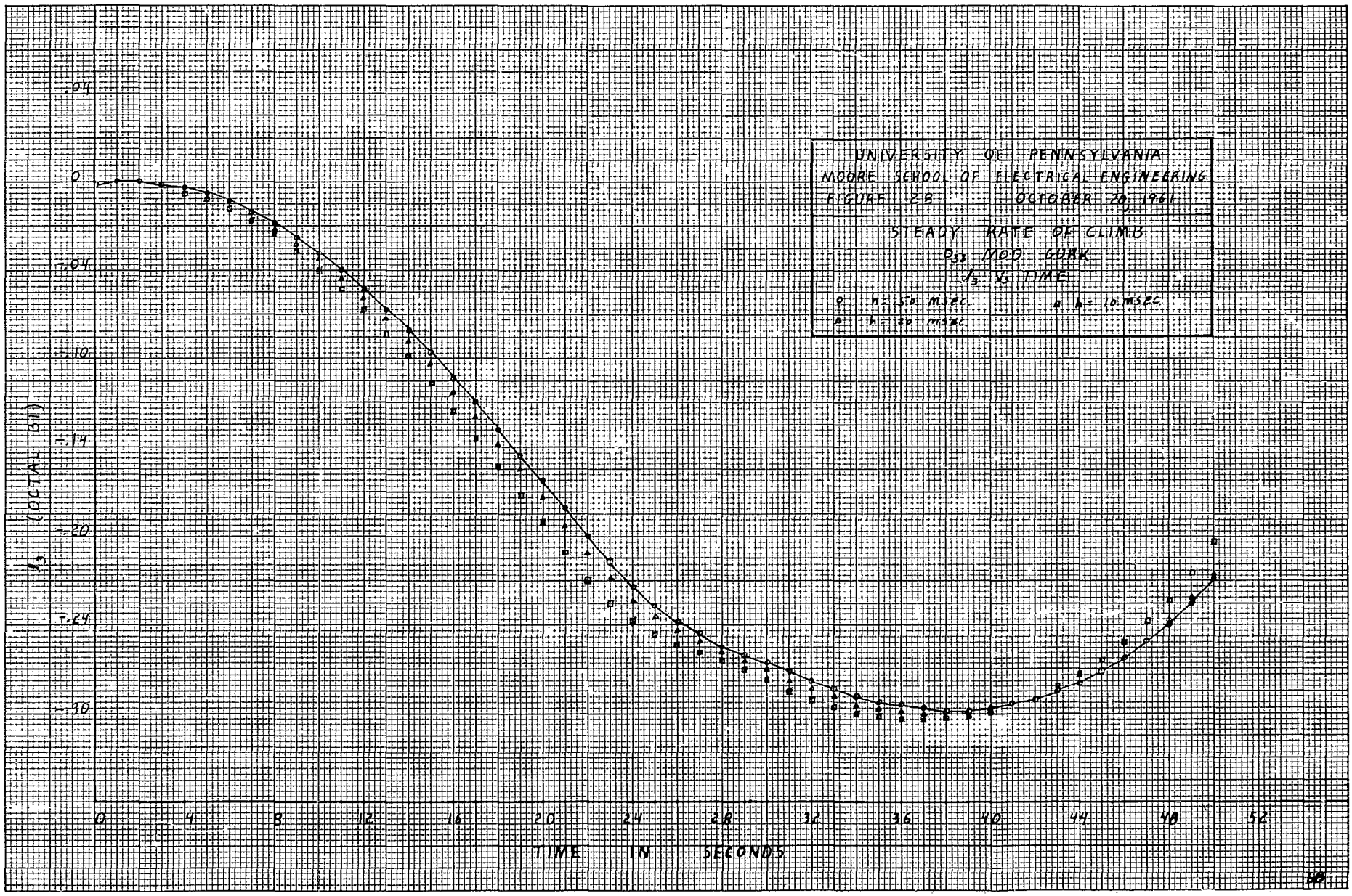
UNIVERSITY OF PENNSYLVANIA
MOORE SCHOOL OF ELECTRICAL ENGINEERING
FIGURE 2.8 OCTOBER 20, 1961
STEADY RATE OF CLIMB
D33 MOD GURK
1/2 V2 TIME
o h = 50 msec.
Δ h = 20 msec.
□ h = 10 msec.
.04
0
-.04
-.10
-.14
-.20
-.24
-.30
I3 (OCTAL BIT)
0
4
8
12
16
20
24
28
32
36
40
44
48
52
TIME IN SECONDS

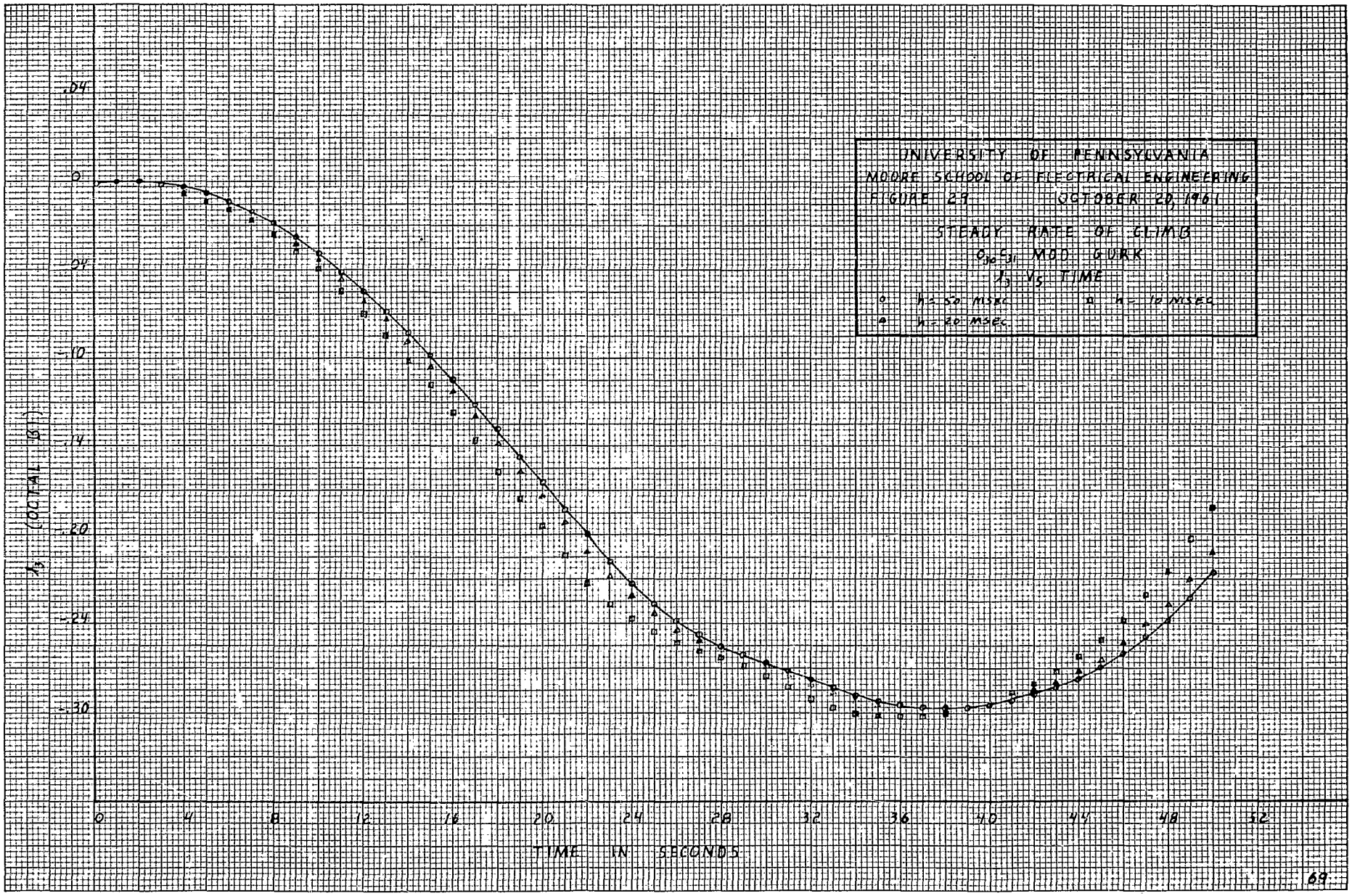
UNIVERSITY OF PENNSYLVANIA
MOORE SCHOOL OF ELECTRICAL ENGINEERING
FIGURE 29 OCTOBER 20, 1961
STEADY RATE OF CLIMB
$C_{y_0} C_{y_1}$ MOD GURK
λ_3 VS TIME
h = 50 msec
h = 20 msec
h = 10 msec
λ_3 (OCTAL 15)
.04
0
-.04
-.10
-.14
-.20
-.24
-.30
0
4
8
12
16
20
24
28
32
36
40
44
48
52
TIME IN SECONDS

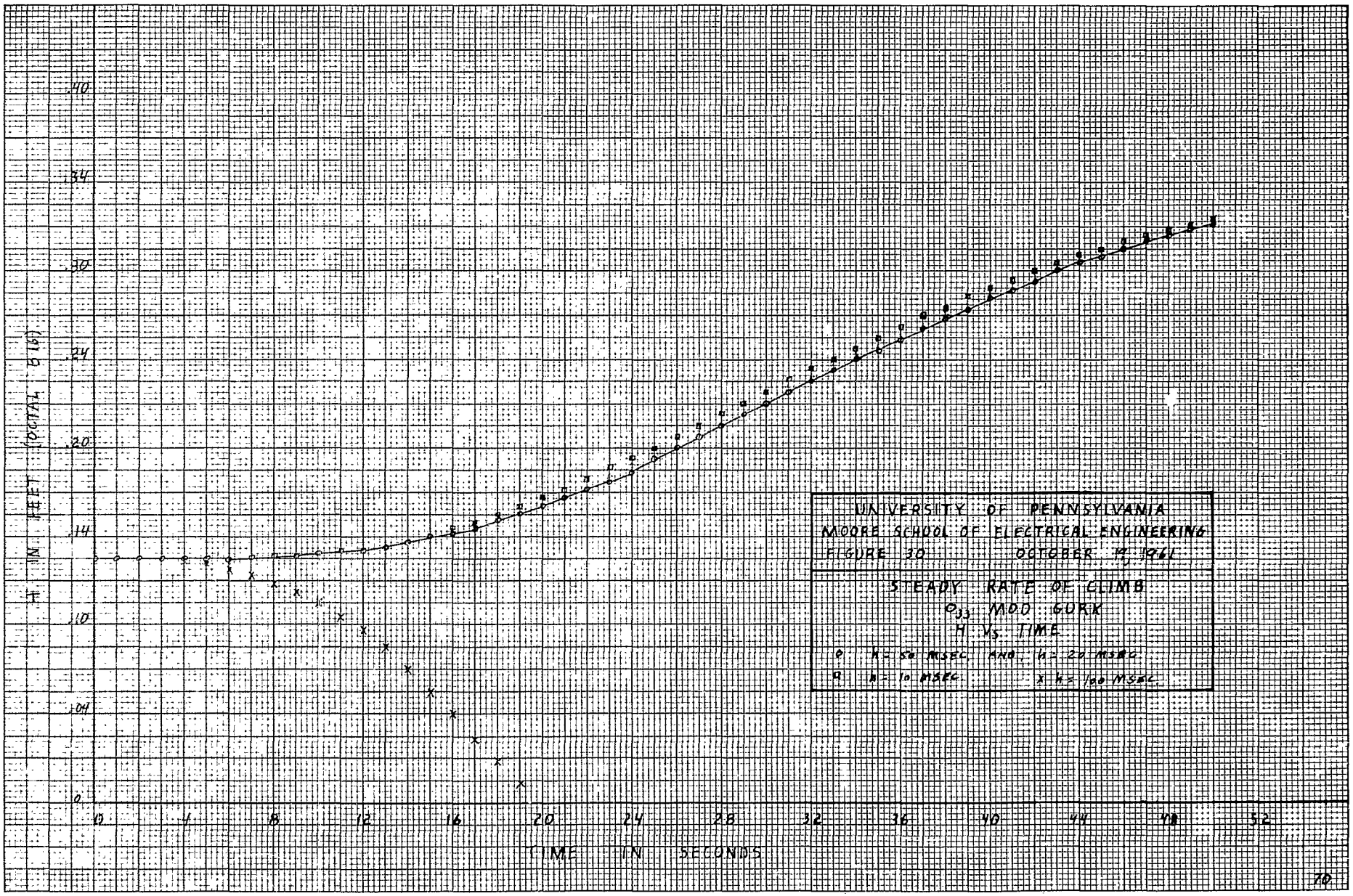
H IN FEET (TOTAL - 8161)
40
34
30
24
20
14
10
04
0
12
4
8
12
16
20
24
28
32
36
40
44
48
52
TIME IN SECONDS
UNIVERSITY OF PENNSYLVANIA
MOORE SCHOOL OF ELECTRICAL ENGINEERING
FIGURE 30 OCTOBER 17, 1961
STEADY RATE OF CLIMB
Θ_{33} MOD GURK
H Vs. TIME
o h = 50 MSEC AND h = 20 MSEC
□ h = 10 MSEC x h = 100 MSEC

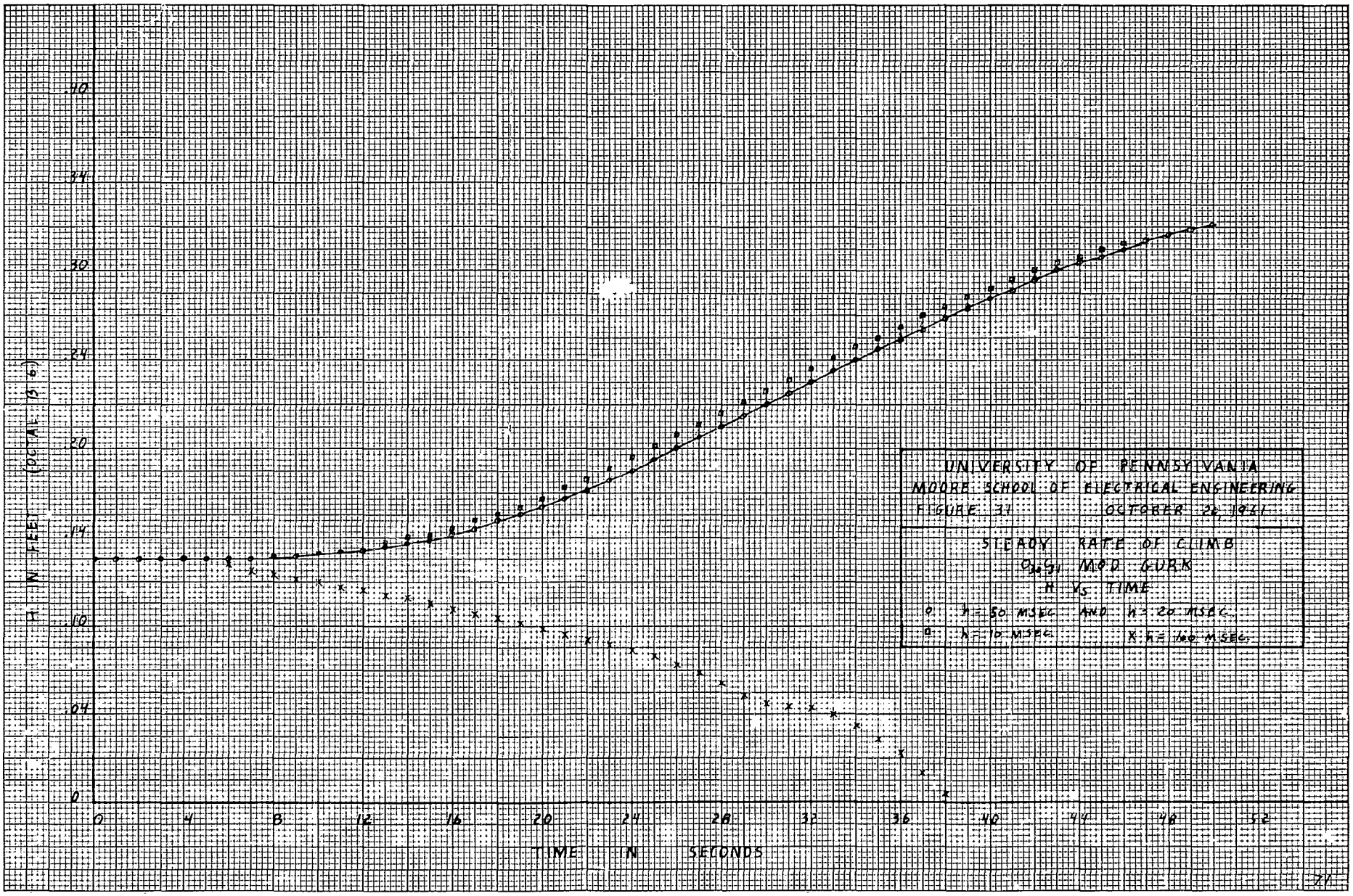
H IN FEET (OCTAL 15.6)
.40
.34
.30
.24
.20
.14
.10
.04
0
0
4
8
12
16
20
24
28
32
36
40
44
48
52
TIME IN SECONDS
UNIVERSITY OF PENNSYLVANIA
MOORE SCHOOL OF ELECTRICAL ENGINEERING
FIGURE 37 OCTOBER 26 1951
STEADY RATE OF CLIMB
Θ_{des} MOD GURK
H VS TIME
o h = 50 MSEC AND h = 20 MSEC.
□ h = 10 MSEC. X h = 100 MSEC.

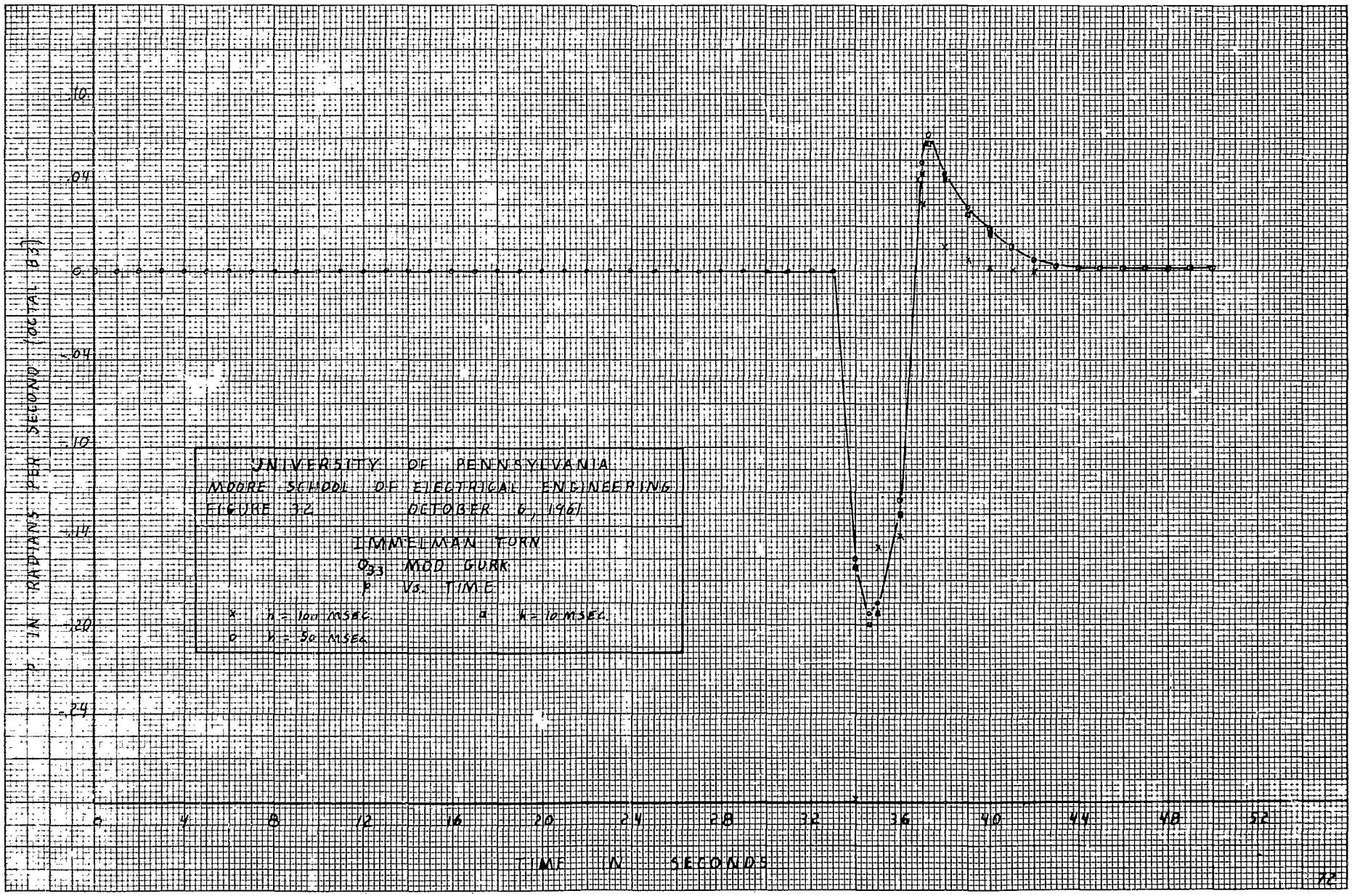
UNIVERSITY OF PENNSYLVANIA
MOORE SCHOOL OF ELECTRICAL ENGINEERING
FIGURE 32. OCTOBER 6, 1961
IMMELMAN TURN
O_{33} MOD GURK
p VS. TIME
x h = 100 MSEC.
o h = 50 MSEC.
a h = 10 MSEC.
p IN RADIANS PER SECOND (OCTAL 63)
.10
.04
0.0
-.04
-.10
-.14
-.20
-.24
0
4
8
12
16
20
24
28
32
36
40
44
48
52
TIME IN SECONDS

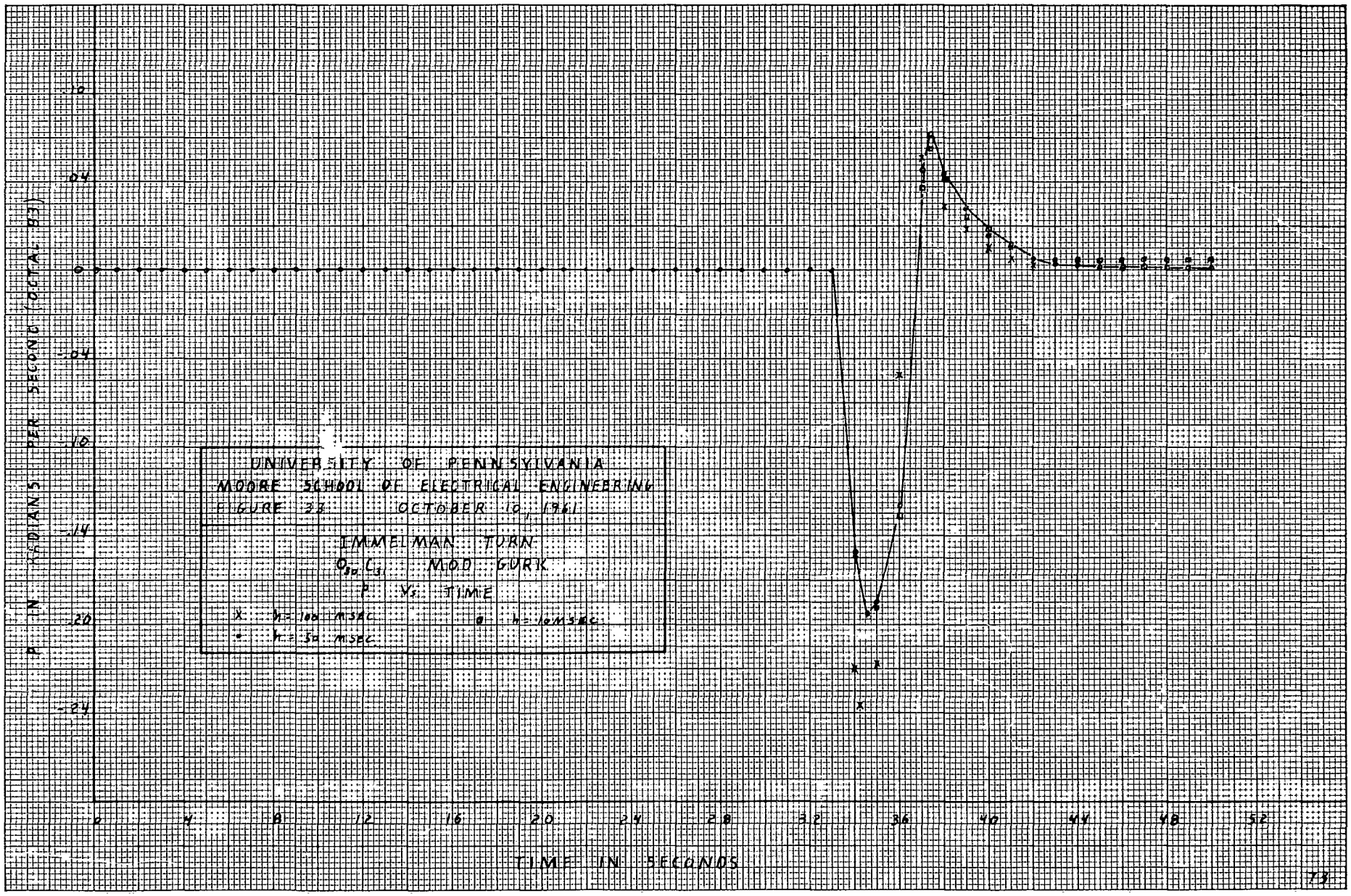
UNIVERSITY OF PENNSYLVANIA
MOORE SCHOOL OF ELECTRICAL ENGINEERING
FIGURE 23 OCTOBER 10, 1961
IMMELMAN TURN
$O_{30}C_3$ MOD GURK
P Vs TIME
X h= 100 msec
• h= 50 msec
0 h= 10 msec
P IN RADIANS PER SECOND (OCTAL 93)
TIME IN SECONDS
.08
0
-.04
-.10
-.14
-.20
-.24
0
4
8
12
16
20
24
28
32
36
40
44
48
52

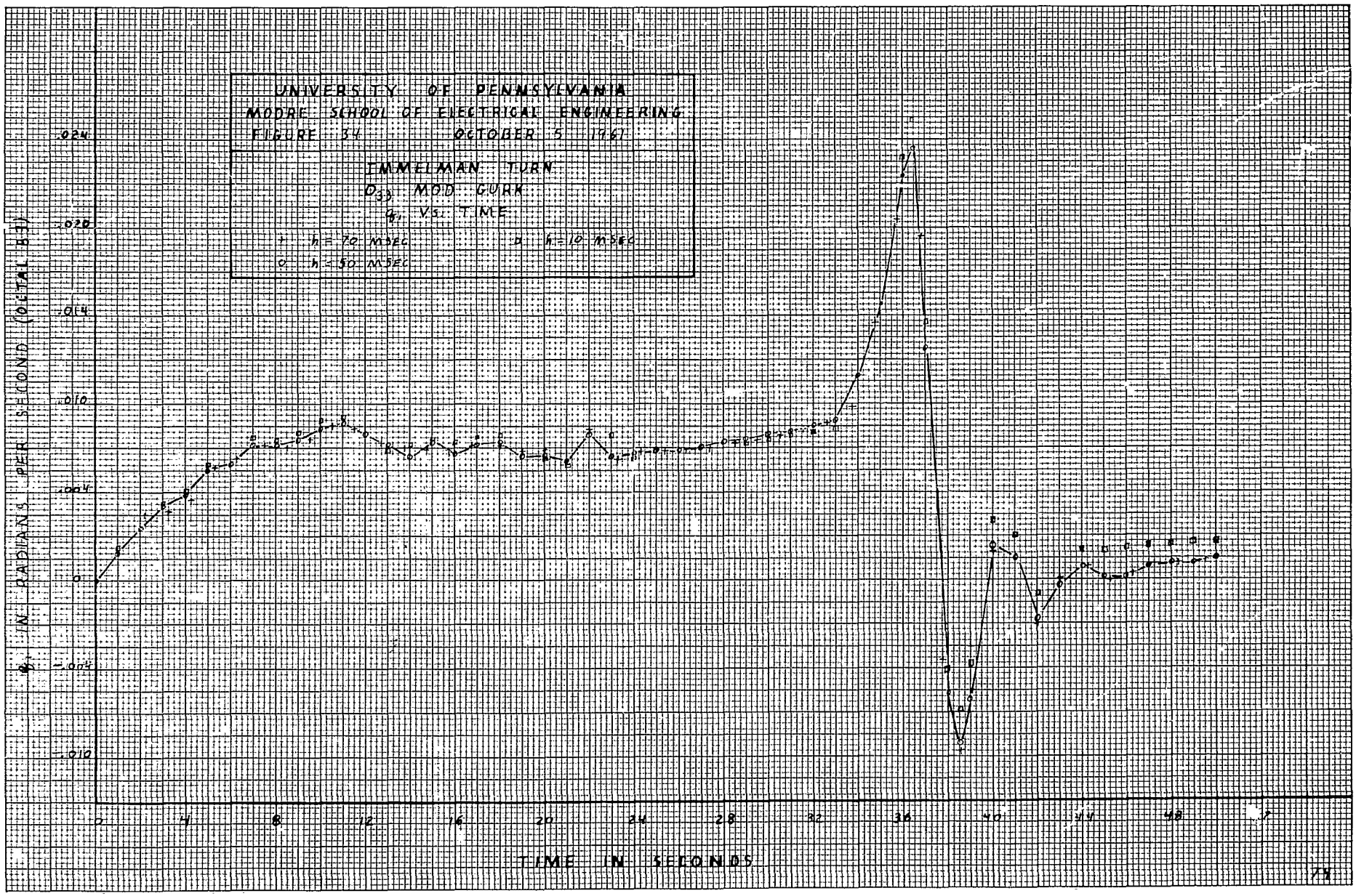
UNIVERSITY OF PENNSYLVANIA
MOORE SCHOOL OF ELECTRICAL ENGINEERING
FIGURE 34 OCTOBER 5 1967
EMMELMAN TURN
D_{33} MOD GURK
θ_4 VS. TIME
+ h = 70 M SEC
o h = 50 M SEC
□ h = 10 M SEC
θ_4 IN RADIANS PER SECOND (TOTAL ERR)
.024
.020
.014
.010
.004
0
-.004
-.010
0
4
8
12
16
20
24
28
32
36
40
44
48
52
TIME IN SECONDS

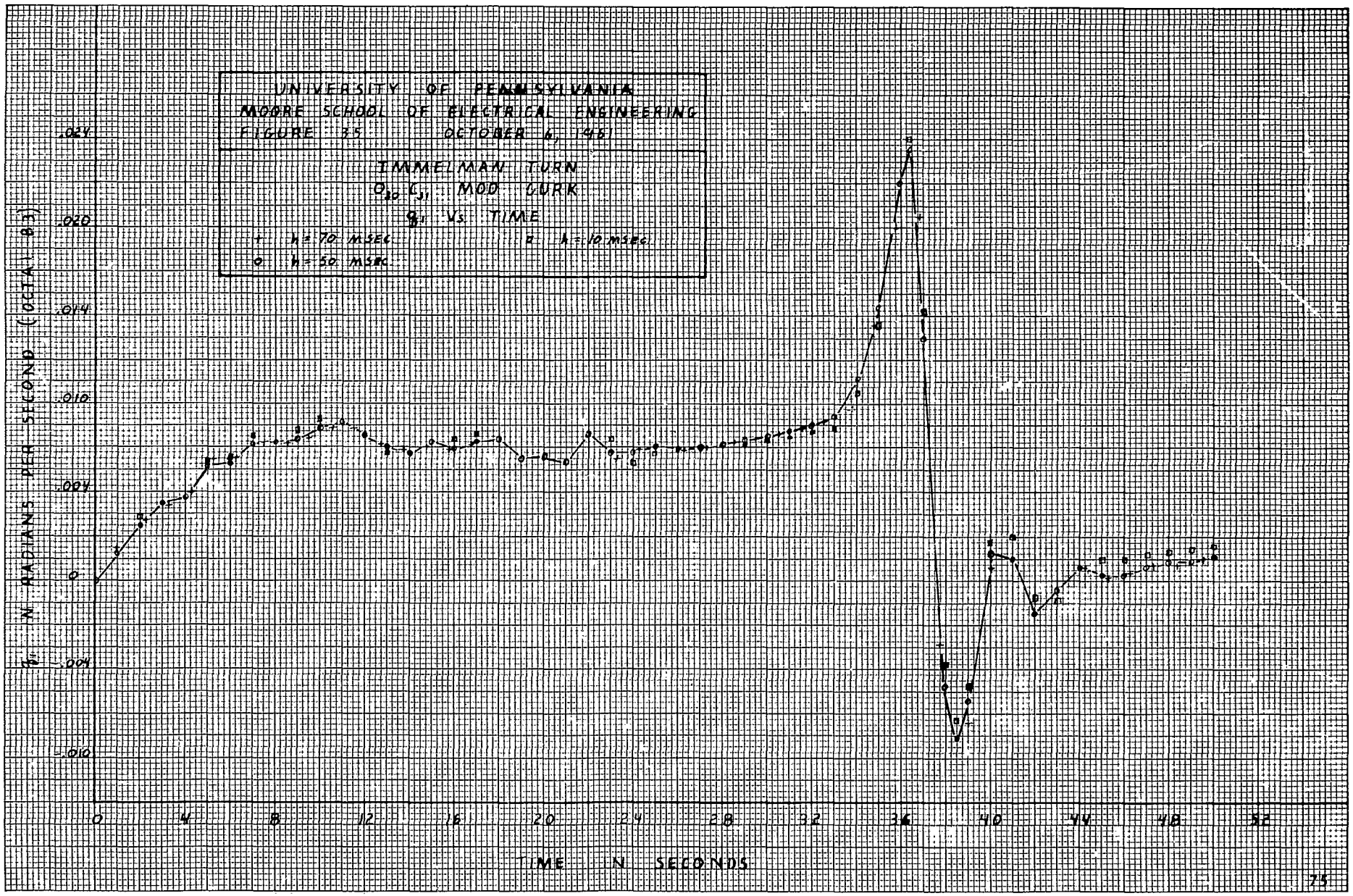
UNIVERSITY OF PENNSYLVANIA
MOORE SCHOOL OF ELECTRICAL ENGINEERING
FIGURE 35 OCTOBER 6, 1951
IMMELMAN TURN
θ_{30} C_{31} MOD CURK
θ_{31} Vs TIME
t h = 70 MSEC
o h = 50 MSEC
□ h = 10 MSEC
$\dot{\theta}_{31}$ IN RADIANS PER SECOND (OCTAL 83)
.024
.020
.014
.010
.004
0
-.004
-.010
0
4
8
12
16
20
24
28
32
36
40
44
48
52
TIME IN SECONDS
75